ACUTE ACTIONS AND SIGNALING TRANSDUCTION OF PROLACTIN ON TRANSEPITHELIAL CALCIUM TRANSPORT IN EPITHELIAL-LIKE CACO-2 MONOLAYER

NARONGRIT THONGON

A THESIS SUMITTED IN PARTIAL FULFILLMENT OF
THE REQUIREMENTS FOR
THE DEGREE OF DOCTOR OF PHILOSOPHY
(PHYSIOLOGY)
FACULTY OF GRADUATE STUDIES
MAHIDOL UNIVERSITY
2008

Thesis
Entitled

ACUTE ACTIONS AND SIGNALING TRANSDUCTION OF PROLACTIN ON TRANSEPITHELIAL CALCIUM TRANSPORT IN EPITHELIAL-LIKE CACO-2 MONOLAYER

Mr. Narongrit Thongon
Candidate

Prof. Nateetip Krishnamra, Ph.D.
Major-Advisor

Assoc. Prof. Tuangporn Suthiphongchai, Ph.D.
Co-Advisor

Asst. Prof. Narattaphol Charoenphandhu, M.D., Ph.D.
Co-Advisor

Assoc. Prof. Sutthasinee Poonyachoti, D.M.V., Ph.D.
Co-Advisor

Prof. Chumpol Pholpramool, Ph.D.
Co-Advisor

Asst. Prof. Auemphorn Mutchimwong, Ph.D
Acting Dean
Faculty of Graduate Studies

Assoc. Prof. Varanuj Chatsudthipong, Ph.D.
Chair
Doctor of Philosophy Programme in Physiology
Faculty of Science

Thesis
Entitled

ACUTE ACTIONS AND SIGNALING TRANSDUCTION OF PROLACTIN ON TRANSEPITHELIAL CALCIUM TRANSPORT IN EPITHELIAL-LIKE CACO-2 MONOLAYER

was submitted to the Faculty of Graduate Studies, Mahidol University
for the degree of Doctor of Philosophy (Physiology)
on
May 23, 2008

Mr. Narongrit Thongon
Candidate

Assoc. Prof. Tuangporn Suthiphongchai, Ph.D.
Member

Assoc. Prof. Chatsri Dechapunya, Ph.D.
Chair

Assoc. Prof. Sutthasinee Poonyachoti, D.M.V., Ph.D.
Member

Prof. Nateetip Krishnamra, Ph.D.
Member

Asst. Prof. Narattaphol Charoenphandhu, M.D., Ph.D.
Member

Prof. Chumpol Pholpramool, Ph.D.
Member

Asst. Prof. Auemphorn Mutchimwong, Ph.D
Acting Dean
Faculty of Graduate Studies
Mahidol University

Prof. Skorn Mongkolsuk, Ph.D.
Dean
Faculty of Science
Mahidol University

ACKNOWLEDGEMENTS

I would like to express my deepest gratitude and sincere appreciation to my major advisor Prof. Nateetip Krishnamra and my project supervisor Asst. Prof. Narattaphol Charoenphandhu for their kindness, excellent guidance, supervision, encouragement, and patience throughout my study.

My cordial gratitude is also expressed to my co-advisors, Prof. Chumpol Pholpramool, Assoc. Prof. Tuangporn Suthiphongchai, and Assoc. Prof. Sutthasinee Poonyachoti, as well as the thesis examining committee, Assoc. Prof. Chatsri Dechapunya, for their valuable suggestions, criticism and correction of the thesis.

I am grateful to Dr. Chureeporn Chitchumroonchokchai and Dr. Kittiporn Phanvijhitsiri at the Institute of Nutrition, Mahidol University, Thailand, for the kind gift of Caco-2 cells. I also would like to express my gratitude to Assoc. Prof. Jonggonnee Wattanapermpool for her excellent guidance in the concept of laboratory planning, scientific writing, and analysis of scientific papers. I thank Dr. La-iad Nakkrasae for assistance in siRNA transfection, Miss Jarinthorn Teerapornpuntakit in assistance of PCR technique, and Miss Jirawan Thongbunchoo in assistance of cell culture technique. I would like to thank the faculty engineers, Mr. Supreecha Jaroonsuck and Mr. Somkid Khammune, for their help in Ussing chamber set up.

I would like to express my gratitude to the Royal Golden Jubilee Ph.D. program (RGJ) for my grant, and to the Commission on Higher Education (CHE) and the Thailand Research Fund (TRF) for research grants to Prof. Nateetip Krishnamra and Asst. Prof. Narattaphol Charoenphandhu. I wish to extend my appreciation to the COCAB members for their kind supports.

My special thanks are also extended to my best friend Miss Siriporn Chamniansawat for her encouragement, care and love.

Finally, I owe the deepest gratitude to my family for their financial support, encouragement, care and love. This thesis, I dedicate to my parents and all teachers who have taught me and took care of me since my school age.

Narongrit Thongon

ACUTE ACTIONS AND SIGNALING TRANSDUCTION OF PROLACTIN ON TRANSEPITHELIAL CALCIUM TRANSPORT IN EPITHELIAL-LIKE CACO-2 MONOLAYER

NARONGRIT THONGON 4736655 SCPS/D

Ph.D. (PHYSIOLOGY)

THESIS ADVISORS: NATEETIP KRISHNAMRA, Ph.D., NARATTAPHOL CHAROENPHANDHU, M.D., Ph.D., CHUMPOL PHOLPRAMOOL, Ph.D., TUANGPORN SUTHIPHONGCHAI, Ph.D., SUTTHASINEE POONYACHOTI, D.M.V., Ph.D.

ABSTRACT

Previous investigations demonstrated the stimulatory effect of prolactin (PRL) on intestinal calcium (Ca) absorption, but the mechanism is unknown. The present study, therefore, aimed to elucidate the mechanism of PRL in the regulation of Ca transport in Caco-2 monolayer. To study intestinal Ca absorption, the Caco-2 monolayer grown on Snapwell for 14 days was exposed to recombinant human PRL (rhPRL) for 1 h before measurement of Ca fluxes in the Ussing chamber.

Human PRL receptors (hPRLR) (short, intermediate, and long isoforms) were identified in Caco-2 cells by PCR and immunocytochemistry, suggesting that Caco-2 cells were targets of PRL action. Results from Ussing experiments showed that rhPRL increased the active Ca flux in a dose-dependent manner with the maximal effective dose of 600 ng/mL. This effect was completely abolished by long-isoform hPRLR (hPRLR-L) knockdown, PI3K inhibitors (wortmannin and LY294002), PKC inhibitor (GF109203X), and ROCK inhibitor (Y27632), but not by MAPK inhibitor (U0126) or JAK2 inhibitor (AG490). PRL also increased the paracellular passive Ca transport and Ca permeability, both of which were abolished by PI3K and ROCK inhibitors. Dilution and cationic diffusion potential experiments demonstrated that rhPRL significantly increased P_{Li}/P_{Cl}, P_{Na}/P_{Cl}, P_{K}/P_{Cl}, P_{Rb}/P_{Cl}, and P_{Cs}/P_{Cl}, i.e., rhPRL increased cation selectivity of the monolayer. This effect was also abolished by PI3K and ROCK inhibitors. Size selectivity of the monolayer was investigated by measuring the dual ^{3}H-mannitol/^{14}C-polyethylene glycol (PEG) fluxes. The results showed that rhPRL had no effect on the size selectivity of Caco-2 monolayer.

In conclusion, PRL rapidly stimulated active Ca transport in Caco-2 monolayer via the non-genomic PI3K, PKC, and ROCK signaling pathways. Such actions of PRL were mediated by hPRLR-L. PRL also enhanced the paracellular passive Ca transport and increased paracellular permeability through the PI3K and ROCK pathways.

KEY WORDS : CACO-2 CELL / CALCIUM TRANSPORT / PROLACTIN / PROLACTIN SIGNALING / PERMEABILITY

113 pp.

กลไกระดับเซลล์ของโพรแลคตินฮอร์โมนในการกระตุ้นการขนส่งแคลเซี่ยมอย่างฉับพลันในเซลล์เพาะเลี้ยง CACO-2 (ACUTE ACTIONS AND SIGNALING TRANSDUCTION OF PROLACTIN ON TRANSEPITHELIAL CALCIUM TRANSPORT IN EPITHELIAL-LIKE CACO-2 MONOLAYER)

ณรงค์ฤทธิ์ ทองอุ่น 4736655 SCPS/D
ปร.ด. (สรีรวิทยา)

คณะกรรมการควบคุมวิทยานิพนธ์: นทีทิพย์ กฤษณามระ, ปร.ด., นรัตถพล เจริญพันธุ์, พ.บ., ปร.ด., ชุมพล ผลประมูล, Ph.D., ตวงพร สุทธิพงษ์ชัย, Ph.D., สุทธาสินี ปุญญโชติ, สพ.บ., Ph.D.

บทคัดย่อ

งานวิจัยที่ผ่านมาพบว่าโพรแลคตินมีฤทธิ์กระตุ้นการขนส่งแคลเซี่ยมในลำไส้ของหนูขาว แต่ยังไม่ทราบแน่ชัดถึงกลไกการออกฤทธิ์ของโพรแลคติน จุดประสงค์ของการวิจัยนี้คือศึกษากลไกการออกฤทธิ์ของโพรแลคตินในเซลล์เพาะเลี้ยงคาโคทู (Caco-2) โดยเลี้ยงแผ่นเยื่อ Caco-2 เป็นเวลา 14 วัน ก่อนที่จะเลี้ยงในสารละลายที่มีโพรแลคตินเป็นเวลา 1 ชั่วโมง จากนั้นจึงศึกษาการขนส่งแคลเซียมผ่านแผ่นเยื่อดังกล่าว

จากการศึกษาด้วยเทคนิคพีซีอาร์ และ คอนโฟคอลอิมมูโนไซโตเคมิสตรี พบว่าเซลล์เพาะเลี้ยง Caco-2 มีตัวรับโพรแลคตินทั้งแบบสั้น กลาง และแบบยาว ทั้งในระดับสารพันธุกรรมอาร์เอ็นเอและระดับโปรตีน ซึ่งบ่งชี้ว่าเซลล์เพาะเลี้ยง Caco-2 สามารถตอบสนองต่อโพรแลคตินได้ จากการศึกษาการขนส่งแคลเซียมพบว่าโพรแลคตินมีฤทธิ์กระตุ้นการขนส่งแคลเซี่ยมแบบใช้พลังงาน โดยโพรแลคตินที่ความเข้มข้น 600 นาโนกรัมต่อมิลลิลิตรมีประสิทธิภาพสูงสุด ทั้งนี้ แอลวาย-294002 (สารยับยั้งฟอสโฟอิโนสิไทด์ 3-ไคเนส) ยีเอฟ-109203เอ็กซ์ (สารยับยั้งโปรตีนไคเนสซี) วาย-27632 (สารยับยั้งโรห์ร็อค) และ การ์น็อคดาว์น ตัวรับโพรแลคตินแบบยาว ยับยั้งฤทธิ์ของโพรแลคตินในการกระตุ้นการขนส่งแคลเซี่ยมแบบใช้พลังงาน นอกจากนี้ยังพบว่าโพรแลคตินมีฤทธิ์ในการกระตุ้นการขนส่งแคลเซี่ยมแบบไม่ใช้พลังงานและเพิ่มการยอมให้แคลเซียมผ่านแผ่นเยื่อ ทั้งนี้ แอลวาย-294002 และ วาย-27632 สามารถยับยั้งฤทธิ์ของโพรแลคตินในการกระตุ้นการขนส่งแคลเซี่ยมแบบไม่ใช้พลังงาน จากการศึกษาด้วยเทคนิคไดลูชั่นโพเทนเชียล และ แค๊ทไอออนิคดิฟฟิวชั่นโพเทนเชียลพบว่า โพรแลคตินเพิ่มคุณสมบัติในการยอมให้อิออนประจุบวกผ่านไม่ว่าจะเป็น ลิเธียม โซเดียม โพแทสเซียม รูบิเดียม และซีเซียม โดยไม่เปลี่ยนคุณสมบัติการยอมให้อิออนประจุลบ คือคลอไรด์ผ่าน ทั้งนี้ แอลวาย-294002 และ วาย-27632 ส่งผลยับยั้งฤทธิ์ของโพรแลคตินในการเพิ่มคุณสมบัติการยอมให้อิออนประจุบวกผ่าน จากการศึกษาการคัดเลือกขนาดสารให้ผ่านแผ่นเยื่อโดยใช้แมนนิทอลล์ติดสลากรังสีและโพลีเอ็ททิลลีนไกลคอลติดสลากรังสี พบว่าโพรแลคตินไม่มีฤทธิ์ต่อการเปลี่ยนแปลงการเลือกขนาดสาร

จากผลการวิจัยสามารถสรุปได้ว่า โพรแลคตินออกฤทธิ์ผ่านกลไก ฟอสโฟอิโนสิไทด์ 3-ไคเนส โปรตีนไคเนสซี และโรห์ร็อคเพื่อกระตุ้นการขนส่งแคลเซี่ยมแบบใช้พลังงาน นอกจากนี้โพรแลคตินยังออกฤทธิ์ผ่านกลไก ฟอสโฟอิโนสิไทด์ 3-ไคเนส และ โรห์ร็อค ในการกระตุ้นการขนส่งแคลเซี่ยมแบบไม่ใช้พลังงาน และการเพิ่มคุณสมบัติในการยอมให้อิออนประจุบวกผ่าน

113 หน้า

CONTENTS

CONTENTS (Cont.)

LIST OF TABLES

LIST OF TABLES (Cont.)

LIST OF FIGURES

LIST OF FIGURES (Cont.)

LIST OF FIGURES (Cont.)

LIST OF FIGURES (Cont.)

LIST OF FIGURES (Cont.)

LIST OF ABBREVIATIONS

$1,25(OH)_2D_3$	1alpha,25-dihydroxyvitamin D_3
%	percent
α	alpha
β	beta
δ	delta
ε	epsilon
γ	gamma
η	eta
ι	iota
λ	lambda
μ	micro
$\mu A. cm^{-2}$	micro-ampere per centimeter-square
μM	micromolar
θ	theta
$\Omega.cm^2$	ohm centimeter-square
ζ	zeta
AG490	(*E*)-*N*-benzyl-2-cyano-3-(3,4-dihydroxyphenyl)acrylamidea-cyano-(3,4-dihydroxy) -N-benzylcinnamide tyrphostin B42
Ag	silver
ANOVA	analysis of variance
AP-1	activator protein-1
bp	base pairs
C°	degree celsius
Ca^{2+}	calcium ionized form
Ca^{2+} ATPase	calcium-adenosine triphosphatase
cDNA	complementary deoxyribonucleic acid

LIST OF ABBREVIATIONS (Cont.)

Cl^-	chloride ionized form
cm	centimeter
cm^2	centimeter-square
$cm.s^{-1}$	centimeter per second
CO_2	carbon dioxide
Cs^+	cesium ion
Cys	cysteine amino acid
DAG	diacyl glycerol
DMSO	dimethyl sulfoxide
DRB	5,6-dichlorobenzimidazole riboside
et al.	and coworkers
g	gram
GF-109203X	2-[1-(3-dimethylaminopropyl) indol-3-yl]-3-(indol-3-yl) maleimide
h	hour
H^+	hydrogen ion
hCR1	human complementary receptor 1
GH	growth hormone
hGAPDH	human glyceraldehyde 3-phosphate dehydrogenase
hPRLR-I	human prolactin receptor intermediate isoform
hPRLR-L	human prolactin receptor long isoform
hPRLR-S	human prolactin receptor short isoform
i.e.	including
IEG	immediate early gene
Isc	Short-circuit current
Jak	janus kinase
JAM	junctional adhesion molecule
K^+	potassium ion

LIST OF ABBREVIATIONS (Cont.)

kb	kilo-base pairs
kDa	kilo-Dalton
Li^+	lithium ion
LY294002	2-(4-morpholinyl)-8-phenyl-4H-1-benzopyran-4-one
MAGUK	membrane-associated guanylate kinase
mg	milligram
mg/day	milligram per day
min	minute
MLCK	myosin light chain kinase
mM	millimolar
mV	millivolt
n	number of samples
Na^+/K^+-ATPase	sodium-potassium-adenosine triphosphatase
NCX	sodium-calcium exchanger
ng/mL	nanogram per milliliter
NHE3	sodium-proton exchanger type III
nM	nanomolar
PBS	standard phosphate buffer solution
P_{Ca}	calcium permeability
P_{Ca}/P_{Na}	relative permeability ratio of calcium and sodium
P_{Cs}/P_{Cl}	relative permeability ratio of cesium and chloride
PD	transepithelial potential difference
PEG	polyethylene glycol
PI3K	phosphoinositide 3-kinase
P_K/P_{Cl}	relative permeability ratio of potassium and chloride

LIST OF ABBREVIATIONS (Cont.)

PKB	protein kinase B
PKC	protein kinase C
P_{Li}/P_{Cl}	relative permeability ratio of lithium and chloride
pm	picometer
PMCA	plasma membrane calcium-adenosine triphosphatase
P_{Na}/P_{Cl}	relative permeability ratio of sodium and chloride
P_{Rb}/P_{Cl}	relative permeability ratio of rubidium and chloride
PRL	prolactin
PRLR	prolactin receptor
r^2	coefficient of determination
r	correlation coefficient
Rb^+	rubidium ion
rhPRL	recombinant human prolactin
ROCK	rho-associated coiled-coil-containing protein kinase
s	second
SE	standard error
Ser	serine amino acid
SGK	serum- and glucocorticoid-inducible kinase
SGLT	sodium-glucose cotransporter
siRNA	small interference ribonucleic acid
STAT	signaling transducer and activator of transcription
TER	transepithelial electrical resistance
TNF	tumor necrosis factor

LIST OF ABBREVIATIONS (Cont.)

TRPV	transient receptor potential vanilloid
Tyr	tyrosine amino acid
U0126	1,4-diamino-2,3-dicyano-1,4-bis[2-aminophenylthio] butadiene
v/v	volume per volume
Vδ	voltage difference
Y27632	(R)-(+)-*trans*-N-(4-pyridyl)-4-(1-aminoethyl)-cyclohexanecarboxamide . 2HCl
ZO	zonula occludens

PUBLICATIONS

1. **Thongon N**, Nakkrasae L-I, Thongbunchoo J, Krishnamra N and Charoenphandhu N. *Prolactin stimulates transepithelial calcium transport and modulates paracellular permselectivity in Caco-2 monolayer: Mediation by PKC and ROCK pathways.* Am J Physiol Cell Physiol 2008; 294(5): C1158–C1168.

2. Jantarajit W, **Thongon N**, Pandaranandaka J, Teerapornpuntakit J, Krishnamra N and Charoenphandhu N. *Prolactin-stimulated transepithelial calcium transport in duodenum and Caco-2 monolayer are mediated by the phosphoinositide 3-kinase pathway.* Am J Physiol Endocrinol Met 2007; 293: E372–E384.

CONFERENCE ABSTACTS

1. Narongrit Thongon. *Acute actions and signaling transduction of prolactin on transepithelial calcium transport in epithelial-like Caco-2 monolayer*. The 8th annual National Grad Research 2007, Mahidol University, Salaya, Nakornpathom, Thailand, September 7 – 8, 2007 (Oral presentation).
2. Narongrit Thongon, Narattaphol Charoenphandhu, Jantarima Pandaranandaka, Jarinthorn Teerapornpuntakit, and Nateetip Krishnamra. *Acute actions and signaling transduction of prolactin on transepithelial calcium transport in epithelial-like Caco-2 monolayer*. The 9th annual RGJ-Ph.D. Congress 2008, Jomtien Palm Beach Resort, Pattaya, Chonburi, Thailand, April 4 – 6, 2008 (Oral presentation).
3. Narongrit Thongon, Narattaphol Charoenphandhu, Jantarima Pandaranandaka, Jarinthorn Teerapornpuntakit, and Nateetip Krishnamra. *Acute actions and*

signaling transduction of prolactin on transepithelial calcium transport in epithelial-like Caco-2 monolayer. the 37th Physiological Society of Thailand's Annual Conference 2008, Garden Sea View Resort, Pattaya, Chonburi, Thailand, May 7 – 9, 2008 (Oral presentation).

CHAPTER I
INTRODUCTION

The higher calcium requirement for fetal growth and milk production leads to disturbances of calcium metabolism in pregnant and lactating mammals (Prentice 2000). The total calcium accretion rate of fetus increases from approximately 50 mg/day at 20 weeks of gestation to 330 mg/day at 35 weeks (Prentice 2000). When calcium supplement is insufficient to meet this extra demand, maternal bone loss and impaired milk calcium secretion may occur (Prentice 2000). Observations of lower bone mineral density and increased rate of bone resorption during pregnancy and throughout lactation were reported (Kalkwarf and Specker 2002; Kovacs 2005; Sarli et al. 2005). Therefore, during these reproductive phases, to maintain adequate calcium availability, the calcium regulating system must increase calcium gain and prevent calcium loss. This is achieved in part by an increase in the intestinal calcium absorption (Halloran and DeLuca 1980).

Normally, the intestine absorbs ~30% of calcium intake. However, during high calcium demand, the fractional calcium absorption markedly increases under hormonal regulation (Berne et al. 2003). It is commonly accepted that $1,25(OH)_2D_3$ is the major regulator that enhances intestinal calcium absorption (Hoenderop et al. 2005). However Pahuja and DeLuca showed that an increase in intestinal calcium transport in pregnant and lactating animals was independent of $1,25(OH)_2D_3$ (Pahuja and DeLuca 1981). Therefore, the question arose as to which hormone did replace $1,25(OH)_2D_3$ as a major regulator of the intestinal calcium absorption. During the reproductive phases, there are several hormones with increased plasma levels, such as progesterone and prolactin (PRL) (Jacobs et al. 1972). Boass and coworker clearly showed that the elevated duodenal calcium absorption during pregnancy and lactation correlated with the change in serum PRL level (Boass and Lovdal 1992). Our laboratory demonstrated that PRL directly enhanced the intestinal calcium absorption

(Charoenphandhu et al. 2001; Krishnamra et al. 2001; Tanrattana et al. 2004). Further studies showed that PRL directly enhanced the transcellular and solvent drag-induced components of the active calcium transport (Charoenphandhu et al. 2001; Tanrattana et al. 2004; Tudpor et al. 2005). The underlying mechanism of PRL action probably involved stimulation of the basolateral Na^+/K^+- and Ca^{2+}-ATPase activities (Charoenphandhu et al. 2006). In addition to the active calcium transport, it has been showed that the passive calcium transport was also enhanced by endogenous PRL, but its mechanism of action has not been elucidated (Krishnamra et al. 1998; Amnattanakul et al. 2005). **Thus, PRL is one of the major regulators of the intestinal calcium transport** (Charoenphandhu and Krishnamra 2007).

PRL is one of the most versatile hormones regulating a number of biological functions, e.g., control of water and electrolyte balance, growth and development, reproduction, immunomodulation and energy metabolism (Bole-Feysot et al. 1998; Freeman et al. 2000). Its activities are mediated by PRL receptors (PRLR) that activate a number of intracellular signaling pathways, the major of which are the JAK2/Stat5 and MAPK pathways (Bole-Feysot et al. 1998). In addition, PI3K/Akt and PKC pathways also mediate the cellular response of PRL in mammary gland and neurons (Bole-Feysot et al. 1998). However, PRL signaling has been extensively studied in mammary glands and neurons, but has never been studied in enterocytes. Moreover, the studied pathways represent the cellular response through the genomic-mediated mechanisms that involve time-consuming transcription and translation processes. Since our laboratory has previously demonstrated an acute stimulatory effects of PRL on the duodenal calcium transport as well as Na^+/K^+- and Ca^{2+}-ATPase activities (Krishnamra et al. 1998; Charoenphandhu et al. 2001; Charoenphandhu et al. 2006), it was, therefore, interesting to investigate the non-genomic signaling pathway(s) of PRL in the intestine.

To study the mechanism of PRL and its signaling pathway, an epithelial model that is closely related to human intestinal cells was used, i.e., Caco-2 cells. They are human colonic adenocarcinoma cell line that spontaneously differentiates into enterocytes with biological and morphological characteristics of differentiated cells from the small intestine (Pinto et al. 1983; Giuliano and Wood 1991; Yee 1997). Caco-2 cells express the brush-border membrane enzyme markers of the small

intestine such as sucrase, isomaltase, lactase, alkaline phosphatase, γ-glutamyltransferase, aminopeptidase N, and dipeptidyl aminopeptidase IV (Chantret et al. 1988; Jamarie and Malo 1991; Yoshioka et al. 1991), and also express proteins involved in calcium transport, such as TRPV6, calbindin, Ca^{2+}-ATPase and Na^{+}/Ca^{2+} exchanger (Wood et al. 2001; Fleet et al. 2002; Taparia et al. 2006). Yee demonstrated a strong correlation between in vivo human absorption and in vitro Caco-2 monolayer permeability for a variety of compounds, e.g., mannitol, glycine, caffeine, ibuprofen, cimetidine, acetyl salicylic acid, and testosterone (Yee 1997), suggesting that Caco-2 monolayer is a suitable model for studying intestinal calcium absorption (Chirayath et al. 1998; Fleet et al. 2002). Moreover, Nagano and coworkers in 1995 provided evidence that Caco-2 cells expressed PRLR, however its isoforms were not identified (Nagano et al. 1995). Hence, Caco-2 cells were chosen as a model for studying the action of PRL on the intestinal calcium transport, and its mechanism in the enhancement of active and passive calcium transport.

The objectives of the present study were:

Main Objective: To investigate the acute action and signaling transduction of PRL on calcium transport across the epithelial-like Caco-2 monolayer.

Specific Objectives:

1. To demonstrate the expression and localization of PRLR in Caco-2 cells.
2. To study the acute effect of PRL and its mechanism of the acute action on the transepithelial calcium transport in Caco-2 monolayer.
3. To elucidate the signaling transduction pathway(s) of the acute PRL action in Caco-2 monolayer.

The hypotheses of the present study were:

1. Caco-2 cells expressed PRLR on their plasma membrane.
2. PRL enhanced both active and passive calcium transport across Caco-2 monolayers via non-genomic signaling pathway(s).
3. PRL enhanced paracellular calcium transport by altering the charge– and size–selective properties of the monolayer.

CHAPTER II
LITERATURE REVIEW

A. INTESTINAL CALCIUM TRANSPORT

Calcium is an important ion that plays a crucial role in many biological processes ranging from the formation and maintenance of the skeleton to the regulation of neuronal function (Hoenderop et al. 2005). Approximately 99% of total calcium is present in hydroxyapatite crystal stored in bone, whereas 1% dissolves in the intracellular and extracellular fluids as ionized calcium (Berne et al. 2003). The extracellular calcium is required for hormonal secretion, neuromuscular function and blood coagulation, while intracellular calcium is required for regulation of several biological processes such as signal transduction and apoptotic activity (Hoenderop et al. 2005). Therefore, the plasma calcium concentration must be tightly regulated within a narrow range of 1.16-1.32 mmol/L (Karbach 1991). Normal calcium balance is maintained by the concerted actions of three organ systems, the gastrointestinal tract, bone and kidney (Hoenderop et al. 2005).

Normally, an adult human ingests an average amount of 1000 mg calcium /day. Of this ingested calcium, only 20% is absorbed by the intestine. However, in the higher calcium requirement condition, the fractional calcium absorption markedly increases under hormonal regulation (Berne et al. 2003). For the small intestine of rats, 88% of calcium absorption occurs in the ileum, 8% in the duodenum, and 4% in the jejunum (Marcus and Lengemann 1962; Charoenphandhu and Krishnamra 2007). The large intestine also has an ability to absorb calcium, but its physiological significance is still controversial (Charoenphandhu and Krishnamra 2007). Although the duodenum is responsible for only 8% of the total intestinal calcium absorption, duodenal calcium absorption is most important since its active transport component can occur during periods of low dietary calcium intake or high calcium requirement, such as pregnancy and lactation (Zhu et al. 1998; Armbrecht et al. 2003). The process by

which, calcium is absorbed across the epithelia involves active and passive transport pathways (Figure 1) (Charoenphandhu et al. 2001; Hoenderop et al. 2005; Charoenphandhu and Krishnamra 2007).

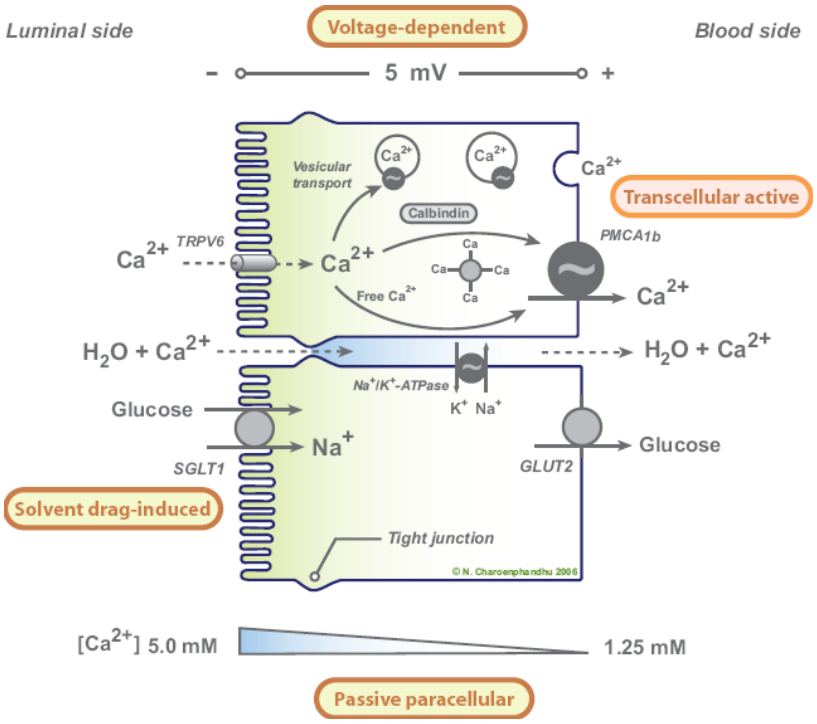

Figure 1. Schematic diagram of intestinal calcium transport (Charoenphandhu and Krishnamra 2007).

A1. Active calcium transport

Active calcium transport is the process that utilizes cellular energy from metabolism to drive calcium transport along the transcellular and paracellular pathway. In the small intestine, it consists of three active calcium transport components, , i.e., (*a*) transcellular active calcium transport, (*b*) solvent drag-induced calcium transport, and (*c*) voltage-dependent calcium transport (Figure 1) (Charoenphandhu et al. 2001; Hoenderop et al. 2005).

A1.1 Transcellular active calcium transport

The transcellular active calcium transport mainly occurs in the duodenum, thereafter it gradually decreases in magnitude and finally becomes absent in the distal intestinal segment (Bronner 2003). It is a multistep transporting process that includes an influx of luminal calcium into the enterocyte, calcium translocation across the cell to the basolateral membrane, and active calcium extrusion from the basolateral side to the circulation (Hoenderop et al. 2005).

Calcium enters the epithelial cells via the calcium selective channels at the luminal membrane under the influence of steep, inwardly directed electrochemical gradient (Hoenderop et al. 2005). It is widely believed that the transient receptor potential vanilloid (TRPV), a member of the transient receptor potential (TRP) channel superfamily, mediates this calcium entry process (Hoenderop et al. 2005). Two TRPVs, , i.e., TRPV5 and 6 are thought to account for calcium influx into the epithelial cells (Clapham 2003). They show strong electrophysiological inwardly rectifying currents and are the most calcium-selective TRP channels with high calcium permeability (permeability ratio P_{Ca}/P_{Na} >100) (Clapham 2003). TRPV5 and 6 are inactivated by high intracellular calcium concentration (Clapham 2003).

For the cytosolic diffusion of influxed calcium, the epithelium must facilitate the transcytosolic calcium diffusion and simultaneously maintain low levels of cytosolic calcium (Hoenderop et al. 2005). This cytosolic calcium diffusion is considered to be the rate limiting step of the transcellular calcium transport (Slepchenko and Bronner 2001). There are two accepted models to explain this cytosolic diffusion, i.e., facilitated diffusion and vesicular transport (Hoenderop et al. 2005). The facilitated diffusion involves the function of calcium-binding protein calbindin-D_{9k}, which serves as shuttles that facilitate calcium movement, at the same time act as cytosolic calcium buffer to maintain low intracellular calcium levels (Feher and Wasserman 1979). Regarding the vesicular model, some cytosolic calcium can also diffuse across the cell in vesicle or by endosome-mediated transport (Lasson and Nemere 2002).

The final step is the active extrusion of calcium from the enterocyte into the circulation against electrochemical gradient. There are two calcium transporters involved in this extrusion process, i.e., plasma membrane calcium-ATPase (PMCA)

isoform 1b and Na^+/Ca^{2+} exchanger 1 (NCX1) (Wasserman et al. 1992; Hoenderop et al. 2005). $PMCA_{1b}$ is the high-affinity calcium pump that is responsible for the maintenance of the resting intracellular calcium (Blaustein et al. 2002) and is responsible for more than 80% of the duodenal calcium extrusion. $PMCA_{1b}$ is stimulated by both calmodulin and calbindin-D_{9k} (Wasserman et al. 1992). The rest of the duodenal calcium extrusion (about 15-20%) involves the function of NCX1 (Wasserman et al. 1992). The active form of vitamin D, 1,25-dihydroxyvitamin D_3 ($1,25(OH)_2D_3$) is the major regulator of the transcellular active calcium transport (Hoenderop et al. 2005) by enhancing the expression of TRPV5, TRPV6, calbindin-D_{9k}, $PMCA_{1b}$, NCX1 (Hoenderop et al. 2005).

A1.2 Solvent drag-induced calcium transport

Solvent drag-induced calcium transport is the paracellular transport pathway by which calcium is carried in the moving stream of water (Charoenphandhu et al. 2006). Although it is not primarily an active calcium transport, solvent drag-induced calcium transport can be characterized as a secondary active transport since it utilizes cellular energy (Tanrattana et al. 2004). It accounts for about 70% of the total active calcium transport (Charoenphandhu et al. 2006).

This type of active calcium transport requires the lateral intercellular standing gradient that is generated by the paracellular hyperosmotic sodium gradient across the epithelia (Karbach 1991) which, inturn, is created by sodium entering the cell with nutrients, mostly glucose, at the brush border membrane (Wright and Loo 2000). The influxed sodium acts as a substrate of the Na^+/K^+ ATPase that pumps sodium out of the cell into the intercellular space (Weinstein and Stephenson 1981). The Na^+/K^+ ATPase creates the hyperosmotic sodium concentration of about 15 mmol/L above the surrounding medium (Chatton and Spring 1995). Thus the osmotic force could generate a downhill flux of water through the TJ into the paracellular space. When water is absorbed along this route, the water-soluble nutrients and ions, including calcium, are also carried along with water (Larsen et al. 2000).

A1.3 Voltage-dependent calcium transport

This transport mechanism is also considered a paracellular calcium transport and also classified as secondary active transport because it requires cellular energy metabolism (Charoenphandhu et al. 2001). It requires the electrogenic activity of the Na^+/K^+ ATPase that generates unequal distribution of charges between the 2 sides of the epithelial sheet (Contreras et al. 1989). In the rat duodenum and jejunum, the transepithelial potential differences are approximately 5-6 and 6-7 mV, respectively, which the luminal side being negative when compared with the serosal side (Tanrattana et al. 2004). This component of active calcium transport in rat duodenum is considered negligible (Charoenphandhu et al. 2001).

A2. Paracellular passive calcium transport

Although the active intestinal calcium transport is considered the most important calcium transport during the periods of low dietary calcium intake as well as high calcium requirement (Zhu et al. 1998; Armbrecht et al. 2003), it is responsible for only 8% of the total intestinal calcium transport (Marcus and Lengemann 1962). The major fractional intestinal calcium absorption, about 92% of the total intestinal calcium transport are accounted for by the passive paracellular mechanism in the jejunum and ileum (Marcus and Lengemann 1962; Karbach 1992). The paracellular passive calcium transport does not require cellular energy metabolism because it is driven by the chemical or electrical gradient across the epithelial sheet (Karbach 1992). It can be modulated in vitro by varying the transepithelial calcium gradient. Under physiological condition, the gradient is passively established by high calcium intake that results in luminal calcium concentration of about 5 mmol/L which is higher than the plasma free calcium concentration of 1.25 mmol/L (Charoenphandhu and Krishnamra 2007). Besides the chemical or electrical gradients, paracellular passive calcium transport can also be regulated through altering the property of the paracellular barrier tight junction (TJ) (Karbach 1992; Goodenough 1999).

B. Prolactin (PRL)

PRL is a peptide hormone of the anterior pituitary gland, with more than 300 diverse biological activities, such as regulation of water and electrolyte balance, growth and development, metabolism, and reproduction (Bole-Feysot et al. 1998). Moreover, it is well known that synthesis and secretion of PRL are not restricted to the anterior pituitary gland, but other organs and tissues, e.g., brain, decidua, myometrium, lacrimal gland, thymus, spleen, circulating lymphocytes, and lymphoid cells of bone marrow, also have this capability (Bole-Feysot et al. 1998).

B1. Chemistry and biology of PRL

B1.1 PRL gene and primary structure

The gene encoding human PRL is localized on chromosome 6 (Owerbach et al. 1981). It is present as a single copy per haploid genome and is composed of five exons and four introns with an overall length of 10 kb (Truong et al. 1984). Berwaer and coworkers clearly showed that the transcription process of the PRL gene is regulated by two independent promoter regions. While the proximal 5,000-bp of human PRL region directs pituitary-specific expression (Berwaer et al. 1991), the upstream promoter region is responsible for the extrapituitary expression (Berwaer et al. 1994). The complementary DNA of human PRL contains 914 nucleotides and is composed of a 681-nucleotide open reading frame encoding a prehormone of 227 amino acids (Cooke et al. 1981). The mature human PRL is composed of 199 amino acids or about 23 kDa (Sinha 1995). The human PRL molecule arranges itself in a single chain of 199 amino acids and contains six cysteines that form three intramolecular disulfide bonds (Cys 4-11, 58-174, and 191-199) (Cooke et al. 1981).

It is widely accepted that the primary structure of PRL is highly conserved (Bole-Feysot et al. 1998) within the given class, for example 97% similarity among the primates (Sinha 1995). However, PRL sequences from the distantly related species show a high degree of difference with only 56% similarity between primates and

rodents (Sinha 1995) and 36% shared between human and crabs (Yasuda et al. 1987). Although the major form of PRL in the anterior pituitary is a 23 kDa protein, variation of PRL has been reported to the result from the posttranslational modification of mature PRL, including glycosylation, phosphorylation, or proteolytic cleavage (Walker 1994; Sinha 1995).

B1.2 Plasma PRL level

In human, plasma PRL levels vary with age, sex, and reproductive period as summarized in the Table 1 (Noel et al. 1974; Soldin et al. 1995; Mazor et al. 1996). In non-reproductive human, the normal plasma PRL level is about 25 ng/mL, higher levels are considered as hyperprolactinemia (Serri et al. 2003). However, high physiological PRL levels during lactation and suckling-induced PRL surge may be as high as 350-650 ng/mL (Arbogast and Voogt 1998).

Table1. Human plasma PRL levels.

	Male (ng/mL)	Female (ng/mL)	References
< 1 month	3.7-81.2	0.3-95.0	Soldin et al. 1995
1-11 months	0.3-28.9	0.2-29.9	
1-3 years	2.3-13.2	1.0-17.0	
4-6 years	0.8-16.9	1.6-13.1	
7-9 years	1.9-11.6	0.3-12.9	
10-12 years	0.9-12.9	1.9-9.6	
13-15 years	1.6-16.6	3.0-14.4	
Adults			
Normal	2.1-17.7	2.8-29.2	Noel et al. 1974;
Pregnant		9.7-208.5	Mazor et al. 1996
Lactation		40.1-252.8	
Post menopausal		1.8-20.3	

B1.3 Site of synthesis and secretion of PRL

The specialized cells called lactotrophs or mammotrophs, comprising 20-50% of the anterior pituitary gland, are the major site that synthesizes and secretes PRL (Freeman et al. 2000). PRL can also be synthesized and secreted by the mammosomatotrophs of the anterior pituitary gland (Frawley et al. 1985). Interestingly, mammosomatotrophs can differentiate into lactotrophs in the presence of maternal signal that appears in early lactation (Porter et al. 1991) or estrogen (Boockfor et al. 1986).

In addition to lactotrophs of anterior pituitary gland, PRL is also produced by numerous cells and tissues, e.g., brain, decidua, myometrium, lacrimal gland, thymus, spleen, circulating lymphocytes, and lymphoid cells of bone marrow, mammary epithelial cells and tumors, skin fibroblasts, and sweat glands (Ben-Jonathan et al. 1996). Therefore, in addition to plasma, PRL can be detected in several fluid compartments such as cerebrospinal fluid, amniotic fluid, tears, milk, follicular fluid, and sweat (Bole-Feysot et al. 1998).

B2. PRL receptor (PRLR)

PRLR, a single glycosylated transmembrane protein that belongs to class I cytokine receptor superfamily, is a membrane-bound protein binding to both PRL and growth hormone (Bole-Feysot et al. 1998).

Gene encoding human PRLR is localized on chromosome 5 that contains at least 10 exons for an overall length exceeding 100 kb (Arden et al. 1990). There are three membrane-bound PRLR isoforms, i.e., short (PRLR-S; 291 amino acids), intermediate (PRLR-I; 393 amino acids), and long isoforms (PRLR-L; 591 amino acids) depending on their length and their cytoplasmic tails (Figure 2) (Goffin and Kelly 1996; Bole-Feysot et al. 1998). In addition to the membrane-bound receptors, soluble PRL-binding proteins are also present in milk (Amit et al. 1997). These PRLR isoforms are results of transcription starting at alternative initiation sites of the different promoter as well as alternative splicing of noncoding and coding exon transcripts (Hu and Dufau 1991; Hu et al. 1998). PRLRs have been identified in a wide range of cells and tissues.

In addition to the previously known PRL targets, such as mammary gland or reproductive organs, many other organs have been found to express PRLR, such as brain, retina, skin, osteoblast, lung, heart, muscle, liver, intestine, kidney and spleen (Bole-Feysot et al. 1998).

The extracellular domain of all PRLR isoforms is composed of ~210 amino acids referred to as the cytokine receptor homology region. This domain can be divided into two subdomains of ~ 100 amino acids, referred to as D1 and D2. Two highly conserved features are found including two pairs of disulfide bond in the N-terminal subdomain D1 (Cys12-Cys22 and Cys51-Cys62) and WS motif in the proximal region of subdomain D2 (Bole-Feysot et al. 1998).

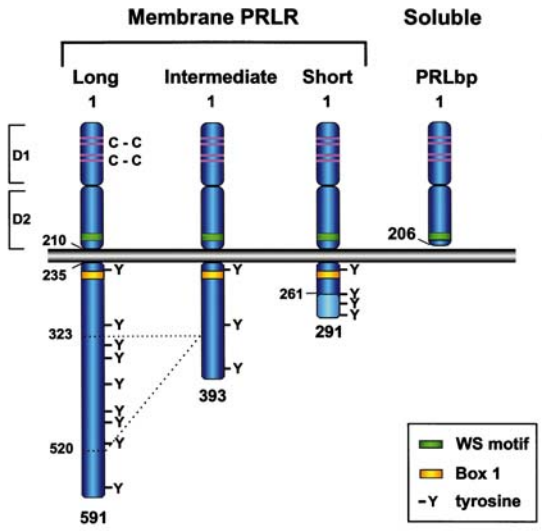

Figure 2. Schematic representation of PRLRs. PRLR; PRL receptor, PRLbp; and soluble PRL binding protein (Bole-Feysot et al. 1998).

The transmembrane domain, like other cytokine receptor that contains single transmembrane protein, is 24 amino acids long. The possible involvement of this region in the functional activity of the receptor is unknown (Bole-Feysot et al. 1998).

The cytoplasmic domain is the only region which distinguishes PRLR isoforms. It is devoid of any intrinsic enzymatic activity. Two regions named Box-1 and Box-2 are conserved (Bole-Feysot et al. 1998). Box-1 is a membrane-proximal region composed of eight amino acids highly enriched in prolines and hydrophilic residues. The second consensus region, Box-2, is less conserved than Box-1 and contains

hydrophilic, negative charged and positive charged residues. Although Box-1 is conserved in all PRL isoforms, Box-2 is absent in PRLR-S (Bole-Feysot et al. 1998).

B3. Activation of PRL receptor

Activation of PRLR is a multistep activation process. Step 1 involves PRL-induced sequential receptor dimerization (Figure 3) (Bole-Feysot et al. 1998). Each PRL molecule contains two binding sites. Interaction of PRLR binding site of PRL with the first PRLR is the prerequisite for the interaction of binding site 2 on the same PRL molecule with a second PRLR (Goffin et al. 1996; Bole-Feysot et al. 1998).

Dimerization of PRLR activates function of Janus kinase 2 (Jak2) (step 2). The membrane proximal region Box-1 of the intracellular domain of PRLR is constitutively associated with a tyrosine kinase termed Janus kinase 2 (Jak2) (Campbell et al. 1994; Freeman et al. 2000). Activation of Jak2 brings two Jak2 molecules close to each other (Ferrage et al. 1998).

Active Jak2 further phosphorylates tyrosine (Tyr) residues of the PRLR (step 3). Phosphotyrosine residues serve as the potential binding/docking sites for the adapter or transducer molecules containing SH2 domains (Freeman et al. 2000). Although phosphorylation of Jak2 occurs in all active PRLR isoforms, Tyr phosphorylation of the receptor itself does not occur upon activation of the PRLR-S, despite the presence of four Tyr residues in its intracellular domain (Goupille et al. 1997). After receptor activation, further activation of several intracellular signalings occurs to mediate PRL action in target cells.

B4. Different effects of short and long PRLR (–S and –L)

As described above, after activation, the phosphorylated Jak2 furthers phosphorylates at a specific Tyr residue in the C-terminus of PRLR. This mechanism occurs only with the PRLR-L isoform (Ali 2000). This isoform is the only PRLR form able to activate the Jak2/STAT5 pathway, which is essential for PRL-induced transcription of milk protein genes, differentiation of normal epithelial cells, and initiation and maintenance of lactation. In contrast to the long isoform, PRLR-S

isoform cannot mediate transcriptional activation of the β-casein gene promoter induced by PRL (Lesueur et al. 1991). Instead, this isoform exerts dominant-negative effects on PRL-induced activation of transcription by the PRLR-L isoform when coexpressed in transfected cells (Hu et al. 2001). Meng and coworkers suggested that PRLR-S isoform also inhibits the PRL induced-long isoform promoting mammary cell proliferation (Meng et al. 2004). Moreover, Qazi and coworkers reported that the PRLR-S isoform exerts inhibitory effect by forming heterodimer with the long isoform in the ligand-independent manner (Qazi et al. 2006). Therefore, it has been suggested that the inhibitory role of the PRLR-S isoform may have physiological significance because the expression of the long and short PRL isoforms of PRLR is regulated in a tissue-specific manner (Lesueur et al. 1991).

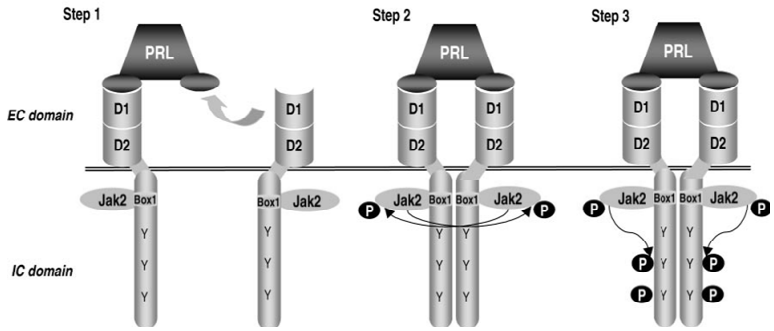

Figure 3. Schematic representation of PRLRs activation (Bole-Feysot et al. 1998).

B5. PRL signaling transduction

Like other peptide hormones, PRL modulates cellular function of its target cells via activating PRLR-associated specific intracellular signaling pathways. This PRL signaling activates specific enzyme or transcription of specific genes resulting in an alteration of cellular function of target cells. There are at least four PRL signaling pathways that have been identified, i.e., Jak2/STAT5, MAPK, PI-3 kinase, and PKC signaling pathways (Figure 4).

The signaling transducer and activator of transcription (STAT) protein family has been shown to be the major transducer of cytokine signaling (Ihle 1995). STAT proteins are 750-850 amino acid proteins that contain six structurally and functionally conserved domains (Paukku and Silvennoinen 2004). There are six members of STAT proteins including STAT1, 2, 3, 4, 5a, and 5b that have been identified in mammalian tissues (Paukku and Silvennoinen 2004). Except STAT2, all of STAT proteins have been identified as important transducer molecules of PRL (Liu et al. 1997; Goffin et al. 1998; Jabbour et al. 1998). When PRLRs are activated, the phosphorylated Tyr residues of activated PRLR interact with the SH2 domain of STAT proteins. Among STAT proteins, STAT5a and 5b are recognized as the most important transducers of PRLR-L and PRLR-I isoform (Liu et al. 1997).

Even though Jak/STAT signaling is the most important signaling pathway of PRL signaling transduction, several reports implicate activation of mitogen-activated protein (MAP) kinase cascade as well (Buckley et al. 1994; Das and Vonderhaar 1996). Phosphotyrosine residues of the activated PRLR can serve as docking sites for adaptor proteins (Shc/Grb2/SOS) connecting the receptor to the MAPK cascade (Avruch et al. 1994; Erwin et al. 1995; Das and Vonderhaar 1996). Intraperitoneal PRL administration to female rats caused a rapid stimulation of hepatic MAPK activity (Piccoletti et al. 1994). Several researchers demonstrated that MAPK pathway plays an important role in PRL-stimulated mitogenesis, proliferation, differentiation, and survival in PRL target cells, e.g., mammary cells (Acosta et al. 2003).

The phosphoinositide 3-kinase (PI3K) is considered a crucial signaling transducing element for several cytokine-activated biological processes (Hirsch et al. 2007). There are three classes of PI3K signaling, classes I, II, and III that have been identified on the basis of the levels of homology of their relevant catalytic subunit. The class I PI3K is further subdivided into IA and IB depending on the distinct regulatory subunit (Hawkins et al. 2006). While class IA PI3Ks are heterodimers of one p50-55 or p85 regulatory subunits and one of three possible catalytic subunits (p110α, p110β, or p110δ) that mediate intracellular signal of tyrosine and non-tyrosine receptor kinase. The class IB PI3Ks are heterodimers of either a p101 or p84 regulatory subunit and a catalytic subunit that mediate intracellular signal of G-protein-coupled receptor (Hawkins et al. 2006). The class IA PI3K is an important

signaling pathway of PRL-mediated cellular response of the target cells (Kelly et al. 2001; Clevenger et al. 2003). The p85 regulatory subunit of PI3K became associated with PRLR after PRL treatment in human embryonic kidney 293, COS, and Chinese hamster ovary cells (Berlanga et al. 1997; Clevenger et al. 2003). Moreover p85 regulatory subunit also acts as downstream element of STAT5, the major adaptor element of PRLR (Constantino et al. 2001). Therefore PRL induces rapid phosphorylation of p85 regulatory subunit (Berlanga et al. 1997), resulting in activation of p110 catalytic subunit of PI3K that further activates downstream Akt/PKB (Krumenacker et al. 2001). Amaral and coworkers demonstrated that PRL increases the islet cell mass and its sensitivity to glucose during pregnancy by activating PI3K/Akt signaling pathway (Amaral et al. 2004). The PI3K inhibitor LY294002 totally abolishes PRL-induced Akt/PKB activation, cell mobility, and cell proliferation (Acosta et al. 2003).

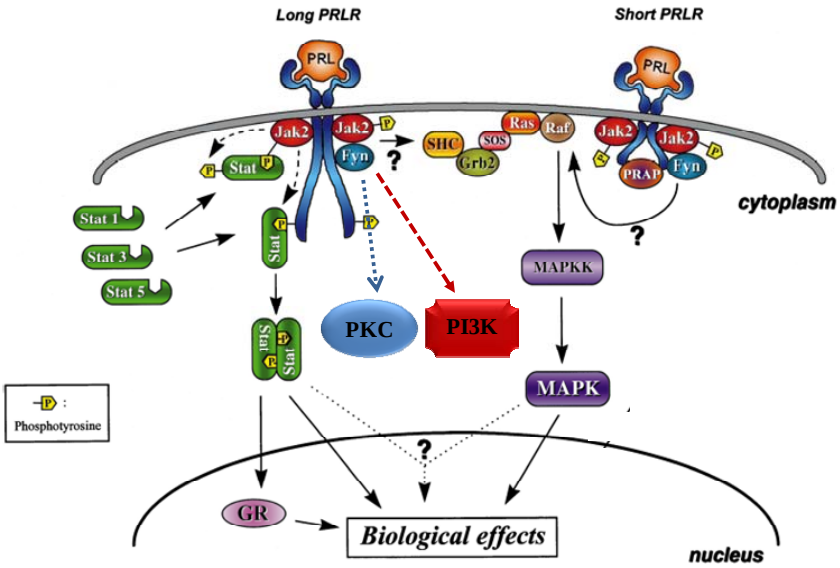

Figure 4. Schematic representation of the PRLR signaling pathway. (Bole-Feysot et al. 1998).

In addition to Jak2/STAT5, MAPK and PI3K, PKC signaling is also considered as one of the PRL signaling transductions. There are at least 10 PKC isoforms that are

divided into 3 groups (conventional PKC, novel PKC, and atypical PKC) depending on their primary structure (Newton 2003; Barnett et al. 2007). While the conventional (α, βI, βII, γ) PKCs are activated by both diacylglycerol (DAG) and Ca^{2+}, the novel (δ, ε, η, θ) PKCs respond only to DAG (Newton 2003). Neither DAG nor Ca^{2+} can activate the atypical (ζ, ι and λ) PKCs (Newton 2003). PRLR activation promotes acute activation of PKC δ in rat luteinized glanulosa cells (Peters et al. 1999). PRL directly activates the activity of PKC in porcine adrenocortical cultured (Kaminska et al. 2002) cells and in cultured islet cells (Tian and Laychock 2003). The PKC inhibitor totally abolishes PRL-induced catecholamine synthesis in hypothalamic cultured cells (Ma et al. 2005). PRL also activates PKC activity to stimulate the proliferation of female rat cholangiocyte cultured cells (Taffetani et al. 2007). Moreover, PRL acted through PKC to enhance nitric oxide synthase activity in rat mammary epithelial cells (Bolander Jr. 2002).

B6. PRL enhances intestinal calcium transport

Since it was clearly proved that vitamin D_3 was not involved in the enhancement of intestinal calcium transport during pregnancy and lactation in mammals (Halloran and DeLuca 1980; Pahuja and DeLuca 1981), PRL became the hormone of interest because its plasma level increases during pregnancy and lactation (Jacobs et al. 1972) and it regulates electrolyte balance (Freeman et al. 2000). Boass and Lovdal (Boass and Lovdal 1992) clearly showed that elevated duodenal calcium absorption during pregnancy and lactation correlated with the change in serum PRL level. It was our group that demonstrated the direct action of PRL in the enhancement of the intestinal calcium transport, independently of vitamin-D_3 activity (Wangdee et al. 1991). Using Ussing chamber technique, duodenum directly exposed to PRL, increased the transcellular active calcium transport in a dose-dependent manner (Charoenphandhu et al. 2001). Tanrattana and coworkers (Tanrattana et al. 2004) further demonstrated that PRL markedly enhanced the solvent drag-induced active calcium transport in the duodenum of female rats. These two studies clearly showed the important role of PRL on the enhancement of active calcium transport, both transcellular and solvent drag-induced active calcium transport components,

independently of other calcium regulating factors. The underlying mechanism of the direct action of PRL can be explained partly by the enhancement of the PMCA and Na^+/K^+ ATPase activities by PRL (Charoenphandhu et al. 2006). Up till now, PRL is considered a calcium-regulating hormone in non-pregnant, as well as pregnant, and lactating rats (Charoenphandhu and Krishnamra 2007).

C. PARACELLULAR BARRIER TIGHT JUNCTION (TJ)

Polarized epithelial cells function, in part, to provide a permeability barrier between two very different environments and to enable vectorial transport across the cellular layer. The junctional complex, between two epithelial cells, includes several well defined structures such as gap junctions, desmosomes, adherens junction, and TJ (Denker and Nigam 1998). TJs are the most apical domain that serves as the major paracellular barrier.

C1. Proteins of TJ

TJ proteins include transmembrane proteins (occludin, junctional adhesion molecule (JAM), and claudins) (Fannings et al. 1999; Balda and Matter 2000) and cytoplasmic plaque proteins (zonula occludens (ZO), cingulin and 7H6) (Citi et al. 1988; Haskins et al. 1998; Gonzalez-Mariscal et al. 2000).

Occludin is a 65 kDa transmembrane phosphorprotein (Anderson and Van Itallie 1995; Fujimoto 1995) composed of four transmembrane domains, two extracellular loops, N-terminal cytosolic domain, and a large C-terminal cytosolic domain (Schneeberger and Lynch 2004).

Claudin is a 22-27 kDa transmembrane protein of TJ (Furuse et al. 1998) composed of four transmembrane-spanning domains, two extracellular and one intercellular loop, and N- and C-terminal cytoplasmic domain (Furuse et al. 1998). The C-terminus of claudin has PDZ-binding motif that binds to PDZ domain containing proteins, such as ZO-1, ZO-2, ZO-3, and MUPP-1 (Multi-PDZ protein) (Itoh et al. 1999; Hamazaki et al. 2002). Up till now, at least 24 members of the claudin family have been identified (Colegio et al. 2003). In contrast to occludins, the

individual claudins are generally expressed in only a restrict number of specific cell types, suggesting that they are associated with tissue specific function of TJ (Furuse and Tsukita 2006).

ZO-1, ZO-2, and ZO-3 belong to a family of membrane-associated guanylate kinase (MAGUK) homologues (Gonzalez-Mariscal et al. 2000). These proteins play an important role in signal transduction of synapse, ion channel, and TJ (Fannings and Anderson 1999).

C2. Regulation of paracellular permeability by TJ

TJ is the major barrier of paracellular transport in epithelial tissues. Although occludin was identified as the first transmembrane protein of TJ, the role of occludin on TJ function remains unclear. Saitou and coworkers demonstrated that occludin-deficient embryonic stem cells differentiate in to epithelial cells with well-developed TJ formed between adjacent epithelial cells (Saitou et al. 1998). This study indicates that occludin is not necessary for TJ formation. On the other hand, injection of cDNA for claudin-1 or -2 but not occludin, into TJ deficient-fibroblasts resulted in the formation of TJ strands (Furuse et al. 1998). These results suggested that claudins are necessary for TJ formation.

Normally TJ can regulate the paracellular barrier by modulating both size and charge selectivity which is regulated by changes in the expression pattern of claudin proteins (Van Itallie and Anderson 2006).

For size selectivity, Nitta and coworkers showed possibility of claudins creating variable pore sizes by studying the vascular permeability in mice in which the claudin-5 gene was deleted. Normally, endothelial cells express mainly claudin-5 and -12. Deletion of claudin-5 resulted in an increase in the size of paracellular tracers allowed to exit from the vascular space into the brain (Salas and Moreno 1982). McLaughlin and coworkers in 2004 clearly showed that ochratoxin A suppressed the expression of claudin-3 and -4, resulting in increaseed paracellular permeability of 4- and 70-kDa FITC dextrans in Caco-2 monolayers (McLaughlin et al. 2004).

Claudin proteins also determine the paracellular charge selectivity of the epithelia (Van Itallie and Anderson 2004; Furuse and Tsukita 2006). For example, in the

claudin system, MDCK cell line is cation selective, whereas the LLC-PK1 cell line is anion selective. While expressions of claudin-4, -5, -8, and -14 decrease cation permeability of MDCK cells (Van Itallie et al. 2001; Ben-Yosef et al. 2003; Yu et al. 2003; Wen et al. 2004), expression of claudin-2 increases cation permeability in these cells (Yu et al. 2003). Expressions of claudin-2, -7, and -15 decrease anion permeability in LLC-PK1 cells (Amasheh et al. 2002; Van Itallie et al. 2003). It is now proved that it is the first extracellular domain of claudin that determines the charge selectivity of the epithelia (Colegio et al. 2003). Since different tissues express different patterns of claudin proteins that lead to different charge selectivities, therefore, the specific pattern of claudin protein expression in each tissue is another major determinant of TJ ion selectivity (Furuse and Tsukita 2006).

D. EPITHELIAL-LIKE CULTURED CACO-2 MONOLAYER

Caco-2 cells are a human colorectal adenocarcinoma cell line (Fogh et al. 1977). In the culturing system, they spontaneously differentiate structurally and functionally into enterocyte-like cells that become polarized columnar epithelium with brush border microvilli, tight intercellular junctions, villin expression, and dome formation (Pinto et al. 1983; Chantret et al. 1988; Hidalgo et al. 1989). When growing on the semipermeable filters, they organize themselves into a polarized monolayer (Le Bevic et al. 1990). Moreover, Caco-2 cells highly express the brush-border membrane enzyme markers of small intestine including sucrase, isomaltase, lactase, alkaline phosphatase, γ-glutamyltransferase, aminopeptidase N, N-acetyltransferase, and dipeptidyl-dipeptidase IV (Chantret et al. 1988; Jamarie and Malo 1991; Yoshioka et al. 1991). After reaching confluence in culture flasks, colon-specific proteins of these cells gradually decline as those reflective of enterocytes markedly increase (Engle et al. 1998). This property renders the Caco-2 cells suitable for studying intestinal transport and permeability. Artursson and Karlson demonstrated a good relationship between the in vivo permeability of a series of drugs to their in vivo bioavailability (Artursson and Karlsson 1991). Comparing transport between Caco-2 cells and in vivo human jejunum, Lennernas and coworkers demonstrated that permeabilities of Caco-2 and jejunum are comparable (Lennernas et al. 1996). Yee demonstrated the strong

correlation between in vivo human intestinal absorption and in vitro Caco-2 monolayer permeability for a variety of compounds (Yee 1997). Thus Caco-2 monolayers are a suitable epithelial model for studying calcium transport in vitro.

D1. Calcium transport in Caco-2 cells

The calcium transport across Caco-2 monolayer was first studied by Giuladino and Wood in 1991 (Giuliano and Wood 1991). By growing Caco-2 cells on permeable filter supports, they found that $1,25(OH)_2D_3$ significantly increased transepithelial calcium transport. After that several researchers used Caco-2 intestinal epithelial model for studying the transcellular and paracellular calcium transport.

Blais and coworkers (Blais et al. 1997) compared paracellular calcium transport across Caco-2 monolayers and HT29 cell monolayer, by growing the cells on permeable filter with the high density of 5×10^5 cells per filter for 15 days to allow the monolayers to express enterocytic differentiation and high epithelial resistance. They reported that Caco-2 cell monolayer is more suitable for studying the paracellular calcium transport pathway (Blais et al. 1997). One year later, Chirayath and coworkers (Chirayath et al. 1998), using 14 days after confluent Caco-2 monolayers, studied the effect of vitamin-D_3 on paracellular calcium transport and showed that vitamin-D_3 increases TJ permeability resulting in increased paracellular calcium transport (Chirayath et al. 1998). Non-digestible disaccharides and conjugated linoleic acids markedly decrease transepithelial electrical resistance and increase paracellular calcium transport in Caco-2 monolayer (Suzuki and Hara 2004; Jewell et al. 2005), possibly by actin rearrangement (Suzuki and Hara 2006).

Fleet and Wood (Fleet and Wood 1999) was the first to demonstrate the transcellular calcium transport across Caco-2 monolayer. They showed that $1,25(OH)_2D_3$ markedly increased transcellular calcium transport. This $1,25(OH)_2D_3$ effect was totally suppressed by calmodulin antagonist, trifluoperazine, which is now used as a transcellular calcium transport inhibitor (Fleet and Wood 1999). Caco-2 cells express all proteins that are involved in transcellular calcium transport including TRPV6, calbindin-D_{9k}, and PMCA (Fleet et al. 2002). Similar to the small intestine, $1,25(OH)_2D_3$ upregulates all of these transcellular calcium transport marker proteins

(Wood et al. 2001; Fleet et al. 2002; Taparia et al. 2006). Besides $1,25(OH)_2D_3$, conjugated linoleic acid also enhances transcellular calcium transport in Caco-2 monolayer by unknown mechanism (Jewell et al. 2005; Murphy et al. 2006)

D2. TJ in Caco-2 Cells

Caco-2 monolayers also express a number of TJ proteins such as occludin, claudin-1, -2, -3, -5, JAM, ZO-1, ZO-2, and ZO-3 (McLaughlin et al. 2004; Murphy et al. 2006). The paracellular route of Caco-2 epithelial monolayer has been estimated to be between 350 to 540 pm with a negatively charged electrostatic field, resulting in the paracellular route showing preferential permeability to cation (Carr et al. 2006). Marano and coworkers (1998), performing the dilution potential technique, reported that Caco-2 epithelial monolayers are the cation selective monolayer. Tumor necrosis factor-α (TNF-α) increases the paracellular permeability and cation selectivity in Caco-2 monolayers (Marano et al. 1998). TNF action is mediated by NF-κB p50/p65 binding and activation of the myosin light chain kinase (MLCK) promoter. NF-κB p50/p65 activation of the MLCK promoter then sequentially leads to the increase in MLCK transcription, expression and activity, and MLCK-mediated opening of the Caco-2 epithelial TJ permeability (Ye et al. 2006). In addition to the charge selectivity, the Caco-2 epithelial monolayer also shows size selectivity. Ochrotaxin A, a small organic toxin that is produced by many common fungal molds, significantly increases the size selectivity of Caco-2 monolyer (McLaughlin et al. 2004). Ochrotoxin A is able to modulate the barrier function of Caco-2 monolayer by suppressing the expression of claudin-3 and -4 (McLaughlin et al. 2004).

CHAPTER III
MATERIALS AND METHODS

A. CELL CULTURE

A1. Maintenance

Caco-2 cells (ATCC® Number: HTB-37), a kind gift from the Institute of Nutrition, Mahidol University, Thailand, were grown in Dulbecco's modified Eagle's medium (DMEM; Sigma, St. Louis, MO, USA) supplemented with 15% heat-inactivated fetal bovine serum (FBS) (GIBCO, Grand Island, NY, USA), 1% nonessential amino acid (Sigma, St. Louis, MO, USA), and 1% penicillin-streptomycin (GIBCO, Grand Island, NY, USA). Cells were maintained in 75-cm^2 T−flask (Corning, Corning, NY, USA) under a humidified atmosphere containing 5% CO_2 at 37° C and subcultured as described in the ATCC protocol.

A2. Experiments

For indirect immunofluorescent staining, Caco-2 cells were plated at density of 1×10^4 cells/cm^2 on a coverslips placed in 6−well culture discs (Corning, Corning, NY, USA). Cells were incubated at 37° C for two days in a humidified atmosphere containing 5% CO_2.

For the calcium transport study, confluent Caco-2 monolayers were prepared by seeding cells at the high density of 5×10^5 cells/cm^2 onto a polyester Snapewell (Snapwell™ inserts, 12 mm diameter, 0.4 μm pore size, Corning, Corning, NY, USA). Culture media was changed daily after 48 h of seeding. Monolayers were incubated at 37° C for 14 days in a humidified atmosphere containing 5% CO_2.

Table 2. Primers used for RT-PCR experiments

Name	Accession No.	Forward and Reverse Primers	Product length (bp)	Cycles
hPRLR-S	AF416619	5′-GGTGACCCCTTGATGTTG-3′	145	40
		5′-TTCTGGTATATGCTCTTCAGC-3′		
hPRLR-I	AF166329	5′-ACCCAAGTCAAGAGAGAGAAC-3′	159	40
		5′-GGCTGATTCTTCAAAGCA-3′		
hPRLR-L	NM_000949	5′-ACTTGCCTCTTTCTCCAG-3′	100	40
		5′-TCCCTCAAGAATACTAAGCAG-3′		
hPRLR-A	NM_000949	5′-CTGTCATCTGTTTGATTATTG-3′	233	40
		5′-CTGGTCCTCACTATCATCTAC-3′		
hGAPDH	NM_002046	5′-CTGGTAAAGTGGATATTGTTG-3′	359	21
		5′-GAGGCTGTTGTCATACTTCTC-3′		

hPRLR-S, short-form human (h)PRLR; hPRLR-I, intermediate-form hPRLR; hPRLR-L, long-form hPRLR; hPRLR-A, hPRLR primers matched to all studied isoforms; GAPDH, glyceraldehyde-3-phosphate dehydrogenase

B. REVERSE TRANSCRIPTASE-PCR

By using TRIzol extract reagent (Invitrogen, Carlsbad, CA, USA), total RNA was prepared from Caco-2 cells according to the manufacture's instruction. One microgram of the total RNA extract was reverse-transcribed with the oligo(dT_{15}) primer and iScript kit (Bio-Rad, Hercules, CA, USA) to cDNA by using a thermal cycler (model Mycycle, Bio-Rad, Hercules, CA, USA). Human glyceraldehyde-3-phosphate dehydrogenase (hGAPDH), a house keeping gene, served as an internal control gene during detection of mRNA expression to check the consistency of the reverse transcription. Sense and antisence primers of human PRLR and hGAPDH were designed by OLIGO6 (Molecular Biology Insight, Cascade, CO, USA) and Primer Validator 1.4 (Naratt software, Bangkok, Thailand) as shown in Table 2. The PCR products were visualized on 2% agarose gel stained with ethidium bromide under a UV transililuminator (Alpha Innotech, San Leandro, CA, USA).

C. CONFOCAL IMMUNOFLUORESCENT STAINING

Caco-2 cells were grown on a coverslip and cultured for 2 days. After removing the culture medium, the confluent cells were washed 3 times with standard phosphate buffer solution (PBS) and then fixed in 3% praraformaldehyde and 2% sucrose for 5 minutes at room temperature. Then cells were treated with 0.2 mM glycine for 5 min followed by the blocking solution (10% FBS and 0.1% tween-20 in PBS (PBST)) for 20 min at room temperature. After blocking the nonspecific binding, cells were incubated overnight at 4 °C with 1:200 rabbit anti-human PRLR antibody (Santa Cruz Biotechnology, Santa Cruz, CA, USA). They were then washed three times for 10 min each time in PBST, and then incubated with AlexaFluo 488-conjugated mouse anti-rabbit secondary antibody (green signal; Molecular Probes, Eugene, OR, USA) for 60 min at room temperature. Nuclei were stained with 1:1000 TO-PRO-3 (red signal; Molecular Probes, Eugene, OR, USA). Negative control was obtained by incubating cells with secondary antibody in the absence of primary antibody. The fluorescent imaging was performed by confocal laser-scanning microscope (model FV1000; Olympus, Tokyo, Japan).

D. USSING CHAMBER EXPERIMENT

Figure 5 shows Ussing chamber, in which the Snapwell acted as a partition between the two halves of the chamber separating the bathing solution into apical and basolateral compartments. To maintain physiological condition, the temperature inside the Ussing chamber was maintained at 37° C, and each hemi-chamber was continuously gased with 95% O_2 and 5% CO_2 to maintain oxygenation and pH of 7.4. Voltage and current electrodes were inserted into the chamber to measure transepithelial potential different (PD) and short-circuit current (Isc), respectively. These two electrical parameters were used to calculate the transepithelial resistance (TER), according to Ohm's law.

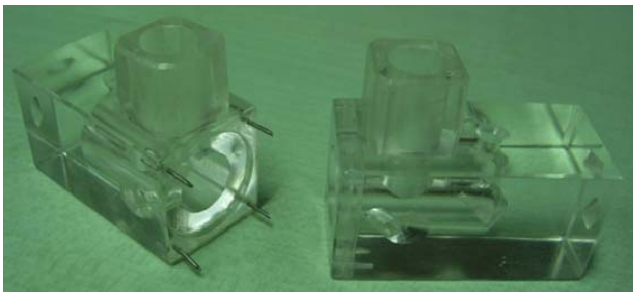

Figure 5. Modified Ussing chamber.

D1. Bathing solution

D1.1 Normal bathing solution

Normal bathing solution contained in mM: 118 NaCl, 4.7 KCl, 1.1 $MgCl_2$, 1.25 $CaCl_2$, 23 $NaHCO_3$, 12 D-glucose, 2.5 L-glutamine, and 2 mannitol. The solution, continuously gassed with humidified 5% CO_2 in 95% O_2, was maintained at 37 °C, pH of 7.4, and had an osmolality of 290-295 mmol kg^{-1} water. Osmolality of the solution was measured by freezing point-based osmometer (model 3320: Advance Instruments, Norwood, MA, USA).

D1.2 Bathing solution for passive calcium transport study

The bathing solution for passive calcium transport study was similar to the normal bathing solution but the $CaCl_2$ concentration on the apical side was 1.25, 2.5, 5, 10, 20, 40, or 80 mM.

D1.3 Bathing solution for dilution potential technique

Two types of bathing solution used in the dilution potential experiments contained 145 mM Na and 72.5 mM Na. While the composition of 145 mM Na-containing bathing solution was similar to that of normal bathing solution, the 72.5 mM Na-containing bathing solution differed from the normal bathing solution in that it contained 47.5 mM NaCl and 125 mM mannitol, the latter of which, was added to maintain normal osmolality.

D1.4 Bathing solution for cationic diffusion potential experiments

The bathing solution used in the cationic diffusion potential experiment contained either 100 mM Li, 50 mM Li, 100 mM Na, 50 mM, 100 mM, 50 mM K, 100 mM Rb, 50 mM, 100 mM Cs, or 50 mM Cs.

The compositions (in mM) of the 10 types of bathing solution were showed below.

100 mM Li-containing bathing solution: 100 LiCl, 10 HEPES/Tris pH 7.4, 4.7 KCl, 1.1 $MgCl_2$, 1.25 $CaCl_2$, 12 D-glucose, 2.5 L-glutamine, 13.991 $NaHCO_3$, 6.009 NaCl, and 17 mannitol.

50 mM Li-containing bathing solution: 50 LiCl, 10 HEPES/Tris pH 7.4, 4.7 KCl, 1.1 $MgCl_2$, 1.25 $CaCl_2$, 12 D-glucose, 2.5 L-glutamine, 13.991 $NaHCO_3$, 6.009 NaCl, and 112 mannitol.

100 mM Cs-containing bathing solution: 100 CsCl, 10 HEPES/Tris pH 7.4, 4.7 KCl, 1.1 $MgCl_2$, 1.25 $CaCl_2$, 12 D-glucose, 2.5 L-glutamine, 10 $NaHCO_3$, 10 NaCl, and 10 mannitol.

50 mM Cs-containing bathing solution: 50 CsCl, 10 HEPES/Tris pH 7.4, 4.7 KCl, 1.1 $MgCl_2$, 1.25 $CaCl_2$, 12 D-glucose, 2.5 L-glutamine, 10 $NaHCO_3$, 10 NaCl, and 100 mannitol.

100 mM Rb-containing bathing solution: 100 RbCl, 10 HEPES/Tris pH 7.4, 4.7 KCl, 1.1 $MgCl_2$, 1.25 $CaCl_2$, 12 D-glucose, 2.5 L-glutamine, 12.416 NaCl, 7.548 $NaHCO_3$, and 10 mannitol.

50 mM Rb-containing bathing solution: 50 RbCl, 10 HEPES/Tris pH 7.4, 4.7 KCl, 1.1 $MgCl_2$, 1.25 $CaCl_2$, 12 D-glucose, 2.5 L-glutamine, 12.416 NaCl, 7.548 $NaHCO_3$, and 100 mannitol.

100 mM Na-containing bathing solution: 100 NaCl, 10 HEPES/Tris pH 7.4, 4.7 KCl, 1.1 $MgCl_2$, 1.25 $CaCl_2$, 12 D-glucose, 2.5 L-glutamine, 10 NaCl, 10 $NaHCO_3$, and 13 mannitol.

50 mM Na-containing bathing solution: 50 NaCl, 10 HEPES/Tris pH 7.4, 4.7 KCl, 1.1 $MgCl_2$, 1.25 $CaCl_2$, 12 D-glucose, 2.5 L-glutamine, 10 NaCl, 10 $NaHCO_3$, and 108 mannitol.

100 mM K-containing bathing solution: 100 KCl, 10 HEPES/Tris pH 7.4, 1.1 $MgCl_2$, 1.25 $CaCl_2$, 12 D-glucose, 2.5 L-glutamine, 12.941 NaCl, 7.059 $NaHCO_3$, and 28 mannitol.

50 mM K-containing bathing solution: 50 KCl, 10 HEPES/Tris pH 7.4, 1.1 $MgCl_2$, 1.25 $CaCl_2$, 12 D-glucose, 2.5 L-glutamine, 12.941 NaCl, 7.059 $NaHCO_3$, and 114 mannitol.

All of these solutions contained extra 20 mM Na, from NaCl and $NaHCO_3$ to maintain pH.

D2. Electrical measurements

A pair of Ag/AgCl electrodes made of 3 M KCl per 4% agar was located near each surface of the tissue for measurement of the transepithelial potential difference (PD) (Figure 6). The other end of electrodes was connected to a pre-amplifier (model ECV-4000, World Precision Instrument, Sarasota, FL, USA).

Another pair of Ag/AgCl electrodes was placed at the end of each of the hemi-chamber to supply short-circuits current (Isc), which was measured by ECV-4000 current-generating unit.

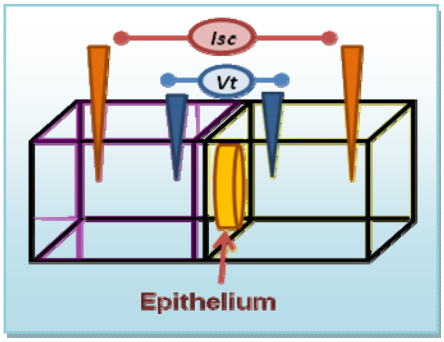

Figure 6. Diagram of electrical measurement in Ussing chamber system.

D3. Dilution potential experiment

This experiment was for studying the charge–selective property of Caco-2 monolayers. Permeability of sodium and chloride ions were measured by dilution potential technique, modified from the methods of Kahle et al. (Kahle et al. 2004) and Hou et al. (Hou et al. 2005). In brief, Caco-2 monolayers were equilibrated in normal bathing solution, which contained 145 mM NaCl, in modified Ussing chamber and electrical parameters were measured for 20 min. Thereafter, the basolateral solution was substituted with 72.5 mM NaCl-containng solution. Changes in PD and Isc were recorded every 0.36 s in 6 min (Figure 7).

The relative permeability ratio of sodium and chloride (P_{Na}/P_{Ca}) was calculated from the dilution potential (Vδ) using the simplified Goldman-Hodgkin-Katz equation (Charoenphandhu et al. 2006). The absolute epithelial permeability to sodium (P_{Na}) and chloride (P_{Ca}) was calculated from the relative permeability ratio using the simplified Kimizuka-Koketsu equation (Charoenphandhu et al. 2006).

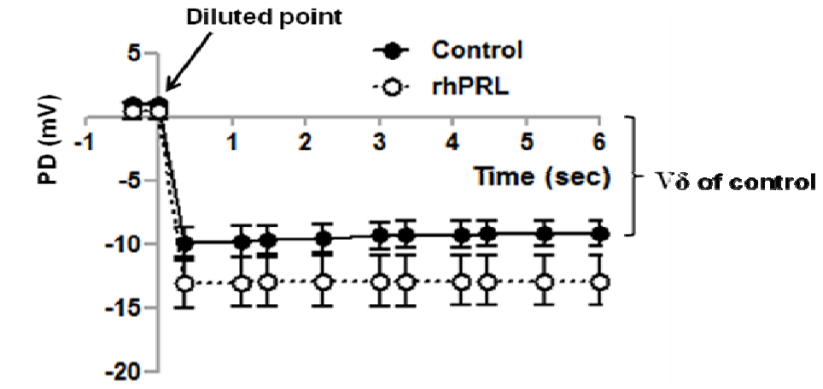

Figure 7. Changes in PD in the dilution potential experiment. Dilution point was the time point at which the basolateral bathing solution was substituted with 72.5 mM NaCl-containing solution. Vδ was the difference of PD, called dilution potential, after diluting the basolateral bathing solution with 72.5 mM NaCl-containing solution.

D4. Cationic diffusion potential experiment

The monovalent cation permeability of Caco-2 monolayers was measured by the cationic diffusion potential technique, modified from the methods of Hou et al. (Hou et al. 2005) and Carr et al. (Carr et al. 2006). Similar to the dilution potential technique, Caco-2 monolayers were equilibrated in normal bathing solution in modified Ussing chamber and electrical parameters were measured for 20 min. Thereafter, the apical bathing solution was substituted with 100 mM LiCl-, NaCl-, KCl-, RbCl-, or CsCl-containing solution, while the basolateral bathing solution was substituted with 50 mM LiCl-, NaCl-, KCl-, RbCl-, or CsCl-containing bathing solution. Changes in PD and Isc were recorded every 0.36 sec for 6 min. The relative permeability ratios of each ion to chloride, i.e., P_{Li}/P_{Cl}, P_{Na}/P_{Cl}, P_{K}/P_{Cl}, P_{Rb}/P_{Cl}, and P_{Cs}/P_{Cl} was calculated from the dilution potential (Vδ) using the simplified Goldman-Hodgkin-Katz equation.

D5. Calcium flux measurement

Calcium transport across Caco-2 monolyers was determined by the method of Charoenphandhu and coworkers (Charoenphandhu et al. 2006). The monolayer was

equilibrated in normal bathing solution for 20 min in modified Ussing chamber. Thereafter, one side of the chamber was replaced with fresh normal bathing solution (cold side), while the other was filled with ^{45}Ca-containing solution (initial amount of 5mCi/mL, final specific activity of ~450–500 mCi/mol; Amersham, Buckinghamshire, UK) (hot side). Seven samples were collected (Figure 8) to calculate the unidirectional flux ($J_{H\rightarrow C}$, in pmol·min^{-1}·cm^{-2}) from the hot side (H) to the cold side (C) with equations 1 and 2,

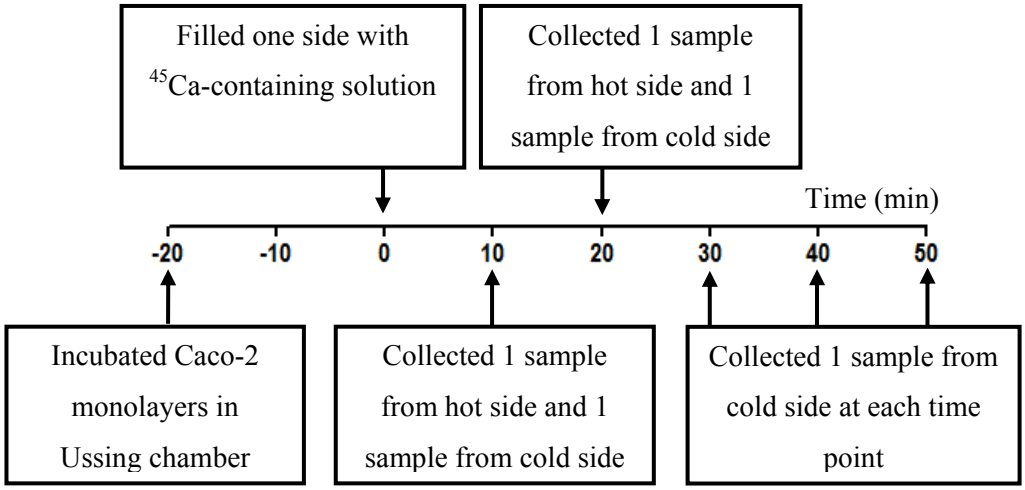

Figure 8. The experiment protocol involved collecting samples from Ussing chamber to study calcium flux.

$$J_{H\rightarrow C} = \frac{R_{H\rightarrow C}}{(S_H \times A)} \qquad (1)$$

$$S_H = \frac{Ca_{45_{Ca}}}{C_T} \qquad (2)$$

where $R_{H\rightarrow C}$ was the rate of tracer appearance in the cold side (in pmol·min^{-1}·cm^{-2}; CPM); S_H is the specific activity in the hot side (cmp/mol); A was the surface area of the Caco-2 monolayers (in cm^2); C_{45Ca} was the mean of radioactivity in the hot side (in counts/min); and C_T was the total calcium in the hot side (in nmol). The radioactivity

of ^{45}Ca was analyzed by liquid scintillation spectrophotometry (model 1219; LKB Wallac, Turku, Finland).

Calcium fluxes in the absence of calcium concentration gradient, i.e., bathing solution in both hemi-chambers contained equal calcium concentration of 1.25 mmol/L , represented the active calcium transport (Charoenphandhu et al. 2001). The calcium gradient-dependent paracellular passive fluxes were measured by determining the calcium fluxes in the presence of varying apical calcium concentrations, i.e., 1.25, 2.5, 5, 10, 20, 40, and 80 mmol/L with the fixed basolateral calcium concentration of 1.25 mmol/L. The calcium permeability (P_{Ca}) via passive paracellular pathway was calculated from equation 3 (Tang and Goodenough 2003)

$$P_{Ca} = \frac{J_{Ca}}{\Delta C} \qquad (3)$$

where J_{Ca} was the paracellular passive calcium flux; and ΔC was the difference between the apical and basolateral calcium concentrations.

D6. Dual ^{3}H-mannitol/^{14}C-polyethylene glycol (PEG) flux measurement

To demonstrate the effect of rhPRL on the size selectivity of Caco-2 monolayer transepithelial dual ^{3}H-mannitol/^{14}C-PEG fluxes, indicator of the widening of tight junction or size selectivity (Tanrattana et al. 2004), were determined. In this experiment, Caco-2 monolayer was bathed in the normal bathing solution containing 1 mmol/L mannitol and 1 mmol/L PEG. Paracellular markers, ^{3}H-mannitol (Amersham; MW 180; molecular radius ~350 pm) and ^{14}C-PEG (Amersham; MW 4000; molecular radius ~2.5 nm) were added in the bathing solution to obtain final specific activities of 750 and 500 mCi/mol, respectively. The sample collection and radioactive flux calculation were similar to the method of calcium flux measurement, as described above. Radioactivities of ^{3}H-mannitol and ^{14}C-PEG were analyzed by liquid scintillation spectrophotometer (model Tri-Carb 3100 TR; Perkin-Elmer, Shelton, CT, USA).

E. PRLR KNOCKDOWN

The oligonucleotides of short interference double-strand RNAs (siRNA) for the knockdown of the expression of human PRLR long isoform (hPRLR-L), with 5′-GGGCUAUAGCAUGGUGACCTT-3′ in the sense strand and 5′-GGUCACCAUGCUAUAGCCCTT-3′ in the antisense strand (siRNA ID 106337, RefSeq number NM_000949; Ambion, Austin, TX, USA) corresponding to nucleotides 1090 to 1109 relative to its start codon, were custom synthesized from Ambion. Twelve day confluence Caco-2 monolayers were used for in vitro siRNA transfection to suppress the expression of hPRLR-L. The in vitro transfection was done using the siPORT Amine transfection reagent (Silencer® siRNA Transfection II kit; Ambion) according to the manufacturer's instructions. The 1 nM siRNA and 4 μl siPORT Amine reagents were incubated in DMEM for 10 min prior addition to the 12 days Caco-2 monolayer to transfect the siRNA. Two days after transfection, the significant role of hPRLR-L on PRL-enhanced transepithelial calcium transport was determined by calcium flux experiment. The hPRLR-L knockdown study had been approved by the Insitutional Biosafety Committee (IBC) of the Faculty of Science, Mahidol University (Licensed to Charoenphandhu et al. 2007).

F. EXPERIMENTAL PROTOCOLS

F1. The experimental protocol of objective 1; To demonstrate the expression and localization of hPRLR in Caco-2 cells.

F1.1 hPRLR mRNA expression in Caco-2 cells

Caco-2 cells were grown in 75-cm^2 T–flask and were maintained to obtaint 80-90% confluency. After that cells were harvested and centrifuged at 1000 g to remove the culture media. The total RNA extraction, reverse transcription, and polymerase chain reaction were performed.

F1.2 hPRLR protein expression and localization in Caco-2 cells

Both expression and localization of PRLR protein in Caco-2 cells were observed by using indirect confocal immunocytochemisty staining technique.

F2. The experimented protocol of objective 2; To study the acute effect of PRL and its mechanism of acute action on the transepithelial calcium transport in Caco-2 monolayer.

F2.1 The acute effect of rhPRL on total active Ca^{2+} transport in Caco-2 monolayers

Caco-2 cells were grown on the Snapwell insert and maintained for 14 days to allow monolayer formation. After 14 days of confluency, Caco-2 monolayers were pre-incubated with 200, 400, 600, 800, or 1000 ng/mL rhPRL (purity > 97%; catalog no. 682-PL; R&D Systems, Minneapolis, MN, USA) in DMEM for 1 h prior to insertion into the modified Ussing chamber. Caco-2 monolayers were equilibrated in normal bathing solution, and electrical parameters were measured for 20 min. The calcium flux study was performed as described above. In this experiment, both apical-to-basolateral and basolateral-to-apical calcium fluxes were studied. The optimal effective dose of rhPRL that enhanced total active calcium transport was used in further experiments.

F2.2 The acute effect of rhPRL on the voltage-dependent active Ca^{2+} transport in Caco-2 monolayers

Caco-2 monolayers were pre-incubated with 600 ng/mL rhPRL (R&D Systems) (an optimal effective dose) in DMEM for 1 h prior to insertion into the modified Ussing chamber. Once inserted, Caco-2 monolayers were equilibrated in normal bathing solution and electrical parameters were measured for 20 min. The external feedback current (short circuit current) was continuously applied to the Ussing chamber system to nullify the PD. The calcium flux study was performed as

described above. This study could determine the significance of the voltage-dependent active calcium transport across Caco-2 monolayer.

F2.3 The acute effect of rhPRL on paracellular passive Ca^{2+} transport in Caco-2 monolayers

Caco-2 monolayers were pre-incubated with 600 ng/mL rhPRL (R&D Systems) (an optimal effective dose) in DMEM for 1 h prior to inserted into the modified Ussing chamber. Once inserted, Caco-2 monolayers were equilibrated in normal bathing solution and electrical parameters were measured for 20 min. The calcium gradient-dependent paracellular passive fluxes were measured by determining calcium fluxes in the presence of varying apical calcium concentrations, i.e., 1.25, 2.5, 5, 10, 20, 40, or 80 mmol/L with a fixed basolateral calcium concentration of 1.25 mmol/L. The calcium flux study was performed as described above.

F2.4 The mechanism of the acute action of rhPRL on paracellular passive Ca^{2+} transport in epithelial-like Caco-2 monolayers

F2.4.1 Calcium permeability

Caco-2 monolayers were pre-incubated with 600 ng/mL rhPRL (R&D Systems) (an optimal effective dose) in DMEM for 1 h prior to insertion into the modified Ussing chamber. The calcium gradient-dependent paracellular passive fluxes were measured by determining calcium fluxes in the presence of varying apical calcium concentrations, i.e., 1.25, 2.5, 5, 10, 20, 40, or 80 mmol/L with a fixed basolateral calcium concentration of 1.25 mmol/L. The P_{Ca} was determined from the paracellular passive calcium flux and the calcium gradient (apical calcium concentration – basolateral calcium concentration) calculated from equation 3.

F2.5 The mechanism of the acute action of rhPRL on paracellular passive tight junction properties in epithelial-like Caco-2 monolayers

F2.5.1 Charge selectivity

Caco-2 monolayers were pre-incubated with 600 ng/mL rhPRL (R&D Systems) in DMEM for 1 h prior to insertion into the modified Ussing chamber. In Ussing chamber set up, Caco-2 monolayers were equilibrated in normal bathing solution and electrical parameters were measured i.e. transepithelial potential (PD) and short-circuit current (Isc) for 20 min. Thereafter, the charge selectivity property of epithelial Caco-2 monolayers was determined by using dilution potential experiment. Moreover, the permeability of monovalent cations also determined using cationic diffusion potential technique.

F2.5.2 Size selectivity

Caco-2 monolayers were pre-incubated with 600 ng/mL rhPRL (R&D Systems) in DMEM for 1 h prior to insertion into the modified Ussing chamber. Caco-2 monolayers were equilibrated in normal bathing solution containing 1 mmol/L mannitol and 1 mmol/L PEG. Electrical parameters were measured for 20 min. Thereafter, the size-selective property of Caco-2 monolayers was determined by using dual ^{3}H-mannitol/^{14}C-PEG flux experiment.

F3. The experimented protocol of objective 3; To elucidate the signaling transduction pathway(s) of the acute PRL action in Caco-2 monolayer

F3.1 The signaling transduction pathway of the acute PRL action on the total active calcium transport

As shown in Figure 9, Caco-2 monolayers were pre-incubated with MEK inhibitor (10 μmol/L U0126; A.G. Scientific, San Diego, CA, USA), JAK2

inhibitor (50 µmol/L AG490; Calbiochem, San Diego, CA, USA), PI3K inhibitor (75 µmol/L LY294002 or 200 nmol/L wortmannin; Tocris Bioscience, Bristol, UK), PKC inhibitor (1 µmol/L GF-109203X, A.G. Scientific), or ROCK I/II inhibitor (1 µmol/L Y27632, Calbiochem, San Diego) in DMEM for 1 h (Figure 9). Thereafter, Caco-2 monolayers were treated with 600 ng/mL rhPRL and each inhibitor in DMEM for 1 h prior to insertion into the modified Ussing chamber. Once properly placed, Caco-2 monolayers were equilibrated in normal bathing solution. Electrical parameters were measured for 20 min. Thereafter, one side of the Ussing chamber was replaced with fresh normal bathing solution (cold side), while the other was filled with ^{45}Ca-containing solution (hot side). The calcium flux study was performed.

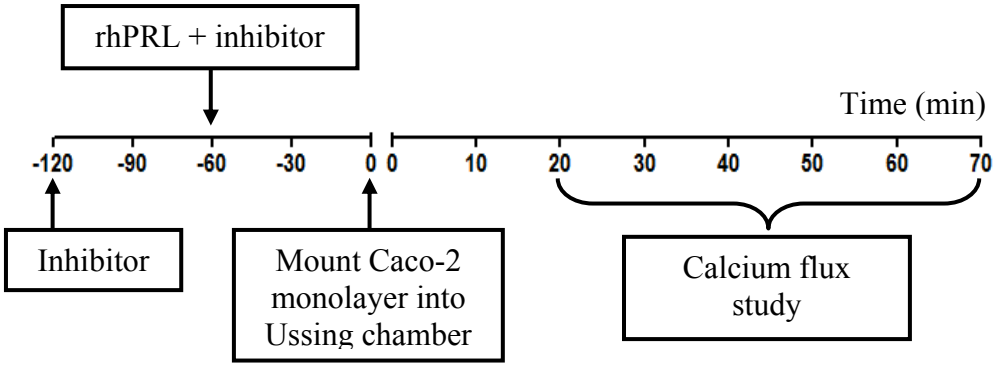

Figure 9. The experimental protocol for PRL signaling study.

F3.2 The non-genomic signaling transduction pathway of the acute PRL action on the total active calcium transport

Caco-2 monolayers were pre-incubated with RNA polymerase inhibitor (50 µM 5,6-dichlorobenzimidazole riboside (DRB); Calbiochem) in DMEM for 1 h. Thereafter, Caco-2 monolayers were treated with 600 ng/mL rhPRL and each inhibitor in DMEM for 1 h prior to insertion into the Ussing chamber. Therefore, Caco-2 monolayers were equilibrated in normal bathing solution. Electrical parameters were measured for 20 min. The calcium flux study was performed.

F3.3 The signaling transduction pathway of the acute PRL action on the paracellular passive calcium transport

Caco-2 monolayers were pre-incubated with MEK inhibitor (10 μmol/L U0126), JAK2 inhibitor (50 μmol/L AG490), PI3K inhibitor (75 μmol/L LY294002 or 200 nmol/L wortmannin), PKC inhibitor (1 μmol/L GF-109203X), or ROCK I/II inhibitor (1 μmol/L Y27632) in DMEM for 1 h (Figure 9). Caco-2 monolayers were treated with 600 ng/mL rhPRL and each inhibitor in DMEM for 1 h prior to insertion into the Ussing chamber. To determining the passive calcium fluxes, apical calcium concentrations were varied to 1.25, 2.5, 5, 10, 20, 40, or 80 mmol/L. The calcium flux study was performed as described above.

F3.4 The signaling transduction pathway of the acute PRL action on the calcium permeability

Caco-2 monolayers were pre-incubated with MEK inhibitor (10 μmol/L U0126), JAK2 inhibitor (50 μmol/L AG490), PI3K inhibitor (75 μmol/L LY294002 or 200 nmol/L wortmannin), PKC inhibitor (1 μmol/L GF-109203X), or ROCK I/II inhibitor (1 μmol/L Y27632) in DMEM for 1 h. Caco-2 monolayers were treated with 600 ng/mL rhPRL plus each inhibitor in DMEM for 1 h prior to insertion into the Ussing chamber. The calcium gradient-dependent paracellular passive fluxes were measured by determining the calcium fluxes in the presence of varying apical calcium concentrations, i.e., 1.25, 2.5, 5, 10, 20, 40, or 80 mmol/L with a fixed basolateral calcium concentration of 1.25 mmol/L. The P_{Ca} was determined from the paracellular passive calcium flux and the calcium gradient (apical calcium concentration – basolateral calcium concentration), using equation 3.

F3.5 The signaling transduction pathway of the acute PRL action on the charge selectivity

Caco-2 monolayers were pre-incubated with MEK inhibitor (10 μmol/L U0126), JAK2 inhibitor (50 μmol/L AG490), PI3K inhibitor (75 μmol/L

LY294002 or 200 nmol/L wortmannin), PKC inhibitor (1 μmol/L GF-109203X), or ROCK I/II inhibitor (1 μmol/L Y27632) in DMEM for 1 h. Caco-2 monolayers were treated with 600 ng/mL rhPRL plus each inhibitor in DMEM for 1 h prior to insertion into the modified Ussing chamber. Thereafter, the charge selectivity property of epithelial Caco-2 monolayers was performed by using dilution and cationic diffusion potential experiments.

F3.6 The significant role of hPRLR-L on PRL-enhanced total active calcium transport in Caco-2 monolayer

12 days confluent Caco-2 monolayers were used for in vitro siRNA transfection to suppress the expression of hPRLR-L. Two days after transfection, the transepithelial calcium transport was determined by the Ussing chamber technique.

G. STATISTICAL ANALYSES

Results were expressed as means ± SE. Two sets of data were compared using the unpaired Student's *t*-test. One-way ANOVA with Dunnett's multiple comparison test was used for multiple sets of data. Linear regression with slope analysis was performed to obtain the apical calcium concentration-calcium flux relationship in the paracellular passive calcium flux study. Nonlinear regression was performed to demonstrate Δcalcium-calcium permeability relationship in calcium permeability study (Charoenphandhu et al. 2006).

CHAPTER IV
RESULTS

A. To demonstrate the expression and localization of PRLR in Caco-2 cells.

The aim of this experiment was to demonstrate the expression and localization of PRLR mRNA and protein in Caco-2 cells by PCR and indirect confocal immunocytochemistry, respectively.

A1. The hPRLR mRNA expression in Caco-2 cells

The short, intermediate, and long isoforms of hPRLR mRNA were identified in Caco-2 cells (Figure 10). In addition to the 3 pairs of primer, each being matched to short, intermediate, or long isoform of hPRLR mRNA. Since all hPRLR mRNA came from the same gene by alternative splicing, another pair of primer was designed to match all of the hPRLR isoforms (All).

The results indicated that Caco-2 cells expressed all isoforms of hPRLR mRNA.

A2. The hPRLR protein expression in Caco-2 cells

The expression and localization of hPRLR were identified by the green signal of AlexaFluo 488-cojugated mouse anti-rabbit secondary antibody (Figure 11A). Nuclei were stained with TO-PRO-3 (red signal) (Figure 11B and 11E). The merge picture of hPRLR and nuclei showed that hPRLR were not present in the nuclei (Figure 11C). As shown in Figure 11C, immunofluorescence was seen as green dots and confined to the cytoplasm, with perinuclear accumulation. Such localization probably corresponded to the vesicles transporting pathway and to elements present in the juxtanuclear Golgi area (Parrot-Applanat et al. 1997).

Negative control was obtained by incubating cells with secondary antibody in the absence of primary antibody (Figure 11D-11F).

These results indicated that Caco-2 cells expressed hPRLR proteins and were a suitable epithelial model for studying the effect of PRL on transepithelial calcium transport.

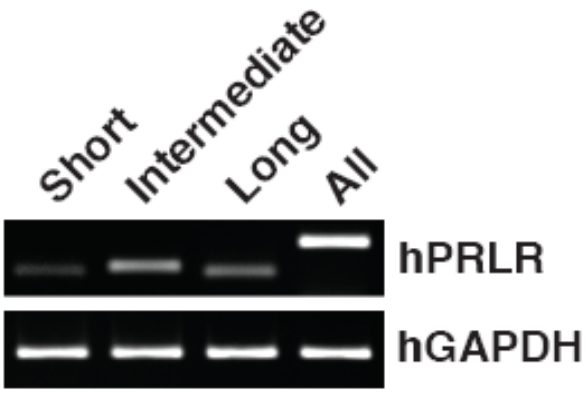

Figure 10. mRNA expressions of short (-S), intermediate (-I), and long (-L) isoforms of human (h)PRLRs in Caco-2 cells (n=5). hPRLR-A primers were used to identify mRNAs of all isoforms (All). hGAPDH was the housekeeping gene that was used as an internal control.

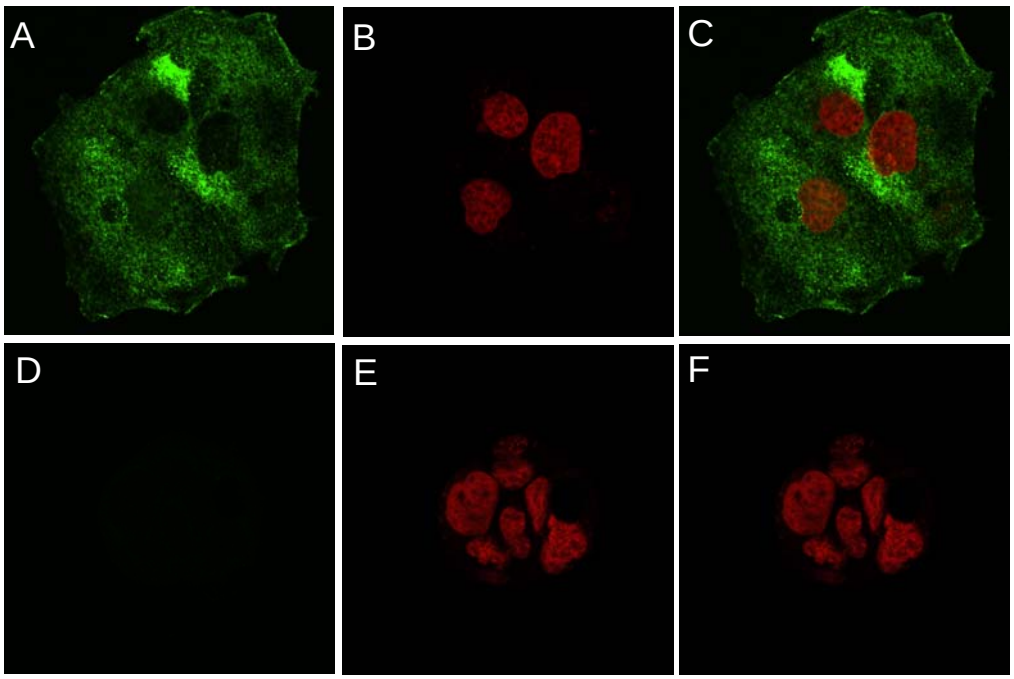

Figure 11. PRLR expression and localization in Caco-2 cells. Cells were treated with 11A or 11D without primary antibody of PRLR (green signal). Nuclei were stained with TO-PRO-3 (red signal) (11B and 11E). The merge picture of PRLR antibody-treated cells and controls were shown in Figure 11C and 11F, respectively. Negative control was obtained by incubating cells with secondary antibody in the absence of primary antibody (Figure 11D-11F).

B. To study the acute effect of rhPRL and its signaling transduction pathway in the acute regulation of the transepithelial calcium transport in Caco-2 monolayer.

B1. The acute effect of recombinant human prolactin (rhPRL) on the apical-to-basolateral total active calcium transport

The aim of this experiment was to study the acute effect of rhPRL on the total apical-to-basolateral active calcium transport across Caco-2 monolayer.

Caco-2 monolayers were pre-incubated with 200, 400, 600, 800, or 1000 ng/mL rhPRL in DMEM for 1 h prior to mounting in the modified Ussing chamber to study the does-dependent response of Caco-2 monolayers and to find the effective dose of rhPRL for further studies. The results indicated that 400 and 600 ng/mL rhPRL enhanced the total active calcium fluxes ($pmol \cdot min^{-1} \cdot cm^{-2}$) from a control value of 156.78 ± 9.66 (n = 8) to 223.15 ± 7.53 ($P < 0.001$) and to 299.66 ± 11.76 ($P < 0.001$), respectively (Figure 12). Higher rhPRL concentrations of 800 and 1,000 ng/mL were without effect, indicating a biphasic response (Figure 12). Moreover, the TER of Caco-2 monolayers was significantly decreased by 400 (291.19 ± 11.13 $\Omega.cm^2$) and 600 ng/mL rhPRL (253.13 ± 10.61 $\Omega.cm^2$) when compared to the control group (372.62 ± 17.66 $\Omega.cm^2$), while other electrical parameters were not changed (Table 3).

These results indicated that rhPRL directly stimulated the apical-to-basolateral active calcium flux in Caco-2 monolayers in a dose-dependent manner. The most effective dose of rhPRL, i.e. 600 ng/mL, was selected for further studies.

B2. The acute effect of rhPRL on the basolateral-to-apical total active calcium transport

The aim of this experiment was to study the acute effect of rhPRL on the basolateral-to-apical calcium transport across Caco-2 monolayer.

Similar to the apical-to-basolateral calcium flux study, Caco-2 monolayers were pre-incubated with 200, 400, 600, 800, or 1000 ng/mL rhPRL in DMEM for 1 h. The results showed no effect of rhPRL on the basolateral-to-apical calcium transport across

(Figure 13). However, 600 ng/mL rhPRL decreased TER but not other electrical parameters (Table 4).

Therefore, rhPRL enhanced the apical to basolateral calcium flux (calcium absorption), but not the basolateral-to-apical calcium flux (calcium secretion).

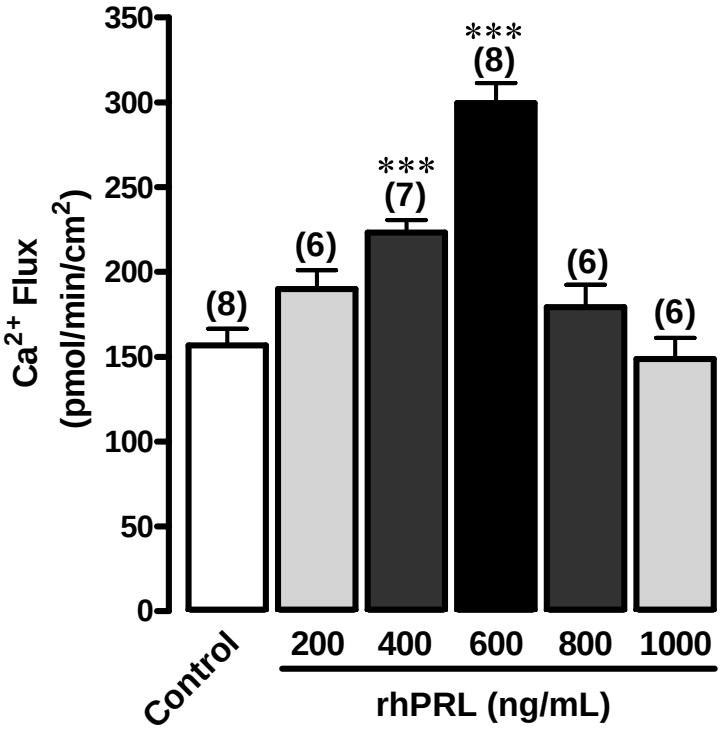

Figure 12. Total active calcium transport in Caco-2 monolayer in the apical-to-basolateral direction. The monolayers were incubated with culture media (control) or 200, 400, 600, 800 or 1000 ng/mL rhPRL-containing culture media 1 h before being inserted into the modified Ussing chamber. Total active calcium transport consists of voltage (PD)-dependent and transcellular active calcium transport. rhPRL, recombinant human PRL.

*** $P<0.001$ compared with control group

Table 3. Electrical parameters under an open-circuit condition of Caco-2 monolayers. The monolayers were incubated with culture media (control) or 200, 400, 600, 800 or 1000 ng/mL rhPRL-containing culture media 1 h before inserted into modified Ussing chamber. Values are means ± SE.

*** P<0.001 compared with control group

Groups	**Electrical parameters**			
	n	**PD (mv)**	**Isc (μA cm^{-2})**	**TER (Ω.cm^2)**
Control	8	0.93±0.2	2.63±0.68	372.62±17.66
rhPRL-treated (ng/mL)				
200	6	0.97±0.13	2.83±0.40	345.83±13.57
400	7	0.97±0.11	3.71±0.42	291.19±11.13***
600	8	0.96±0.11	3.75±0.45	253.13±10.61***
800	6	0.82±0.11	2.67±0.42	319.44±19.44
1000	6	0.88±0.16	2.50±0.50	362.50±12.50

rhPRL, recombinant human PRL; PD, transepithelial potential difference; Isc, short-circuit current; TER, transepithelial resistance.

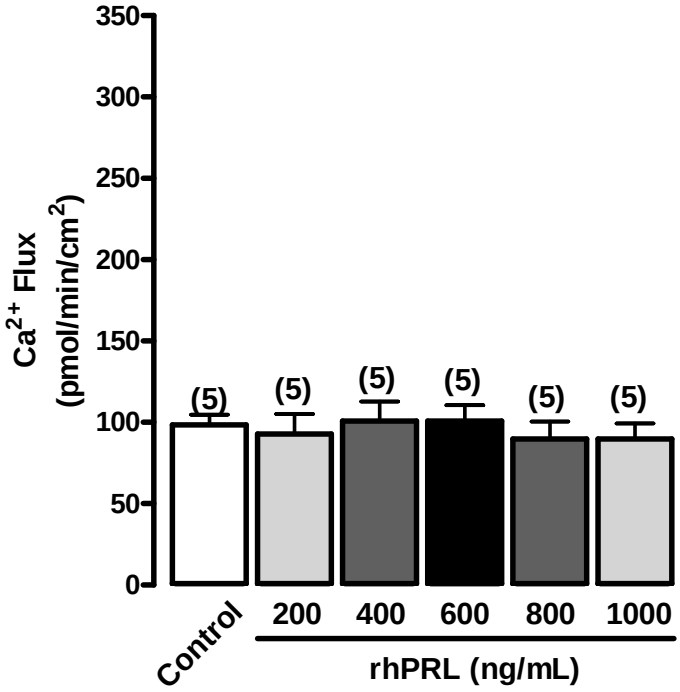

Figure 13. Total active calcium transport in Caco-2 monolayer in the basolateral-to-apical direction. The monolayers were incubated with culture media (control) or 200, 400, 600, 800 or 1000 ng/mL rhPRL-containing culture media 1 h before being inserted into the modified Ussing chamber. rhPRL, recombinant human PRL

Table 4. Electrical parameters of Caco-2 monolayers under an open-circuit condition. The monolayers were incubated with culture media (control) or 200, 400, 600, 800 or 1000 ng/mL rhPRL-containing culture media 1 h before being inserted into the modified Ussing chamber. Values are means ± SE.

***** P<0.05 compared with control group

Condition		**Electrical parameters**		
	n	**PD (mv)**	***Isc* (μA cm^{-2})**	**TER (Ω cm^2)**
Control	5	0.76±1.30	2.20±0.49	360.00±18.71
rhPRL-treated (ng/mL)				
200	5	1.06±0.09	3.00±0.32	356.67±16.33
400	5	0.92±0.08	3.20±0.49	301.33±29.09
600	5	0.82±0.12	3.20±0.49	258.00±11.91*
800	5	1.00±0.10	3.00±0.55	351.33±29.47
1000	5	0.82±0.11	2.20±0.20	370.00±33.91

rhPRL, recombinant human PRL; PD, transepithelial potential difference; Isc, short-circuit current; TER, transepithelial resistance.

B3. The acute effect of rhPRL on the voltage-dependent active calcium transport

The aim of this experiment was to study the acute effect of rhPRL on the voltage-dependent active calcium transport across Caco-2 monolayers.

The short circuit current was continuously applied to the system to nullify the PD. As depicted in Figure 14, the basal total active calcium transport (156.78 ± 9.66 $pmol \cdot min^{-1} \cdot cm^{-2}$) in the presence of PD (open circuit), was not different from that in the absence of PD (short circuit), i.e. 156.84 ± 11.66 $pmol \cdot min^{-1} \cdot cm^{-2}$. The stimulatory effect of rhPRL on the active calcium transport was not affected by the presence of PD, since rhPRL significantly increased the active calcium fluxes to the same level i.e. 299.66 ± 11.76 $pmol \cdot min^{-1} \cdot cm^{-2}$ in the presence of PD, and 292.31 ± 17.23 $pmol \cdot min^{-1} \cdot cm^{-2}$ in the absence of PD.

This result indicated that the PD had no effect on calcium transport, i.e., voltage-dependent active calcium transport was negligible in Caco-2 monolayer.

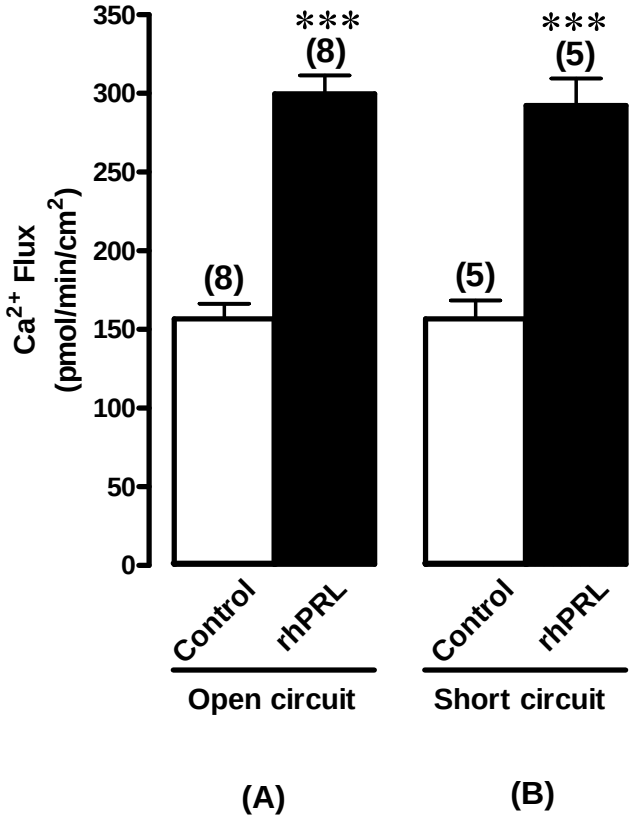

Figure 14. Total active calcium transport across the epithelial-like Caco-2 monolayer in the apical-to-basolateral direction. The monolayers were incubated in the culture medium (control) or 600 ng/mL rhPRL-containing culture medium 1 h before mounting in the modified Ussing chamber to study the calcium transport. The transepithelial potential difference (PD) was present in (A) and was absent in (B). rhPRL, recombinant human PRL.

*** $P<0.001$ compared with control group

B4. The PRL signaling transduction pathway mediating the rhPRL-enhanced total active calcium flux.

The aim of this experiment was to study the PRL signaling transduction pathway that mediated the acute rhPRL-enhanced total active calcium flux by pre-incubating with various inhibitors.

As shown in Figure 15, none of the inhibitors had effect on the basal total active calcium flux ($pmol \cdot min^{-1} \cdot cm^{-2}$) when added alone, calcium fluxes of PI3K inhibitor LY294002 (158.05 ± 13.48), another PI3K inhibitor wortmannin (151.99 ± 11.15), PKC inhibitor GF-109203X (164.89 ± 17.02), Jak2 inhibitor AG490 (177.01 ± 10.18), MEK inhibitor U0126 (177.26 ± 16.55), and ROCK I/II inhibitor Y27632 (150.37 ± 10.34)- treated group were not different from the respective control groups (156.78 ± 9.66). rhPRL at 600 ng/mL significantly increased the total active calcium flux to 299.66 ± 11.76 $pmol \cdot min^{-1} \cdot cm^{-2}$, $p < 0.001$. AG490 and U0126 had no effect on the rhPRL-enhanced total active calcium flux, because the calcium flux in AG490 + rhPRL (299.09 ± 21.91 $pmol \cdot min^{-1} \cdot cm^{-2}$) and U0126 + rhPRL (267.64 ± 20.57 $pmol \cdot min^{-1} \cdot cm^{-2}$)- treated groups were the same as that of the rhPRL-treated group (299.66 ± 11.76 $pmol/min/cm^2$). However, LY294002, wortmannin, GF-109203X, and Y27632 totally suppressed the stimulatory effect of rhPRL on total active calcium flux. Moreover, TER-reducing effect of rhPRL was also abolished by LY294002, wortmannin, and Y27632 (Table 5).

Therefore, rhPRL acted through PI3K, PKC, and Rho/ROCK signaling transduction pathways to enhance the total active calcium flux in Caco-2 monolayer.

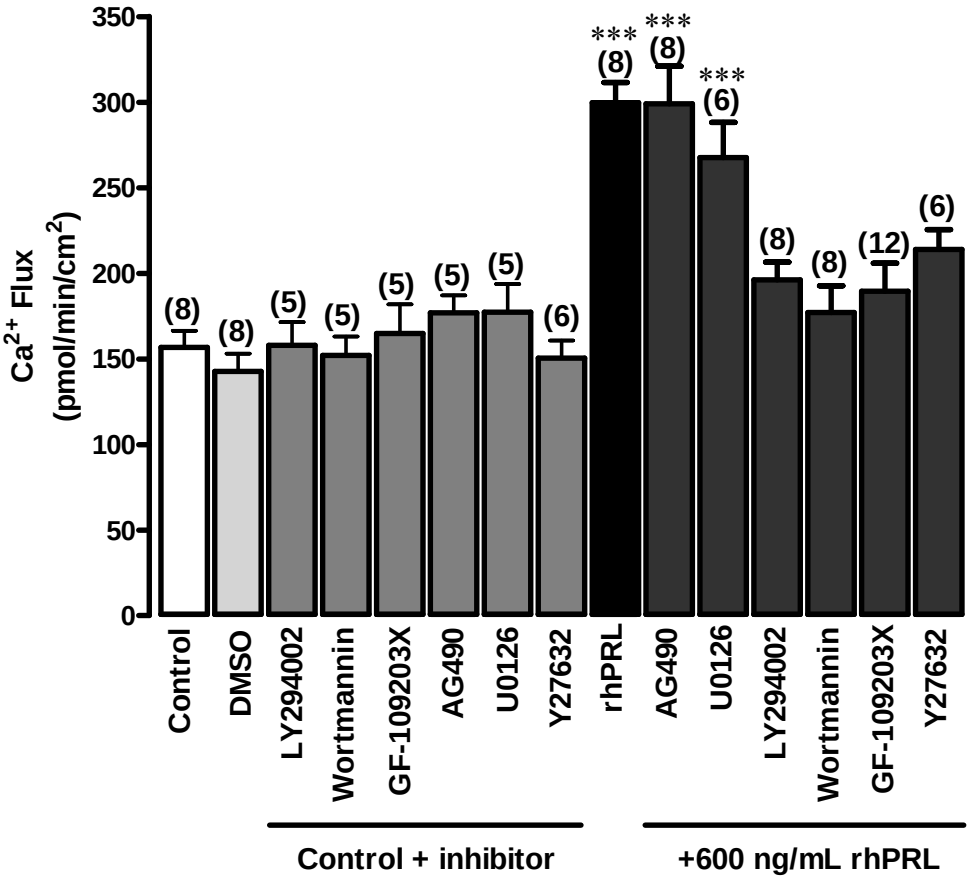

Figure 15. Total active calcium transport across the epithelial-like Caco-2 monolayer in the apical-to-basolateral direction. The monolayers were incubated in the culture medium (control), 0.3% v/v DMSO (vehicle for preparation of inhibitors), 10 µmol/L U0126 (MEK inhibitor), 50 µmol/L AG490 (JAK2 inhibitor), 75µmol/L LY294002 (PI3K inhibitor), 200 nmol/L wortmannin (PI3K inhibitor), 1 µmol/L GF-109203X (PKC inhibitor), or 5 µmol/L Y27632 (ROCK inhibitor)-containing culture medium 1 h before being added with or without 600 ng/mL rhPRL. rhPRL, recombinant human PRL.

*** $P<0.001$ compared with control group

Table 5 Electrical parameters under an open-circuit condition. The monolayers were incubated with culture medium (control), 0.3% v/v DMSO (vehicle for preparation of inhibitors), 10 μmol/L U0126 (MEK inhibitor), 50 μmol/L AG490 (JAK2 inhibitor), 75μmol/L LY294002 (PI3K inhibitor), 200 nmol/L wortmannin (PI3K inhibitor), 1 μmol/L GF-109203X (PKC inhibitor), or 5 μmol/L Y27632 (ROCK inhibitor)-containing culture media 1 h before adding 600 ng/mL rhPRL. Values are means±SE. rhPRL, recombinant human PRL.

* P<0.05 compared with control group

** P<0.01 compared with control group

Condition		**Electrical parameters**		
	n	**PD (mv)**	***Isc* (μA.cm^{-2})**	**TER (Ω.cm^2)**
Control	8	0.93±0.20	2.62±0.67	372.58±17.66
DMSO	8	1.00±0.15	2.50±0.38	383.33±10.45
AG490	5	0.86±0.17	2.40±0.40	356.67±27.69
U0126	5	0.92±0.32	2.40±0.75	376.67±32.32
GF-109203X	5	0.82±0.34	2.20±0.80	340.00±40.00
LY294002	5	1.04±0.19	2.80±0.49	375.00±19.36
wortmannin	5	0.88±0.22	2.40±0.60	366.67±27.89
Y27632	6	0.55±0.13	2.00±0.52	373.33±1829
600 ng/mL rhPRL	8	0.96±0.09	3.75±0.45	253.09±10.61**
600 ng/mL rhPRL+				
AG490	8	0.75±0.10	3.00±0.46	262.30±18.80**
U0126	6	1.03±0.23	3.67±0.49	269.45±22.94*
GF-109203X	6	0.72±0.28	3.00±1.13	247.17±18.47**
LY294002	8	0.96±0.10	3.25±0.37	302.92±18.53
wortmannin	8	1.04±0.13	3.00±0.38	355.42±25.15
Y27632	6	0.88±0.17	2.50±0.43	348.33±15.20

B5. The rhPRL acted through the non-genomic signaling pathway to enhance total active calcium flux.

The aim of this experiment was to demonstrate that rhPRL acted through the non-genomic signaling pathway to enhance total active calcium flux.

In this experiment Caco-2 monolayers were pre-incubated with RNA polymerase II inhibitor (5,6-dichlorobenzimidazole riboside, DRB) for 1 h, and later, incubated with 600 ng/mL rhPRL for 1 h. The basal total active calcium transport ($pmol \cdot min^{-1} \cdot cm^{-2}$) in DRB-treated group (135.10 ± 9.17) was not different from that of control group (156.78 ± 9.66) (Figure 16). This inhibitor had no effect on rhPRL-enhanced total active calcium flux since the calcium flux in rhPRL + DRB group (309.71 ± 43.66) was not statistically different from that of the rhPRL-treated group (299.66 ± 11.76). The TER of Caco-2 monolayer was decreased by rhPRL + DRB and rhPRL to 264.39 ± 13.06 $\Omega.cm^2$ ($p < 0.001$) and 253.13 ± 10.61 $\Omega.cm^2$ ($p < 0.001$), respectively (Table 6).

These results demonstrated that rhPRL acted through a non-genomic signaling pathways to enhance the total active calcium flux in Caco-2 monolayer.

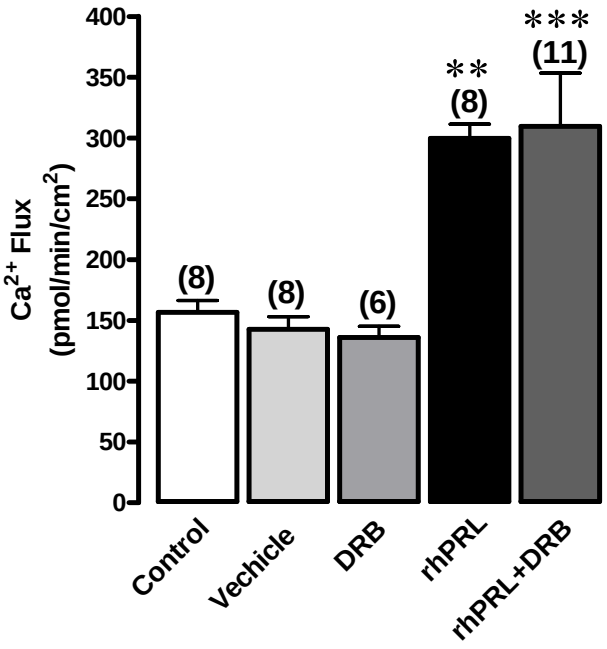

Figure 16. Total active calcium transport across the epithelial-like Caco-2 monolayer in the apical to basolateral direction. The monolayers were incubated in the culture medium (control), 0.3% v/v DMSO, or 50 μM DRB (RNA polymerase inhibitor)-containing culture medium 1 h before being added with or without 600 ng/mL rhPRL. rhPRL, recombinant human PRL.

** $P<0.01$ compared with control group

*** $P<0.001$ compared with control group

Table 6. Electrical parameters under an open-circuit condition. The monolayers were incubated with culture medium (control), 0.3% v/v DMSO (vehicle for preparation of inhibitor), or 50 μmol/L DRB (RNA polymerase inhibitor)-containing culture medium 1 h before being added with or without 600 ng/mL rhPRL. Values are means±SE. rhPRL, recombinant human PRL.

*** P<0.001 compared with control group

Condition		Electrical parameters		
	n	PD (mv)	*Isc* (μA.cm^{-2})	TER (Ω.cm^2)
Control	8	0.93±0.20	2.62±0.67	372.70±17.66
DMSO	8	1.00±0.15	2.50±0.38	383.33±10.45
DRB	6	0.97±0.13	2.50±0.34	382.50± 26.89
600 ng/mL rhPRL	8	0.96±0.09	3.75±0.45	253.13±10.61***
600 ng/mL rhPRL+DRB	11	0.95±0.92	3.64±0.34	264.40±13.06***

B6. The acute effect and signaling transduction pathway of rhPRL on the enhancement of paracellular passive calcium transport.

The aim of this experiment was to demonstrate both the acute effect and signaling transduction pathway of rhPRL on the passive calcium flux.

The calcium gradient-dependent paracellular passive fluxes were determined by measuring calcium fluxes in the presence of varying apical calcium concentrations, i.e., 1.25, 2.5, 5, 10, 20, 40, and 80 mmol/L with a fixed basolateral calcium concentration of 1.25 mmol/L. Caco-2 monolayers were also pre-incubated with various inhibitors prior to incubation with rhPRL. Apical calcium concentrations from 1.25 to 80 mmol/L increased the paracellular passive calcium fluxes in a linear manner, i.e., control group [$y = (3.76 \pm 0.13)x + (0.92 \pm 4.45)$, $r^2 = 0.96$], as well as in rhPRL-treated group [$y = (6.41 \pm 0.24)x + (4.51 \pm 8.36)$, $r^2 = 0.96$] (Figure 17A). At each apical calcium concentration, calcium flux in the rhPRL-treated group was significantly greater than that of the control group ($p < 0.05$). Moreover, the slope of the regression line was increased from 3.76 ± 0.13 in control group to $6.41 \pm 0.24 \times 10^{-3}$ cm/h in rhPRL-treated group ($p < 0.001$). Figures 17B and 17D show that LY294002 and Y27632 completely abolished the rhPRL-enhanced passive calcium flux, while GF-109203X had no effect (Figure 17C).

These results demonstrated that rhPRL acted through PI3K and Rho/ROCK signaling pathways to enhance the paracellular passive calcium flux in Caco-2 monolayers.

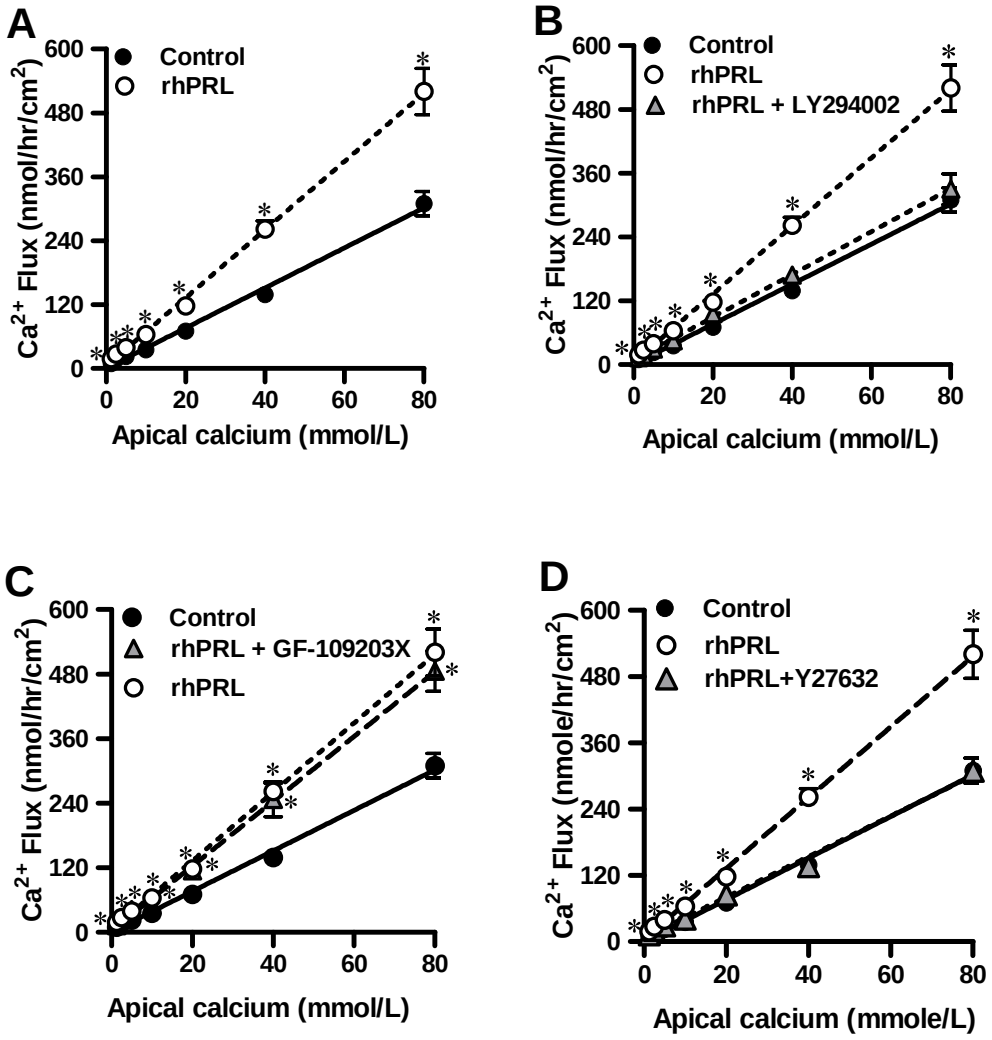

Figure 17. Paracellular passive calcium transport of epithelial-like Caco-2 monolayer. The monolayers were incubated with culture medium (control), 0.3% v/v DMSO (vehicle for preparation of inhibitors), 75μmol/L LY294002 (PI3K inhibitor), 1 μmol/L GF-109203X (PKC inhibitor), or 5 μmol/L Y27632 (ROCK inhibitor)-containing culture medium 1 h before adding 600 ng/mL rhPRL. The basolateral solution contained calcium at 1.25 mmol/L, whereas the apical calcium concentration was 1.25, 2.5, 5, 10, 20, 40, or 80 mmol/L. n=5 at each point.

* $P<0.05$ compared with control group at the same apical calcium concentration

C. To study the mechanism of acute PRL action on the transepithelial calcium transport in Caco-2 monolayer

C1. The mechanisms of acute PRL action on the enhancement of paracellular passive calcium transport

C1.1 rhPRL increased calcium permeability of Caco-2 monolayers

The aim of this experiment was to demonstrate the underlying mechanism of rhPRL-enhanced paracellular passive calcium transport by studying the calcium permeability of the monolayer.

In this experiment, the calcium gradient-dependent paracellular passive fluxes were determined by measuring calcium fluxes at varying apical calcium concentrations with or without pre-incubation with PI3K inhibitor (LY294002) PKC inhibitor (GF-109203X), or ROCK I/II inhibitor (Y-27632)**.** Calcium permeability was calculated from the paracellular passive calcium flux and the difference between the apical and basolateral calcium concentrations (Δ calcium). Calcium permeability via the paracellular pathway was increased by rhPRL (Figure 18A). At each Δ calcium, calcium permeability in the rhPRL-treated group was significantly greater than that in the control group ($p < 0.05$). Consistent with the passive calcium flux, the rhPRL-enhanced calcium permeability was diminished after exposure to LY294002 (Figure 18B) or Y27632 (Figure 18D), but not GF-109203X (Figure 18C).

These results demonstrated that rhPRL increased calcium permeability of Caco-2 monolayers by acting through PI3K and Rho/ROCK signaling pathways.

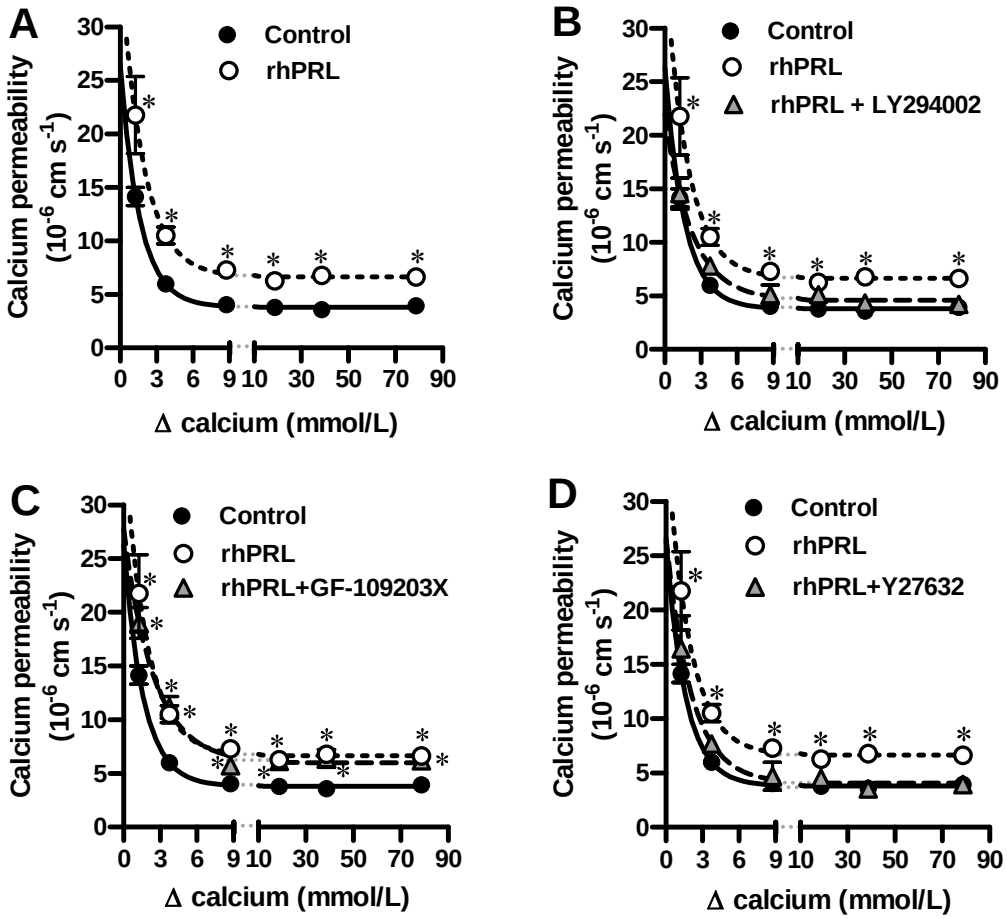

Figure 18. Calcium permeability in Caco-2 monolayer. The monolayers were incubated with culture medium (control), 0.3% v/v DMSO (vehicle for preparation of inhibitors), 75 μmol/L LY294002 (PI3K inhibitor), 1 μmol/L GF-109203X (PKC inhibitor), or 5 μmol/L Y27632 (ROCK inhibitor)-containing culture medium 1 h before adding 600 ng/mL rhPRL. The basolateral solution contained calcium at 1.25 mmol/L, whereas the apical calcium concentration was 1.25, 2.5, 5, 10, 20, 40, or 80 mmol/L. n=5 at each point.

* $P<0.05$ compared with control group at the same Δ calcium

C1.2 rhPRL had no effect on the size-selective property of Caco-2 monolayers

The aim of this experiment was to demonstrate the mechanism of the rhPRL-enhanced paracellular passive calcium transport by studying the size-selective property of Caco-2 monolayer.

As an indicator of widening of the tight junction or size selectivity, the transepithelial dual ^{3}H-mannitol and ^{14}C-PEG fluxes were determined. As shown in Table 7, transepithelial ^{3}H-mannitol and ^{14}C-PEG fluxes of the rhPRL-treated groups were not different from those of the control group.

Therefore, rhPRL had no effect on the size selectivity of Caco-2 monolayer.

Table 7. Transepithelial ^{3}H-mannitol/^{14}C-PEG fluxes. The monolayers were incubated with or without 600 ng/mL rhPRL. Values are means±SE. rhPRL, recombinant human PRL.

Condition	**n**	**Flux (nmol/hr/cm^2)**	
		Mannitol	**PEG**
Control	**7**	5.60±0.27	3.89±0.58
600 ng/mL rhPRL	**7**	5.36±0.34	3.96±0.28

C1.3 rhPRL increased cation selectivity of Caco-2 monolayers

The aim of this experiment was to demonstrate the underlying mechanism of the rhPRL-enhanced paracellular passive calcium transport by studying charge selective property of Caco-2 monolayer.

The charge-selective property of Caco-2 monolayers was elucidated by the dilution potential technique. As shown in Figure 19A, the relative permeability ratio of Na^+ to Cl^- (P_{Na}/P_{Cl}) of the control group, i.e., 3.70 ± 0.31, was greater than 1, implying that, Caco-2 monolayers were normally cation selective. rhPRL significantly increased the P_{Na}/P_{Cl} to 7.05 ± 1.01, $p < 0.05$. LY294002, wortmannin, and Y27632 completely abolished the rhPRL-enhanced cation selectivity of Caco-2 monolayers, whereas AG490, GF-109203X, and U0126 were without effect. Moreover, rhPRL significantly increased the absolute sodium permeability to 10.94 ± 0.68 10^{-6} cm^{-1}, $p < 0.01$ when compared with the control group of 8.15 ± 0.29 10^{-6} cm^{-1}. Consistent with the P_{Na}/P_{Cl}, rhPRL-enhanced the absolute sodium permeability was diminished after exposure to LY294002, wormannin, and Y-27632, but not AG490, GF-109203X, and U0126 (Figure 19B). The rhPRL and all inhibitors had no effect on the absolute chloride permeability (Figure 19C).

Moreover, Figure 20A shows relative permeability (P_x/P_{Cl}) of the monolayers in control condition to cations in the following order $Na^+ > K^+ > Rb^+ > Cs^+ > Li^+$, i.e., 2.70 ± 0.12, 2.14 ± 0.07, 1.75 ± 0.07, 1.69 ± 0.03, and 1.08 ± 0.02, respectively. Therefore, the paracellular pores of Caco-2 monolayers were classified as series VII of the Eisenman's sequences (Eisenman and Horn 1983). rhPRL significantly increased the permeability ratio of Li^+, Na^+, K^+, Rb^+, and Cs^+ to the values of 1.86 ± 0.09 (Figure 20A and 20B; $p < 0.001$), 5.96 ± 0.89 (Figure 20A and 20C; $p < 0.001$), 3.41 ± 0.17 (Figure 20A and 21D; $p < 0.001$), 2.19 ± 0.15 (Figure 20A and 21E; $p < 0.01$), and 1.91 ± 0.08 (Figure 20A and 21F; $p < 0.05$), respectively. LY294002 and Y27632 diminished the rhPRL-enhanced monovalent cation permeability in Caco-2 monolayer (Figures 20B-20F). Figure 21 shows the TER of the cationic diffusion potential experiment that was V-shaped with the lowest value of TER for Na^+. While GF-109203X had no effect on the rhPRL-induced decrease in TER, LY294002 and Y27632 abolished the effect of rhPRL (Figures 21B-21D).

These results demonstrated that Caco-2 monolayer represented a cation selective epithelium. Moreover, rhPRL acted through PI3K and Rho/ROCK signaling pathways to enhance the cation selectivity of Caco-2 monolayer.

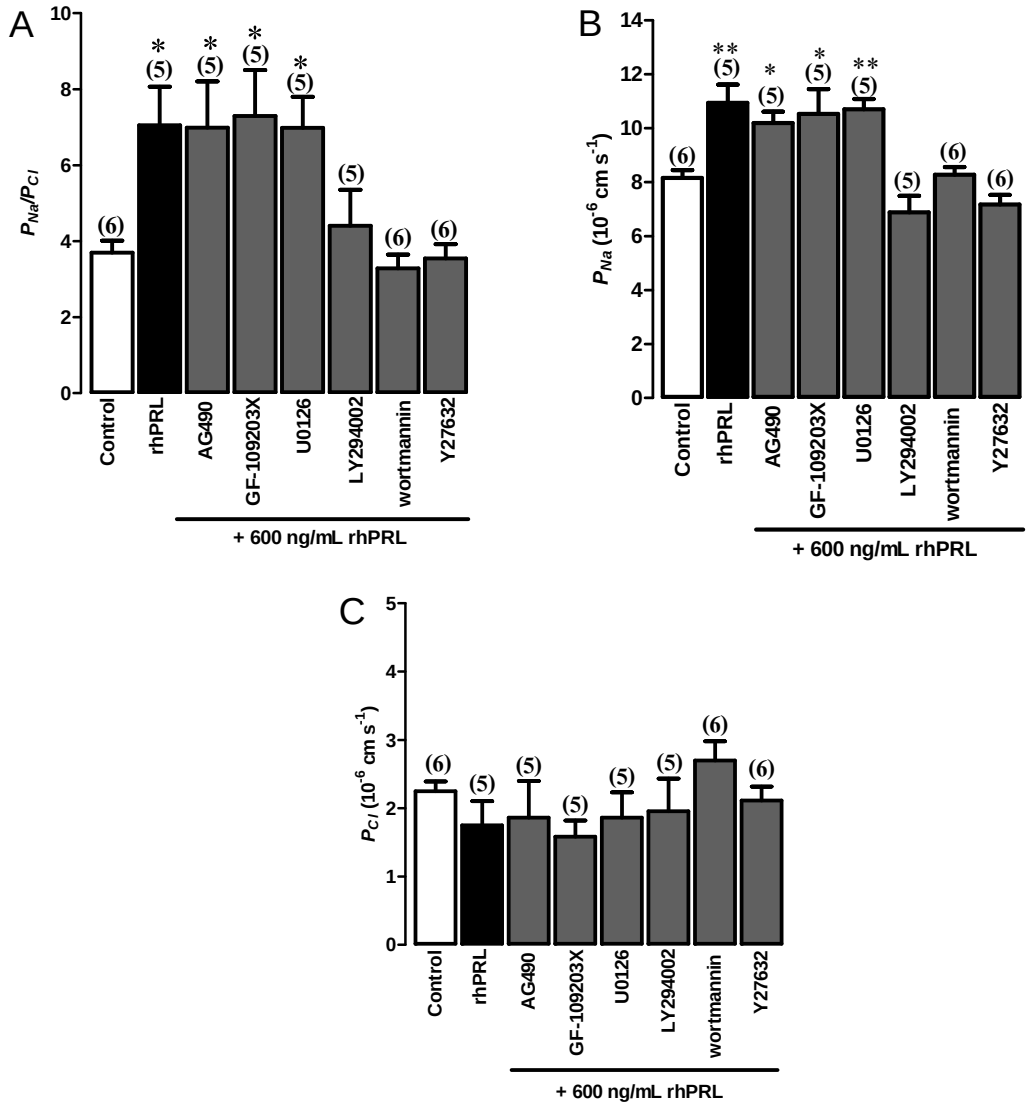

Figure 19. Charge-selective property of Caco-2 monolayer. The monolayers were incubated in the culture medium (control), 0.3% v/v DMSO (vehicle for preparation of inhibitors), 10 µmol/L U0126 (MEK inhibitor), 50 µmol/L AG490 (JAK2 inhibitor), 75 µmol/L LY294002 (PI3K inhibitor), 200 nmol/L wortmannin (PI3K inhibitor), 1 µmol/L GF-109203X (PKC inhibitor), or 5 µmol/L Y27632 (ROCK inhibitor) containing culture medium 1 h before added with 600 ng/mL rhPRL. P_{Na}/P_{Cl}; relative permeability ratio of Na^+ to Cl^-, P_{Na}; absolute Na^+ permeability, P_{Cl}; absolute Cl^- permeability.

* P<0.05 compared with control group,

** P<0.01 compared with control group

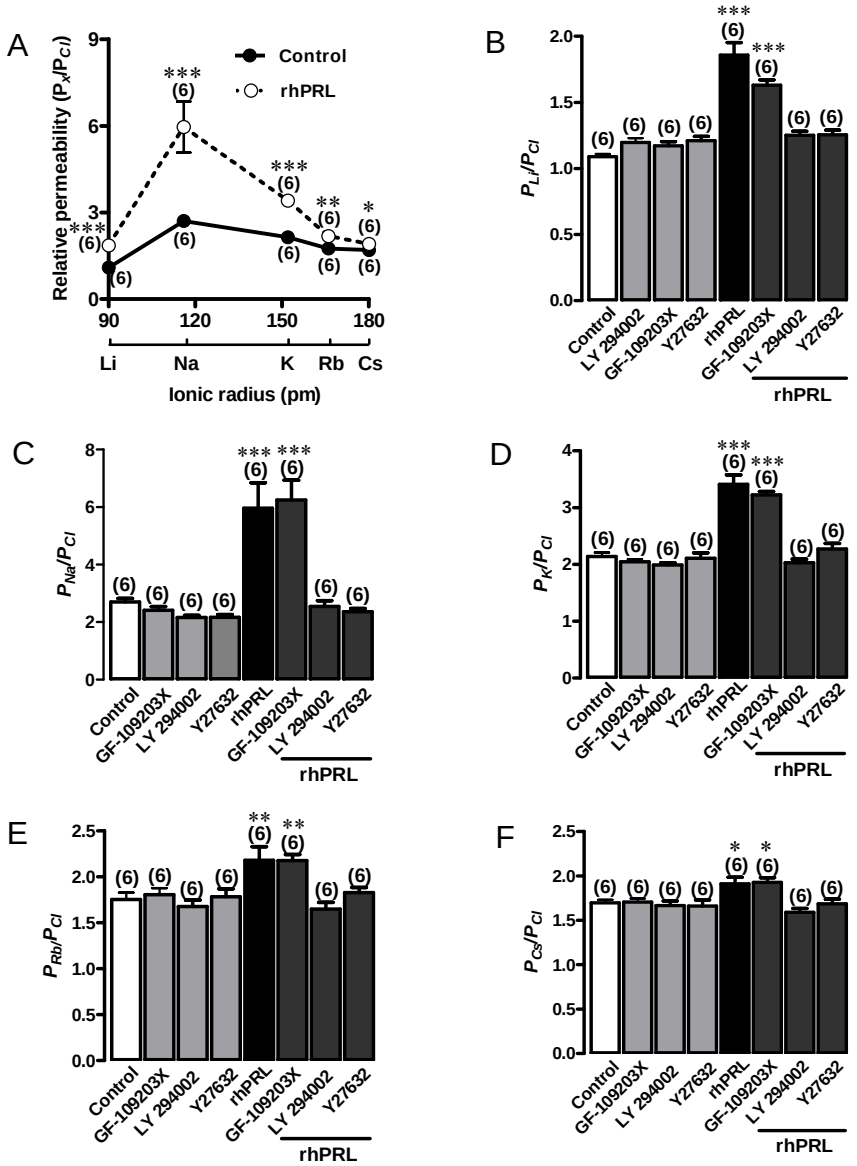

Figure 20. Monovalent cation permeability of Caco-2 monolayers. The monolayers were incubated with culture media (control), 75 µmol/L LY294002 (PI3K inhibitor), 1 µmol/L GF-109203X (PKC inhibitor), or 5 µmol/L Y27632 (ROCK inhibitor)-containing culture media 1 h before added with or without 600 ng/mL rhPRL.

* $P<0.05$, ** $P<0.01$, *** $P<0.05$ compared with control group at the same relative ion permeability ratio

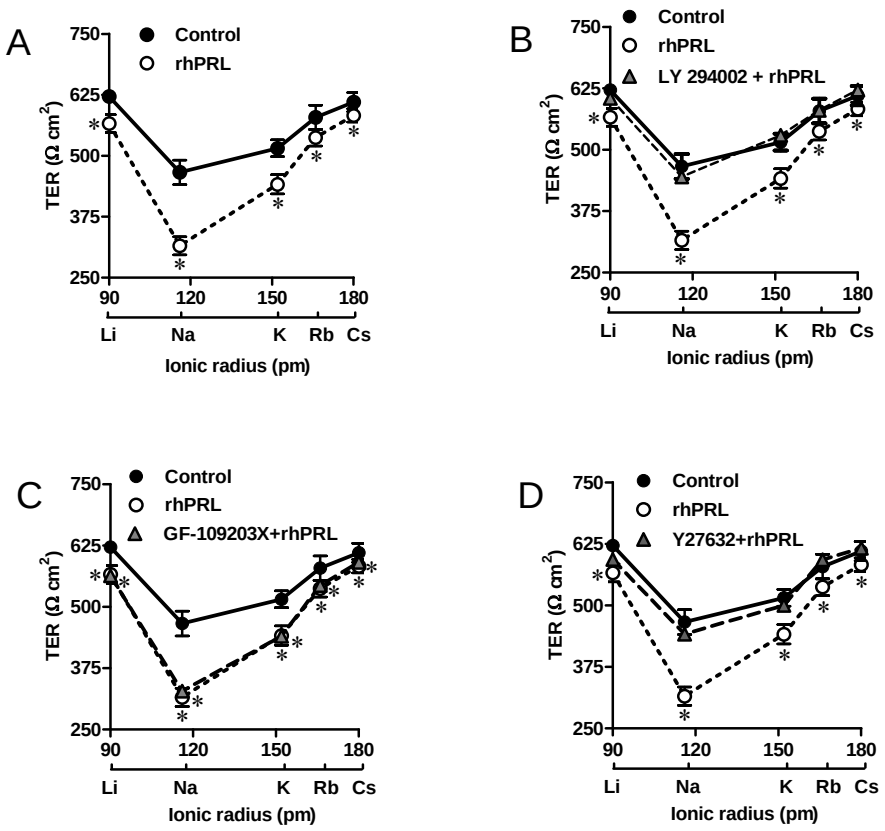

Figure 21. Line graph of TER from the cationic diffusion potential experiment. The monolayers were incubated with culture media (control), 75 μmol/L LY294002 (PI3K inhibitor), 1 μmol/L GF-109203X (PKC inhibitor), or 5 μmol/L Y27632 (ROCK inhibitor) containing culture media 1 h before added with or without 600 ng/mL rhPRL.

* $P<0.05$ compared with control group

C2. hPRLR-L mediated rhPRL actions.

Since the PRLR-L was suggested as the activated isoform that mediated PRL action in mammalian cells, e.g., mammary gland (Lesueur et al. 1991), this experiment aimed to determine whether PRLR-L took part in the mediation of rhPRL action in Caco-2 cells.

PRLR-L expression was suppressed by siRNA. The results from RT-PCR showed that siRNA significantly suppressed the PRLR-L expression with no change in other PRLR isoform (see Appendix E). Caco-2 monolayers were pre-incubated with 600 ng/mL rhPRL in DMEM for 1 h prior to insertion into the Ussing chamber to study the role of PRLR-L on the rhPRL-enhanced calcium fluxes. siPORT Amine transfection reagent and PRLR-L siRNA had no effect on the basal active calcium fluxes ($pmol \cdot min^{-1} \cdot cm^{-2}$), i.e, calcium flux of siPORT (154.22 ± 17.98) and siRNA (163.36 ± 17.15) groups were not different from that of control group (160.91 ± 9.55) (Figure 22). 600 ng/mL rhPRL significantly increased the total active calcium flux to 287.21 ± 9.27 $pmol \cdot min^{-1} \cdot cm^{-2}$ ($p < 0.001$). PRLR-L siRNA totally abolished the rhPRL-enhanced calcium fluxes in Caco-2 monolayer.

The results demonstrated that rhPRL stimulated total active calcium transport in Caco-2 monolayer via PRLR-L.

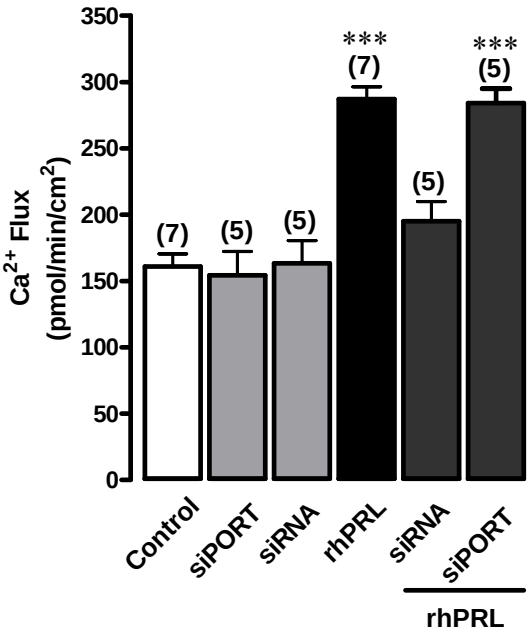

Figure 22. The effect of PRLR-L siRNA on the total active calcium flux. Two days prior to the study of calcium flux, Caco-2 monolayers were transfected with PRLR-R siRNA. siPORT is an amine transfection reagent.

*** $P<0.001$ compared with control group

CHAPTER V
DISCUSSION

Increases in calcium demand during pregnancy and lactation for fetal growth and milk production led to negative calcium balance in mother. Previous investigation showed that PRL, the milk producing hormone, may alleviate the calcium imbalance partly by stimulating the intestinal calcium absorption in a vitamin D-independent manner. However, the mechanism underlying the PRL-induced increase in the intestinal calcium absorption was not known. By using the Caco-2 epithelial model, the present study elucidated the mechanisms and signaling pathways of PRL action in the regulation of the duodenal active and passive calcium transport.

A. Experimental of hPRLR in Caco-2 epithelial model of intestinal calcium absorption

Since there is correlation between human intestinal drug absorption and Caco-2 monolayer permeability (Yee 1997), Caco-2 epithelial model has been widely used in the pharmacological studies of drug absorption (Volpe 2007). Caco-2 monolayer has also been used as a suitable model for the studies of calcium absorption in humans (Giuliano and Wood 1991; Fleet and Wood 1999).

In the present study, Caco-2 monolayer grown on a Snapwell was used to demonstrate calcium transport, the low passage number of Caco-2 cells (25–40th) was more appropriate for studies of both active and passive calcium transport than the high passage numbers (93–108th) because the high passage number Caco-2 cells had lower carrier-mediated transport, higher TER, and lower alkaline phosphatase activity (a marker of the small intestinal cell differentiation) (Yu et al. 1997). Low passage number Caco-2 cells (25–60th) has been shown to be appropriate for the study of both the transcellular and the paracellular calcium transport (Blais et al. 1997; Fleet and Wood 1999). In contrast, transcellular active calcium transport was absent at high in

cells from passage number (Chirayath et al. 1998).

Moreover, Seki and coworkers evaluated the establishment of tight junction in Caco-2 monolayer after cells were plated into Transwell at the density of 4.5×10^5 cell/cm^2 and found that tight junction formation in Caco-2 epithelial monolayer apparently occurred after 13 day-post seeding (Seki et al. 2008). In this study, Caco-2 cells were grown on Snapwell at high density of 5×10^5 cell/cm^2 and maintained for 14 days to allow Caco-2 cells to form epithelial monolayers.

The presence of hPRLR mRNAs, i.e., hPRLR-S, hPRLR-I, and hPRLR-L, in Caco-2 cells was demonstrated by using PCR. The localization and expression of hPRLR protein was demonstrated by confocal immunocytochemistry. hPRLR expression was found on the plasma membrane and in the cytoplasm, but not in the nucleus. hPRLRs in the cytoplasm could serve as an intracellular store. Cellular activation probably activated the translocation and insertion of cytoplasmic hPRLR into the membrane as seen with other proteins in neutrophils. Jost and coworkers reported the process of cytosolic store of human complementary receptor 1 (hCR 1) in neutrophils. Activation of the neutrophils resulted in the translocation of these cytosolic hCR 1 to the plasma membrane (Jost et al. 1998). Moreover, the perinuclear accumulation of the intracellular hPRLR probably represented the vesicle transporting pathway which appeared to concentrated in the juxtanuclear Golgi area (Figure 11 and 24). Perrot-Applanat and coworkers using confocal immunocytochemistry reported similar perinuclear accumulation of PRLR in COS-7, CHO and NIH-3T3 PRLR-transfected fibroblasts (Figure 24A) (Parrot-Applanat et al. 1997). They proposed that the perinuclear PRLR might correspond to the endocytotic pathway of the juxtanuclear Golgi apparatus (Parrot-Applanat et al. 1997).

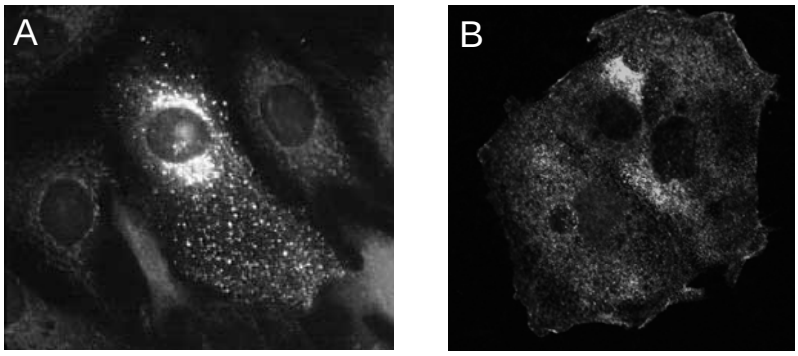

Figure 23. Immunofluorescent image of Flag-PRLR (long isoform) expressed in NIH-3T3 cells (A) (Parrot-Applanat et al. 1997) and hPRLR expressed in Caco-2 cells (B).

B. PRL enhanced active and passive calcium flux in Caco-2 monolayer and altered its charge selective property via PRLR-L isoforms.

High physiological concentrations of PRL, i.e., 200, 400, and 600 ng/mL (Boass and Lovdal 1992; Arbogast and Voogt 1998) as well as the pharmacological concentration of 800 ng/mL and pathological concentration of 1000 ng/mL (Serri et al. 2003) rapidly stimulated the total active calcium transport in Caco-2 monolayers in a dose-dependent manner. The present optimal effective dose of 600 ngPRL/mL was consistent with the optimum effective dose that was previously shown to enhance the active calcium transport in the duodenal tissue of rat (Tanrattana et al. 2004). This PRL concentration was considered as a high physiological level since it was equivalent to the levels of 350-650 ng/mL during suckling in lactating rats (Weitzman et al. 1980; Arbogast and Voogt 1998). Moreover, the typical biphasic action of PRL seen in vivo was also observed in Caco-2 monolayers, i.e., in contrast to the high physiological doses, the pharmacological dose of 800 ng/mL and pathological dose of 1000 ng/mL were unable to increase the calcium flux. This phenomenon could be explained as follow. To activate the cellular response of target cells to PRL, binding of the PRL to PRLR in a normal 1 PRL: 2 PRLR was prerequisite for activating the intracellular signaling (Bole-Feysot et al. 1998). At very high concentrations of PRL,

most available PRLRs were occupied as 1 : 1 complexes that could not activate the intracellular signal transduction (Fuh et al. 1993; Ilondo et al. 1994).

The total active calcium flux consists of three components, namely the transcellular active, solvent drag-induced and voltage-dependent paracellular active transport (Charoenphandhu et al. 2001). The transcellular and solvent drag-induced active calcium transport generally leads to calcium absorption, whereas the voltage-dependent active calcium transport leads to calcium secretion. In this experiment, 600 ng/mL PRL enhanced the total apical-to-basolateral active calcium flux by about 2 fold of that in control group. On the other hand, 600 ng/mL PRL had no effect on the total basolateral-to-apical active calcium flux. Therefore it was possible to conclude that PRL enhanced active calcium absorption in a unidirectional manner in Caco-2 epithelial model. The possible underlying mechanism could involve PRL-enhanced apical calcium uptake, possibly by increasing TRPV activity, and basolateral calcium extrusion by increasing PMCA activity (Charoenphandhu et al. 2006). Both transport activities constitute the unidirectional apical-to-basolateral active calcium transport. Although PRL increased the transcellular active calcium transport, change in the PD was very small and not detectable by the Ussing technique because the transcellular active calcium transport was of a small magnitude (Charoenphandhu et al. 2001). That was the major reason for using radioactive calcium to demonstrate calcium fluxes. The present data support our previous finding that PRL enhanced the total active calcium absorption and that the voltage-dependent active calcium flux was negligible in rat duodenum (Charoenphandhu et al. 2001). Interestingly, the TER of Caco-2 monolayer was decreased by PRL, similar to that observed after exposure to vitamin D (Chirayath et al. 1998). When the monolayer was short-circuited, the external current (Isc) moved across the monolayer via the low-resistance pathway, i.e., the paracellular pathway (Greger 1996). Therefore, the decrease in TER that was calculated from PD and Isc in the presence of PRL must have resulted from the PRL-induced increase in the paracellular permeability.

The gradient-dependent paracellular calcium transport was a passive process (Wallis et al. 1996) that became prominent when the apical calcium concentration was greater than 5 mmol/L. Thus, to observe the paracellular passive calcium transport, apical calcium concentration was varied, i.e., 1.25, 2.5, 5, 10, 20, 40, or 80 mmol/L

with a constant basolateral calcium concentration of 1.25 mmol/L. The present finding that the passive calcium transport and paracellular calcium permeability were increased by PRL confirmed the previous report from in vivo experiments (Krishnamra et al. 1998). The results also showed a linear correlation between apical calcium concentration and calcium flux in both control group and PRL-treated group. Since PRL enhanced paracellular calcium transport, it may alter the charge- and/or size-selective properties of the tight junction, which were known to regulate the paracellular ion movement (Van Italli and Anderson 2006).

Regarding the paracellular transport, ions and non-charge solutes move across epithelium by going through the major paracellular barrier, i.e., tight junction that handles the paracellular transport by regulating its size and charge selectivity (Van Itallie and Anderson 2006). The size restriction of paracellular pore of tight junctions in Caco-2 monolayer has been estimated to be 350–540 pm (Carr et al. 2006), thus, could not be a limiting factor for paracellular fluxes of calcium and mannitol (Table 8). As paracellular transport markers, mannitol and PEG have been used to determine the widening of tight junction (Tanrattana et al. 2004). Interestingly, PRL had no effect on mannitol flux across Caco-2 monolayer, even though the hydrated radius of mannitol was quite similar to that of calcium. Moreover, PRL had no effect on the larger paracellular marker PEG (molecular radius ~2,500 pm). On the other hand, PRL significantly increased the relative permeability of Na^+, K^+, Rb^+, Cs^+, and Li^+ to Cl^-, implying that the enhancing effect of PRL on the paracellular passive calcium transport and calcium permeability was due to the modulation of charge selectivity rather than size selectivity of tight junction. The present finding was consistant with the previous report of no effect of PRL on the widening of the tight junction or size selectivity of the duodenum (Tanrattana et al. 2004). Moreover, similar to the report in other epithelia, e.g., MDCK II, the greatest conductance of the monolayer (reciprocal of TER) was found when NaCl was used as the primary conductor (Tang and Goodenough 2003), which confirmed the present conclusion that Caco-2 monolayer was selectively permeable to Na^+ than other monovalent cation.

Table 8. The ionic and hydrated radius of various chemicals.

	Ionic or molecular redius (pm)	Hydrated radius (pm)
PEG	2500	
Mannitol	350	410
Ca^{2+}	116	420
Li^{+}	90	340
Na^{+}	114	276
K^{+}	152	232
Rb^{+}	166	228
Cs^{+}	180	228

For the charge selectivity, it is widely accepted that claudin proteins determine the paracellular charge selectivity of the epithelia (Van Itallie and Anderson 2004; Furuse and Tsukita 2006). Since there are 24 members of claudin proteins identified so far and different tissues express various combinations of different claudin proteins resulting in varying degrees of charge selectivity, therefore, specific pattern of claudin protein expression is likely to be the major determinant of tight junction ion selectivity (Furuse and Tsukita 2006). For example, claudin-16 has been shown to increase the cation permeability in LLP-CK1 epithelial monolayers (Hou et al. 2008). Co-expression of claudin-16 and claudin-19 further increased the cation selectivity in this epithelial model (Hou et al. 2008). These findings thus support the hypothesis that the expression of claudin proteins determines the charge selectivity property. Furthermore, the present study demonstrated the P_{Na}/P_{Cl} of 3.73 (in control condition) which was comparable to that in the previous study (Carr et al. 2006). Thus, Caco-2 monolayer obviously favored cationic transport which was significantly increased by PRL. The possible underlying mechanism of PRL action probably involved changes in the localization and combination of claudin proteins in the tight junction. Ikari and coworkers (Ikari et al. 2006) reported that 1 h preincubation with specific PKA activator (H-89) induced phosphorylation of claudin-16 at Ser217 residue as well as enhanced claudin-16 localization at the tight junction, resulting in greater cation selectivity of the MDCK epithelial model. On the other hand, dephosporylated

claudin-16 or claudin-16 with Ser217 mutation, which induced claudin-16 internalization into the cytoplasm for degradation, decreased the cation selectivity**.**

Since PRLR-L mediates PRL actions in several tissues such as ovary (Lesueur et al. 1991), the significant role of PRLR-L in the regulation of calcium flux in Caco-2 monolayer was investigated. PRLR-L knockdown by using siRNA completely abolished the PRL-enhanced calcium flux, indicating that PRLR-L mediated PRL signaling in Caco-2 monolayer. This finding was similar to that found in other models such as transcription of milk protein gene in Chinese hamster ovary (CHO) K1 cells (Lesueur et al. 1991).

C. The intracellular pathways of the acute non-genomic action of PRL

The immediate early genes (IEGs) are activated transiently and rapidly in response to a wide variety of cellular stimuli. One important member of IEGs is the activating protein-1 (AP-1) which is composed of fos family proteins (c-fos, fosB, fra-1, fra-2) and jun family proteins (c-jun, junB, junD). PRL markedly increased c-fos mRNA expression within the first 30 min of incubation (Dominguez-Caceres et al. 2004). In addition, PRL treatment rapidly increased AP-1 activity through PI3K activation in the first hour and peaked at 4 h in MCF-7 cells (Gutzman et al. 2004). Although AP-1 is well known as an early regulator of cell growth and differentiation, it might also affect other cellular processes, e.g., calcium absorption. Therefore, to confirm the non-genomic nature of PRL action on calcium transport in Caco-2 monolayers, 50 μM 5,6-dichloro-1β-D-ribofuranosylbenzimidazole (DRB) was used to exclude the involvement of transcriptional processes. This adenosine analog is a selective inhibitor of RNA polymerase II (RNA Pol II). It inhibits several protein kinases e.g. casein kinase II and transcription factor IIH-associated protein kinase that phosphorylate the C-terminal domain of RNA polymerase II (Yankulov et al. 1995), thereby preventing the transition of the initiation step to the elongation step in the transcription process (Zhu al. 1997). Moreover, DRB also inhibits the positive transcription-elongation factor b, resulting in an inhibition of the transcriptional process (Zhu et al. 1997). DRB has been extensively used to validate non-genomic actions of several hormones, e.g., vitamin D (Yankulov et al. 1995; Yamaguchi et al.

1998). The present results showed that DRB had no effect on the PRL-enhanced calcium transport in Caco-2 monolayer, comfirming that PRL exerted its action via the non-genomic signaling mechanism to enhance both active and passive calcium transport in Caco-2 monolayer.

Similar to other peptide hormones, PRL modulates cellular function of its target cells via activation of the PRLR-associated intracellular signaling pathways. There are at least four PRL signaling pathways that have been identified, namely Jak/STAT, MAPK, PI3K, and PKC pathways (Figure 4) (Bole-Feysot et al. 1998; Freeman et al. 2000). Although these PRL signalings have been extensively studied, almost all of those investigations were concerned with the genomic signaling mechanism. Moreover, these PRL signaling pathways have been extensively studied in neurons, mammary cells and T-lymphocytes, but never in enterocytes. The present study therefore looked into demonstrate the acute non-genomic action of PRL in Caco-2 epithelial monolayers. To demonstrate the signaling pathways of PRL in Caco-2 monolayers, several inhibitors, i.e., MAPK inhibitor (U0126), Jak2 inhibitor (AG490), PI3K inhibitors (LY294002 or wortmannin), PKC inhibitor (GF-109203X), or ROCK I/II inhibitor (Y27632) were used. Results showed that PRL acted through the PI3K, PKC, and Rho/ROCK signaling pathways to enhance the total active calcium transport. Moreover, PRL acted through PI3K and Rho/ROCK signaling pathways to stimulate the paracellular passive calcium transport in Caco-2 monolayer.

Regarding the active calcium transport, the present investigation showed that the stimulatory action of PRL was via PI3K pathway in Caco-2 monolayers. Previous investigation reported that PRL rapidly enhanced the apical calcium uptake and the plasma membrame Ca^{2+}-ATPase (PMCA) activity in rat duodenum (Charoenphandhu et al. 2006). Rosado and coworkers demonstrated that PI3K activation led to rapid tyrosine phosphorylation and increased activity of PMCA, resulting in enhanced calcium extrusion in human platelets (Rosado and Sage 2000). Moreover, serum- and glucocorticoid-inducible kinase (SGK) activation via PI3K-dependent pathway was shown to increase TRPV activity (Lang et al. 2006). Thus, PRL may also activate TRPV and PMCA activities via the PI3K-dependent pathway to enhance calcium uptake into the cells and calcium extrusion across the basolateral membrane, respectively, thereby increasing the active calcium transport in Caco-2 monolayer.

Considering the present finding that showed the PRL-induced increases in paracellular passive calcium transport, calcium permeability, and charge selectivity being abolished by PI3K inhibitors, and the fact that tight junction is the major paracellular barrier, it could be said that PRL probably modulated the tight junction function via the PI3K signaling. The role PI3K in the regulation of tight junction transport has apparently been proposed before. PI3K activation by oxidative stress was found to decrease TER and increase paracellular permeability in Caco-2 monolayer (Sheth et al. 2003). In addition, PI3K activation by HIV-1 Tat proteins was found to alter claudin-5 experssion and increase paracellular permeability in brain microvascular endothelial cells (Andras et al. 2005). Moreover, PI3K activation by reactive oxygen species altered cytoskeletal rearrangement and plasma membrane claudin-5 expression, resulting in increased paracellular permeability in human blood-brain barrier cells (Schreibelt et al. 2007). Nevertheless, it was not possible to speculate the mechanism of PRL action on tight junction function from the present data, and whether the PRL-PI3K-dependent pathway mediated cytoskeletal rearrangement and expression pattern of claudin proteins on tight junction permeability requires further study.

The present study also showed that PRL exerted its actions through PKC signaling to enhance the active calcium transport in Caco-2 monolayer. Since PKC was known to enhance calcium absorption by activating TRPV activity (Gkika et al. 2006), and increasing calcium extrusion via PMCA on the basolateral membrane (Usachev et al. 2002; Triphan et al. 2007), it could be deduced that PRL-PKC-dependent pathway regulated the active calcium transport via activating both calcium influx and calcium extrusion processes.

The Rho proteins are subfamily of the Ras-superfamily of small (~21 kDa) GTPase, which includes the Ras, Arf, Rab, and Ran families (Wennerbergn et al. 2005). There are 20 Rho GTPases that can be classified into 6 subgroups, namely the Rho proteins (RhoA, RhoB, RhoC), the Cdc42-like proteins (Cdc4, TC10, TCL, Wrch1, Chp), the Rac proteins (Rac1, Rac2, Rac3, RhoG), the Ran proteins (Rnd1, Rnd2, Rnd3/RhoE), the RhoBTB proteins (RhoBTB1, RhoBTB2, RhoBTB3) and the Miro proteins (Miro1, Miro2) (Ellenbroek and Collard 2007). Rho GTPase proteins, especially RhoA, have been known to regulate actin cytoskeleton in response to

several receptor stimuli (Ellenbroek and Collard 2007). Activated RhoA interacts with its effector serine/threonine kinases, named Rho-associated coiled-coil-containing proteins kinases (ROCK-I and ROCK-II), which subsequently activate myosin light chain kinase, thereby resulting in contraction and formation of actin stress fiber of non-muscle cells (Ellenbroek and Collard 2007). In the recent years, several investigators demonstrated that the Rho/ROCK signaling pathway modulates paracellular permeability by inducing perijunctional actomyosin ring contraction and enhancing size selectivity of tight junction (Jou et al. 1998; Sahai and Marshall 2002; Russo et al. 2005). However, it was presently founded that PRL did not alter the size selectivity of Caco-2 monolayers. The activation of Rho/ROCK signaling by PRL, therefore, may not involve the actomyosin ring contraction to increase paracellular pore size. Herein, PRL acted through the Rho/ROCK signaling pathway to enhance paracellular permeability by altering charge selectivity in Caco-2 monolayer. In brain endothelial cells, the Rho/ROCK signaling enhanced blood-brain barrier permeability by inducing occludin and claudin-5 phosphorylation at Ser and Tyr residues (Persidsky et al. 2006). Thus, Rho/ROCK signaling may alter paracellular permeability and charge selectivity of Caco-2 monolayer through phosphorylation of the tight junction proteins. Moreover, activation of Rho/ROCK signaling by PRL also enhanced the active calcium transport across Caco-2 monolayer. However, the underlying mechanism by which Rho/ROCK signaling enhanced active calcium transport is still unknown.

It is known that PI3K is the ultimate upstream kinase of several downstream kinases, e.g., PKC and Rho/ROCK (Kapus and Szászi 2006; Hirsch et al. 2007), which are recognized as the activators of several downstream targets involved in the transcellular and paracellular calcium transport, i.e., TRPV, PMCA, and claudins. Therefore, it should be concluded that PRL exerted its action via PRLR-L to activate PI3K/PKC/Rho/ROCK dependent pathway, which further activated apical calcium uptake by increasing TRPV activity and basolateral calcium extrusion by increasing PMCA activity, resulting in increased the transcellular active calcium transport in Caco-2 monolayer (Figure 24). It was possible that PRL exerted its action through PI3K/Rho/ROCK dependent pathways to induce an increase in the activity of cation selective claudin(s) in the tight junction and/or affect the localization of cation

selective claudin(s) in the tight junction, which led to increases in the paracellular passive calcium transport, calcium permeability, and cation selectivity in Caco-2 monolayer (Figure 25). However the sequence of kinase activations and specific effector proteins involved in the acute cellular response to PRL need to be elucidated by further investigations.

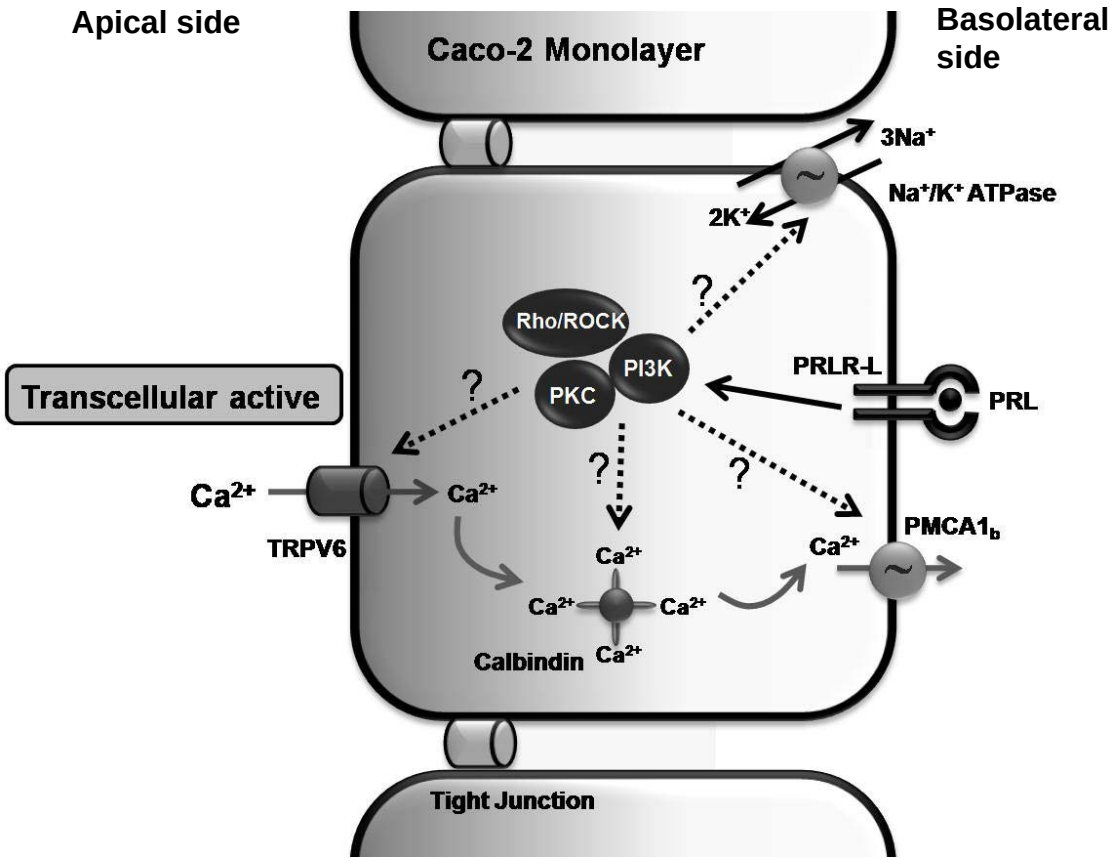

Figure 24. Proposed mechanism of the PRL-enhanced total active calcium flux.

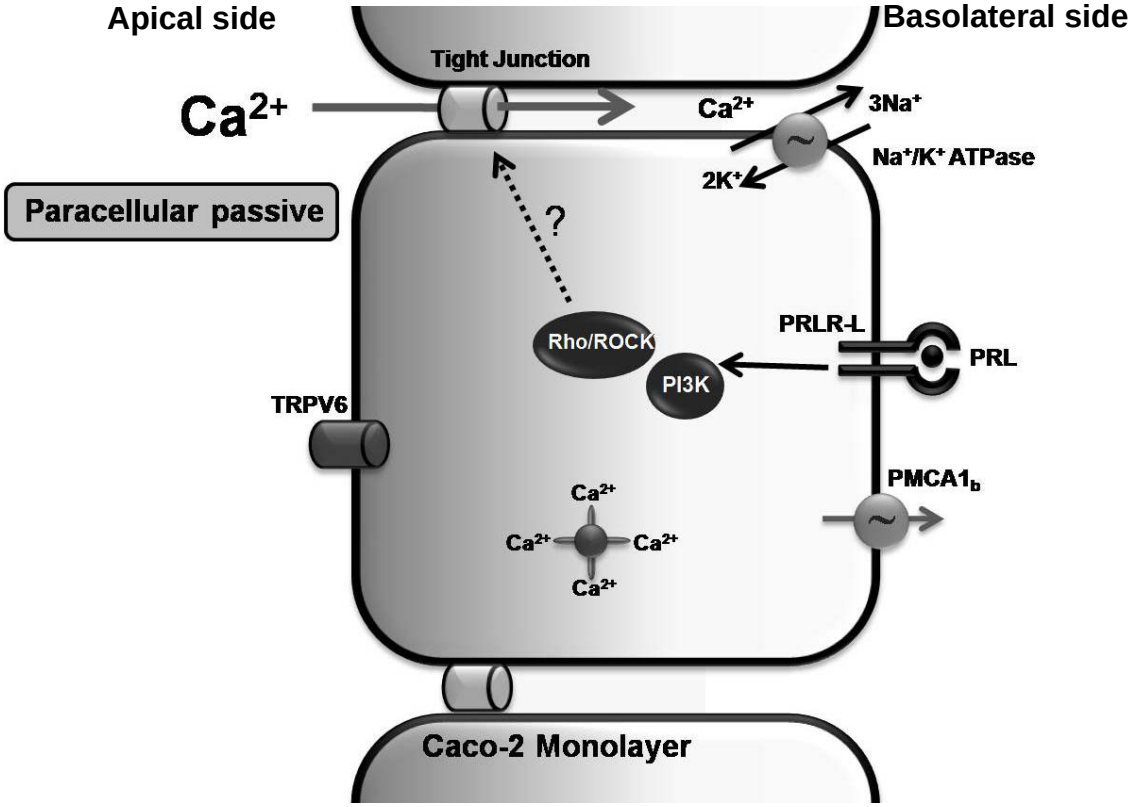

Figure 25. Proposed mechanism of the PRL-enhanced paracellular passive calcium transport and calcium permeability in Caco-2 monolayer.

CHAPTER VI
CONCLUSIONS

The present study aimed to investigate acute action and signaling transduction of PRL on the transepithelial calcium transport across Caco-2 monolayer. The monolayer was established by growing Caco-2 cells on 0.4–µm pore size polyester Snapwell. The main findings could be divided into 4 aspects as follow.

1. Caco-2 monolayer was a suitable model for studying the effect of PRL on calcium fluxes.

1.1 Caco-2 cells expressed mRNA of all hPRLR isoforms, i.e., hPRLR-S, hPRLR-I, and hPRLR-L.

1.2 As shown by immunocytochemistry, hPRLR was expressed on the plasma membrane and in the intracellular compartment of Caco-2 cells.

2. As demonstrated by the PRLR-L knockdown study, PRL acted through hPRLR-L to enhance transepithelial calcium flux across the epithelial-like Caco-2 monolayers.

3. PRL enhanced transepithelial active calcium fluxes across Caco-2 monolayers.

3.1 PRL enhanced apical-to-basolateral total active Ca fluxes (i.e., absorption), but not basolateral-to-apical calcium fluxes (i.e., secretion), across Caco-2 monolayer.

3.2 PRL exerted its actions through non-genomic PI3K, PKC, and Rho/ROCK signaling pathways to increase the total active calcium fluxes across Caco-2 monolayers (Figure 24).

3.3 Voltage-dependent active calcium flux was negligible, and PRL had no effect on this active component.

4. PRL enhanced transepithelial passive calcium fluxes and calcium permeability of the Caco-2 monolayer (Figure 25).

4.1 PRL exerted its action through PI3K and Rho/ROCK signalings to enhance the gradient-dependent paracellular passive calcium fluxes in Caco-2 monolayer.

4.2 PRL exerted its action through PI3K and Rho/ROCK signaling to enhance calcium permeability and cation selectivity of Caco-2 monolayer.

REFERENCES

Acosta JJ, Munoz RM, Gonzalez L, Subtil-Rodriguez A, Dominguez-Caceres MA, Garcia-Martinez JM, Calcabrini A, Lazaro-Trueba I, Martin-Perez J. Src mediates prolactin-dependent proliferation of T47D and MCF7 cells via the activation of focal adhesion kinase/Erk1/2 and phosphatidylinositol 3-kinase pathways. Mol Endocrinol 2003; 17(11): 2268–2282.

Adson A, Raub TJ, Burton PS, Barsuhn CL, Hilgers AR, Audus KL, Ho NF. Quantitative approaches to delineate paracellular diffusion in cultured epithelial cell monolayers. J Pharm Sci 1994; 83(11): 1529–1536.

Ali S. Recruitment of the protein-tyrosine phosphatase SHP-2 to the C-terminal tyrosine of the prolactin receptor and to the adaptor protein Gab2. J Biol Chem 2000; 275(50): 39073–39080.

Amaral ME, Cunha DA, Anhe GF, Ueno M, Carneiro EM, Velloso LA, Bordin S, Boschero AC. Participation of prolactin receptors and phosphatidylinositol 3-kinase and MAP kinase pathways in the increase in pancreatic islet mass and sensitivity to glucose during pregnancy. J Endocrinol 2004; 183(3): 469–476.

Amasheh S, Meiri N, Gitter AH, Schoneberg T, Mankertz J, Schulzke JD, Fromm M. Claudin-2 expression induces cation-selective channels in tight junctions of epithelial cells. J Cell Sci 2002; 115(Pt 24): 4969–4976.

Amit T, Dibner C, Barkey RJ. Characterization of prolactinand growth hormone-binding proteins in milk and their diversity among species. Mol Cell Endocrinol 1997; 130: 167–180.

Amnattanakul S, Charoenphandhu N, Limlomwongse L, Krishnamra N. Endogenous prolactin modulated the calcium absorption in the jejunum of suking rats. Can J Physiol Pharmacol 2005; 83(7): 595–604.

Anderson JM and Van Itallie CM. Tight junctions and the molecular basis for regulation of paracellular permeability. Am J Physiol 1995; 269(4 Pt 1): G467–G475.

Andras IE, Pu H, Tian J, Deli MA, Nath A, Hennig B, Toborek M. Signaling mechanisms of HIV-1 Tat-induced alterations of claudin-5 expression in brain endothelial cells. J Cereb Blood Flow Metab 2005; 25(9): 1159–1170.

Arbogast LA and Voogt JL. Endogenous opioid peptides contribute to suckling-induced prolactin release by suppressing tyrosine hydroxylase activity and messenger ribonucleic acid levels in tuberoinfundibular dopaminergic neurons. Endocrinology 1998; 139(6): 2857–2862.

Arden KC, Boutin J-M, Djiane J, Kelly PA, Cavenee WK. The receptors for prolactin and growth hormone are localized in the same region of human chromosome 5. Cytogenet Cell Genet 1990; 53: 161–165.

Armbrecht HJ, Boltz MA, Bruns ME. Effect of age and dietary calcium on intestinal calbidin D-9k expression in the rat. Arch Biochem Biophys 2003; 420: 194–200.

Artursson P and Karlsson J. Correlation between oral drug absorption in humans and apparent drug permeability coefficients in human intestinal epithelial (Caco-2) cells. Biochem Biophys Res Commun 1991; 175(3): 880–885.

Avruch J, Zhang X-F, Kyriakis JM. Raf meets Ras: completing the framework of a signal transduction pathway. Trends Biochem Science 1994; 19: 279–283.

Balda MS and Matter K. Transmembrane proteins of tight junctions. Semin Cell Dev Biol 2000; 11(4): 281–289.

Barnett ME, Madgwick DK, Takemoto DJ. Protein kinase C as a stress sensor. Cell Signal 2007; 19(9): 1820–1829.

Ben-Jonathan N, Mershon JL, Allen DL, Steinmetz RW. Extrapituitary prolactin: distribution, regulation, functions, and clinical aspects. Endocr Rev 1996; 17: 639–669.

Ben-Yosef T, Belyantseva IA, Saunders TL, Hughes ED, Kawamoto K, Van Itallie CM, Beyer LA, Halsey K, Gardner DJ, Wilcox ER, Rasmussen J, Anderson JM, Dolan DF, Forge A, Raphael Y, Camper SA, Friedman TB. Claudin 14 knockout mice, a model for autosomal recessive deafness DFNB29, are deaf due to cochlear hair cell degeneration. Hum Mol Genet 2003; 12(16): 2049–2061.

Berlanga JJ, Gualillo O, Buteau H, Applanat M, Kelly PA, Edery M. Prolactin activates tyrosyl phosphorylation of insulin receptor subatrate 1 and phosphatidylinositol-3-OH kinase. J Biol Chem 1997; 272: 2050–2052.

Berne RM, Levy MN, Koeppen BM, Stanton BA. Endocrine regulation of calcium and phosphate metabolism 2003. St. Louis, Missouri, Elsevier Science.

Berwaer M, Martial JA, Davis JR. Characterization of an up-stream promoter directing extrapituitary expression of the human prolactin gene. Mol Endocrinol 1994; 8(5): 635–642.

Berwaer M, Monget P, Peers B, Mathy-Hartert M, Bellefroid E, Davis JR, Belayew A, Martial JA. Multihormonal regulation of the human prolactin gene expression from 5000 bp of its upstream sequence. Mol Cell Endocrinol 1991; 80(1-3): 53–64.

Blais A, Aymard P, Lacour B. Paracellular calcium transport across Caco-2 and HT29 cell monolayers. Pflügers Arch 1997; 434(3): 300–305.

Blaustein MP, Juhaszova M, Golovina VA, Church PJ, Stanley EF. Na^{+}/Ca^{2+} exchanger and PMCA localization in neurons and astrocytes: functional implications. Ann NY Acad Sci 2002; 976: 356–366.

Boass A and Lovdal J. Pregnancy- and lactation-induced changes in active intestinal calcium transport in rat. Am J Physiol 1992; 263: G127–G134.

Bolander Jr. F. Prolactin activation of mammary nitric oxide synthase: molecular mechanisms. J Mol Endocrinol 2002; 28: 45–51.

Bole-Feysot C, Goffin V, Edery M, Binart N, Kelly PA. Prolactin (PRL) and its receptor: actions, signal transduction pathways and phenotypes observed in PRL receptor knockout mice. Endocr Rev 1998; 19(3): 225–268.

Boockfor FR, Hoeffler JP, Frawley LS. Estradiol induces a shift in cultured cells that release prolactin or growth hormone. Am J Physiol Endocrinol Metab 1986; 250: E100–E103.

Bronner F. Mechnisms of intestinal calcium absorption. J Cell Biochem 2003; 88: 387–393.

Buckley AR, Raoy YP, Buckley DJ, Gout PW. Prolactin-induced phosphorylation and nuclear translocation of MAP kinase in Nb2 lymphoma cells. Biochem Biophys Res Commun 1994; 204: 1158–1164.

Campbell GS, Argetsignger LS, Ihle JN, Kelly PA, Rillema JA, Carter-Su C. Activation of JAK2 tyrosine kinase by prolactin receptors in Nb2 cells and mouse mammary gland explants. Proc Natl Acad Sci USA 1994; 91: 5232–5236.

Carr G, Haslam IS, Simmons NL. Voltage dependence of transepithelial guanidine permeation across Caco-2 epithelia allows determination of the paracellular flux component. Pharm Res 2006; 23(3): 540–548.

Chantret I, Barbat A, Dussaulx E, Brattain MG, Zweibaum A. Epithelial polarity, villin expression, and enterocytic differentiation of cultured human colon carcinoma cells: a survey of twenty cell lines. Cancer Res 1988; 48(7): 1936–1942.

Charoenphandhu N and Krishnamra N. Prolactin is an important regulator of intestinal calcium transport. Can J Physiol Pharmacol 2007; 85: 569–581.

Charoenphandhu N, Limlomwongse L, Krishnamra N. Prolactin directly stimulates transcellular active calcium transport in the duodenum of femals rats. Can J Physiol Pharmacol 2001; 79(5): 430–438.

Charoenphandhu N, Limlomwongse L, Krishnamra N. Prolactin directly enhanced Na^+/K^+- and Ca^{2+}-ATPase activities in the duodenum of female rats. Can J Physiol Pharmacol 2006; 84: 555–563.

Charoenphandhu N, Tudpor K, Pulsok K, Krishnamra N. Chronic metabolic acidosis stimulated trascellular and solvent drag-induced calcium transport in the duodenum of female rats. Am J Physiol Gastrointest Liver Physiol 2006; 291: G446–G455.

Chatton JY and Spring KR. The sodium concentration of the lateral intercellular spaces of MDCK cells: a microspectrofluormetric study. J Membr Biol 1995; 144: 11–19.

Chirayath MV, Gajdzik L, Hulla W, Graf J, Cross HS, Peterlik M. Vitamin D increases tight-junction conductance and paracellular Ca^{2+} transport in Caco-2 cell cultures. Am J Physiol 1998; 274(2 Pt 1): G389–G396.

Citi S, Sabanay H, Jakes R, Geiger B, Kendrick-Jones J. Cingulin, a new peripheral component of tight junctions. Nature 1988; 333(6170): 272–276.

Clapham DE. TRP channels as cellular sensors. Nature 2003; 426: 517–524.

Clevenger CV, Furth PA, Hankinson SE, Schuler LA. The role of prolactin in mammary carcinoma. Endocr Rev 2003; 24(1): 1–27.

Colegio OR, Van Itallie CM, Rahner C, Anderson JM. Claudin extracellular domains determine paracellular charge selectivity and resistance but not tight junction fibril architecture. Am J Physiol Cell Physiol 2003; 284(6): C1346–C1354.

Constantino S, Santos R, Lacronique V, Bouchaert I, Monni R, Bernard O, Gisselbrecht S, Gouilleux F. Constitutively active STAT5 variants induce growth and survial of hematopoietic cells through a PI 3-kinase /Akt dependent pathway. Oncogene 2001; 20: 2080–2090.

Contreras RG, Avila G, Gutierrez C, Bolivar JJ, Gonzalez-Mariscal L, Darzon A. Repolarization of Na^{+}-K^{+} pumps during establishment of epithelial monolayers. Am J Physiol 1989; 257: C896–C905.

Cooke NE, Coit D, Shine J, Baxter JD, Martial JA. Human prolactin. cDNA structural analysis and evolutionary comparisons. J Biol Chem 1981; 256(8): 4007–4016.

Das R and Vonderhaar BK. Activation of raf-1, MEK and MAP kinase in prolactin responsive mammary cells. Breast Cancer Res Treat 1996; 40: 141–149.

Das R and Vonderhaar BK. Involvement of SHC, GRB2, SOS, and Ras in prolactin signaling transduction in mammary epithelial cells. Oncogene 1996; 13: 1139–1145.

Denker BM and Nigam SK. Molecular structure and assembly of the tight junction. Am J Physiol 1998; 274: F1–F9.

Dominguez-Caceres MA, Garcia-Martinez JM, Calcabrini A, Gonzalez L, Porque PG, Leon J, Martin-Perez J. Prolactin induces c-Myc expression and cell survival

through activation of Src/Akt pathway in lymphoid cells. Oncogene 2004; 23(44): 7378–7390.

Eisenman G and Horn R. Ionic selectivity revisited: the role of kinetic and equilibrium processes in ion permeation through channels. J Membr Biol. 1983; 76(3): 197–225.

Ellenbroek S and Collard J. Rho GTPases: functions and association with cancer. Clin Exp Metastasis 2007; 24(8): 657–672.

Engle MJ, Goetz GS, Alpers DH. Caco-2 cells express a combination of colonocyte and enterocyte phenotypes. J Cell Sci 1998; 174: 362–369.

Erwin RA, Kirken RA, Malabarba MG, Farar WL, Rui H. Prolactin activates Ras via signaling protein SHC, growth factor receptor bound2, and son of sevenless. Endocrinology 1995; 136: 3512–3518.

Fannings AS and Anderson JM. PDZ domain: fundamental building blocks in the organization of protein complexes at the plasma membrne. J Clin Invest 1999; 103(6): 767–772.

Fannings AS, Mitic LL, Anderson JM. Transmembrane proteins in the tight junction barrier. J Am Soc Nephrol 1999; 10(6): 1337-1345.

Feher JJ and Wasserman RH. Calcium absorption and intestinal calcium-binding protein: quantitative relationship. Am J Physiol Endocrinol Metab Gastrointest Physiol 1979; 236: E556–E561.

Ferrage F, Pezet A, Chiarenza A, Buteau H, Nelson BH, Goffin V. Heterodimerization of IL-2 receptor belta chain is necessary and sufficient to activate Jak2 and downstream signaling pathways. FEBS Lett 1998; 420: 32-36.

Fleet JC, Eksir F, Hance KW, Wood RJ. Vitamin D-inducible calcium transport and gene expression in three Caco-2 cell lines. Am J Physiol Gastrointest Liver Physiol 2002; 283(3): G618–G625.

Fleet JC and Wood RJ. Specific 1,25$(OH)_2D_3$-mediated regulation of transcellular calcium transport in Caco-2 cells. Am J Physiol 1999; 276(4 Pt 1): G958–G964.

Fogh J, Fogh JM, Orfeo T. One hundred and twenty-seven cultured human turmor cell lines producing tumors in nude mice. J Nalt Cancer Inst 1977; 59: 221–226.

Frawley LS, Boockfor FR, Hoeffler JP. Identification by plaque assays of a pituitary cell type that secretes both growth hormone and prolactin. Endocrinology 1985; 116: 734–737.

Freeman ME, Kanyicska B, Lerant A, Nagy G. Prolactin: structure, function, and regulation of secretion. Physiol Rev 2000; 80(4): 1523–1631.

Fuh G, Colosi P, Wood WI, Wells JA. Mechanism-based design of prolactin receptor antagonists. J Biol Chem 1993; 268(8): 5376–81.

Fujimoto K. Freeze-fracture replica electron microscopy combined with SDS digestion for cytochemical labeling of integral membrane proteins. Application to the immunogold labeling of intercellular junctional complexes. J Cell Sci 1995; 108 (Pt 11): 3443–3449.

Furuse M, Fujita K, Hiiragi T, Fujimoto K, Tsukita S. Claudin-1 and -2: novel integral membrane proteins localizing at tight junctions with no sequence similarity to occludin. J Cell Biol 1998; 141(7): 1539–1550.

Furuse M, Hirase T, Itoh M, Nagafushi A, Yonemura S, Tsukita S. Occludin: a novel integral membrane protein localizing at tight junctions. J Cell Biol 1993; 125(6 Pt 2): 1777–1788.

Furuse M, Sasaki H, Fujimoto K, Tsukita S. A single gene product, claudin-1 or -2, reconstitutes tight junction strands and recruits occludin in fibroblasts. J Cell Biol 1998; 143(2): 391–401.

Furuse M and Tsukita S. Claudins in occluding junctions of humans and flies. Trends Cell Biol 2006; 16(4): 181–188.

Giuliano AR and Wood RJ. Vitamin D-regulated calcium transport in Caco-2 cells: unique in vitro model. Am J Physiol 1991; 260: G202–G121.

Gkika D, Topala CN, Chang Q, Picard N, Thebault S, Houillier P, Hoenderop JG, Bindels RJ. Tissue kallikrein stimulates Ca^{2+} reabsorption via PKC-dependent plasma membrane accumulation of TRPV5. Embo J 2006; 25(20): 4707–4716.

Goffin V, Bouchard B, Ormandy CJ, Weimann E, Ferrag F, Touraine P, Bole-Feysot C, Maaskant RA, Clement-Lacroix P, Edery M, Binart N, Kelly PA.

Prolactin: a hormone at the crossroads of neuroimmunoendocrinology. Ann N Y Acad Sci 1998; 840: 498–509.

Goffin V and Kelly PA. The prolactin/growth hormone receptor family: structure/function relationships. J Mammary Gland Biol Neopl 1996; 2: 7–17.

Goffin V, Kinet S, Ferrage F, Binart N, Martial JA, Kelly PA. Antagonistic properties of human prolactin analogues that show paradoxical agonistic activity in the Nb2 bioassay. J Biol Chem 1996; 271: 16573–16579.

Gonzalez-Mariscal L, Betanzos A, Avila-Flores A. MAGUK proteins: structure and role in tight junction. Semin Cell Dev Biol 2000; 11(4): 315–324.

Goodenough DA. Pluggings the leaks. Proc Nalt Acad Sci USA 1999; 96: 319–321.

Goupille O, Daniel N, Bignon C, Jolivet G, Djiane J. Prolactin signal transduction to milk protein genes: carboxy-terminal part of the prolactin receptor and its tyrosine phosphorylation are not obligatory for JAK2 and STAT5 activation. Mol Cell Endocrinol 1997; 127: 55–169.

Greger R, Epithelial transport. In: Comprehensive Human Physiology: From Cellular Mechanisms to Integration, edited by Greger R, Windhorst U. Berlin: Springer, 1996.

Gutzman JH, Rugowski DE, Schroeder MD, Watters JJ, Schuler LA. Multiple kinase cascades mediate prolactin signalings to activating proten-1 in brest cencer cells. Mol Endocrinol 2004; 18: 3064–3075.

Halloran B and DeLuca H. Calcium transport in small intestine during pregnancy and lactation. Am J Physiol 1980; 239: E64–E68.

Hamazaki Y, Itoh M, Sasaki H, Furuse M, Tsukita S. Multi-PDZ domain protein 1 (MUPP1) is concentrated at tight junctions through its possible interaction with claudin-1 and junctional adhesion molecule. J Biol Chem 2002; 277(1): 455–461.

Haskins J, Gu L, Wittchen ES, Hibbard J, Stevenson BR. ZO-3, a novel member of the MAGUK protein family found at the tight junction, interacts with ZO-1 and occludin. J Cell Biol 1998; 141(1): 199–208.

Hawkins PT, Anderson KE, Davidson K, Stephens LR. Signalling through Class I PI3Ks in mammalian cells. Biochem Soc Trans 2006; 34(Pt 5): 647–662.

Hidalgo IJ, Raub TJ, Borchardt RT. Characterization of the human colon carcinoma cell line (Caco-2) as a model system for intestinal epithelial permeability. Gastroenterology 1989; 96(3): 736–749.

Hirsch E, Costa C, Ciraolo E. Phosphoinositide 3-kinases as a common platform for multi-hormone signaling. J Endocrinol 2007; 194(2): 243–256.

Hoenderop JG, Nilius B, Bindels RJ. Calcium absorption across epithelia. Physiol Rev 2005; 85(1): 373–422.

Hou J, Paul DL, Goodenough DA. Paracellin-1 and the modulation of ion selectivity of tight junctions. J Cell Sci 2005; 118: 5109–5118.

Hou J, Renigunta A, Konrad M, Gomes AS, Schneeberger EE, Paul DL, Waldegger S, Goodenough DA. Claudin-16 and claudin-19 interact and form a cation-selective tight junction complex. J Clin Invest 2008; 118(2): 619–628.

Hu Z and Dufau ML. Multible and differential regulation of ovarian prolactin receptor messenger RNAs and their expression. Biochem Biophys Res Commun 1991; 181: 219–225.

Hu Z, Zhuang L, Meng J, Dufau ML. Transcription regulation of the generic promoter III of the rat prolactin receptor gene by C/EBP belta and Sp1. J Biol Chem 1998; 273: 26225–26235.

Ihle JN. Cytokine receptor signalling. Nature 1995; 377(6550): 591–594.

Ikari A, Matsumoto S, Harada H, Takagi K, Hayashi H, Suzuki Y, Degawa M, Miwa M. Phosphorylation of paracellin-1 at Ser217 by protein kinase A is essential for localization in tight junctions. J Cell Sci 2006; 119(Pt 9): 1781–1789.

Ilondo MM, Damholt AB, Cunningham BA, Wells JA, De Meyts P, Shymko RM. Receptor dimerization determines the effects of growth hormone in primary rat adipocytes and cultured human IM-9 lymphocytes. Endocrinology 1994; 134(6): 2397–23403.

Itoh M, Furuse M, Morita K, Kubota K, Saitou M, Tsukita S. Direct binding of three tight junction-associated MAGUKs, ZO-1, ZO-2, and ZO-3, with the COOH termini of claudins. J Cell Biol 1999; 147(6): 1351–1363.

Jabbour HN, Critchley HO, Boddy SC. Expression of functional prolactin receptors in nonpregnant human endometrium: janus kinase-2, signal transducer and

activator of transcription-1 (STAT1), and STAT5 proteins are phosphorylated after stimulation with prolactin. J Clin Endocrinol Metab 1998; 83(7): 2545–2553.

Jacobs LS, Mariz IK, Daughaday WH. A mixed heterologous radioimmunoassay for human prolactin. J Clin Endocrinol Metab 1972; 34(3): 484–490.

Jamarie C and Malo C. Caco-2 cells cultured in serum-free medium as a model for the study of enterocytic differentiation in vitro. J Cell Physiol 1991; 149(1): 24–33.

Jewell C, Cusack S, Cashman KD. The effect of conjugated linoleic acid on transepithelial calcium transport and mediators of paracellular permeability in human intestinal-like Caco-2 cells. Prostaglandins Leukot Essent Fatty Acids 2005; 72(3): 163–171.

Jost C, Klickstein L, Wetzler E, Kumar A, Berger M. Intracellular storage and regulated plasma membrane expression of human complement receptor type 1 in rat basophil leukemia cell transfectants. Blood 1998; 92(1): 300–309.

Jou TS, Schneeberger EE, Nelson WJ. Structural and functional regulation of tight junctions by RhoA and Rac1 small GTPases. J Cell Biol 1998; 142(1): 101–115.

Kahle KT, Macgregor GG, Wilson FH, Van Hoek AN, Brown D, Ardito T, Kashgarian M, Giebisch G, Hebert SC, Boulpaep EL, Lifton RP. Paracellular Cl^- permeability is regulated by WNK4 kinase: insight into normal physiology and hypertension. Proc Natl Acad Sci U S A 2004; 101(41): 14877–14882.

Kalkwarf H and Specker B. Bone mineral changes during pregnancy and lactation. Endocrine 2002; 17(1): 49–53.

Kaminska B, Ciereszko RE, Opalka M, Dusza L. Prolactin signaling in porcine adrenocortical cells: involvement of protein kinases. Domest Anim Endocrinol 2002; 23(4): 475–491.

Kapus A and Szászi K. Coupling between apical and paracellular transport process. Biochem Cell Biol 2006; 84: 870–880

Karbach U. Segmental heterogeneity of cellular and paracellular calcium transport across rat duodenum and jejunum. Gastroenterology 1991; 100: 47–58.

Karbach U. Paracellular calcium transport across the small intestine. J Nutr 1992; 122: 672–677.

Kelly PA, Binart N, Freemark M, Lucas B, Goffin V, Bouchard B. Prolactin receptor signal transduction pathways and actions determined in prolactin receptor knockout mice. Biochem Soc Trans 2001; 29(Pt 2): 48–52.

Kovacs C. Calclium and bone metabolism during pergnancy and lactation. J Mammary Gland Biol Neoplasia 2005; 10(2): 105–118.

Krishnamra N, Ousingsawat J, Limlomwongse L. Study of acute pharmacologic effects of prolactin on calcium and water transport in the rat colon by an in vivo perfusion technique. Can J Physiol Pharmacol 2001; 79(5): 415–421.

Krishnamra N, Wirunrattanakij Y, Limlomwongse L. Acute effects of prolactin on passive calcium absorption in the small intestine by in vivo perfusion technique. Can J Physiol Pharmacol 1998; 76(2): 161–168.

Krumenacker JS, Narang VS, Buckley DJ, Buckley AR. Prolactin signaling to pim-1 expression: a role for phosphatidylinositol 3-kinase. J Neuroimmunol 2001; 113(2): 249–259.

Lang F, Bohmer C, Palmada M, Seebohm G, Strutz-Seebohm N, Vallon V. (Patho)physiological significance of the serum- and glucocorticoid-inducible kinase isoforms. Physiol Rev 2006; 86(4): 1151–1178.

Larsen EH, Nedergaard S, Ussing HH. Role of lateral intercellular space and sodium recirculation for isotonic transport in leaky epithelia. Rev Physiol Biochem Pharmacol 2000; 141: 153–212.

Lasson D and Nemere I. Vectorial transcellular calcium transport in intestine: integration of current models. J Biomed Biotechnol 2002; 2: 117–119.

Le Bevic A, Quaroni A, Nichols B, Rodriguez-Boulan E. Biodenetic pathways of plasma membrane proteins in Caco-2 cells, a human intestinal epithelial cell line. J Cell Biol 1990; 111: 1351–1361.

Lennernas H, Palm K, Fagerholm U, Artursson P. Comparison between active and passive drug transport in human intestinal epithelial (Caco-2) cells in vitro and human jejunum in vivo. Intl J Pharm 1996; 127: 103–107.

Lesueur L, Edery M, Ali S, Paly J, Kelly PA, Djiane J. Comparison of long and short forms of the prolactin receptor on prolactin-induced milk protein gene transcription. Proc Nalt Acad Sci USA 1991; 88: 824–828.

Liu X, Robinson GW, Wagner KU, Garrett L, Wynshaw-Boris A, Hennighausen L. Stat5a is mandatory for adult mammary gland development and lactogenesis. Genes Dev 1997; 11(2): 179–186.

Ma FY, Grattan DR, Goffin V, Bunn SJ. Prolactin-regulated tyrosine hydroxylase activity and messenger ribonucleic acid expression in mediobasal hypothalamic cultures: the differential role of specific protein kinases. Endocrinology 2005; 146(1): 93–102.

Marano CW, Lewis SA, Garulacan LA, Peralta Soler A, Mullin JM. Tumor necrosis factor-a increase sodium and chloride conductant across the tight junction of Caco-2 BBE, human intestinal epithelial cell line. J Membr Biol 1998; 161: 263–274.

Marcus CS and Lengemann FW. Absorption of ^{45}Ca and ^{85}Sr from solid and liquid food at various levels of the alimentary tract of the rat. J Nutr 1962; 77: 155–160.

Mazor M, Hershkowitz R, Ghezzi F, Cohen J, Chaim W, Wiznitzer A, Levy J, Leiberman JR, Glezerman M. Prolactin concentrations in preterm and term pregnancy and labour. Arch Gynecol Obstet 1996; 258(2): 69-74.

McLaughlin J, Padfield PJ, Burt JPH, O'Neill CA. Ochratoxin A increases permeability through tight junctions by removal of specific claudin isoforms. Am J Physiol Cell Physiol 2004; 287: C1412–C1417.

Meng J, Tsai-Morris CH, Dufau ML. Human prolactin receptor variants in breast cancer: low ratio of short forms to the long-form human prolactin receptor associated with mammary carcinoma. Cancer Res 2004; 64(16): 5677–5682.

Murphy EF, Jewell C, Hooiveld GJ, Muller M, Cashman KD. Conjugated linoleic acid enhances transepithelial calcium transport in human intestinal-like Caco-2

cells: an insight into molecular changes. Prostaglandins Leukot Essent Fatty Acids 2006; 74(5): 295–301.

Nagano M, Chastre E, Choquet A, Bara J, Gespach C, Kelly PA. Expression of prolactin and growth hormone receptor genes and their isoforms in the gastrointestinal tract. Am J Physiol 1995; 268(3 Pt 1): G431–G442.

Newton AC. Regulation of the ABC kinases by phosphorylation: protein kinase C as a paradigm. Biochem J 2003; 370(Pt 2): 361–371.

Noel GL, Suh HK, Frantz AG. Prolactin release during nursing and breast stimulation in postpartum and nonpostpartum subjects. J Clin Endocrinol Metab 1974; 38(3): 413–423.

Owerbach D, Rutter WJ, Cooke NE, Martial JA, Shows TB. The prolactin gene is located on chromosome 6 in humans. Science 1981; 212(4496): 815-816.

Pahuja D and DeLuca H. Stimulation of intestinal calcium transport and bone calcium mobilization by prolactin in vitamin D-deficient rats. Science 1981; 214: 1038-1039.

Parrot-Applanat M, Gualillo O, Buteau H, Edery M, Kelly PA. Internalization of prolactin receptor and prolactin in transfected cells does not involve nuclear translocation. J Cell Sci 1997; 110: 1123–1132.

Paukku K and Silvennoinen O. STATs as critical mediators of signal transduction and transcription: lessons learned from STAT5. Cytokine Growth Factor Rev 2004; 15(6): 435–455.

Persidsky Y, Heilman D, Haorah J, Zelivyanskaya M, Persidsky R, Weber GA, Shimokawa H, Kaibuchi K, Ikezu T. Rho-mediated regulation of tight junctions during monocyte migration across the blood-brain barrier in HIV-1 encephalitis (HIVE). Blood 2006; 107(12): 4770–4780.

Peters CA, Maizels ET, Hunzicker-Dunn M. Activation of PKC δ in the rat corpus luteum during pregnancy. Potential role of prolactin signaling. J Biol Chem 1999; 274(52): 37499–37505.

Piccoletti R, Maroni P, Bendinelli P, Bernelli-Zazzera A. Rapid stimulation of mitogen-activated protein kinase of rat liver by prolactin. Biochem J 1994; 303: 429–433.

Pinto M, Robin-Leon S, Appay MD, Kedinger M, Triadow N, Dussaulx E. Enterocyte-like differentiation and polarization of the human colon carcinoma cell line Caco-2 in culture. Biol Cell 1983; 47: 323–330.

Porter TE, Chapman LE, Van Dolah FM, Frawley LS. Normal differentiation of prolactin cells in neonatal rats requires a maternal signal specific to early lactation. Endocrinology 1991; 128: 792–796.

Prentice A. Calcium in pregnancy and lactation. Annu Rev Nutr 2000; 20: 249–272.

Rosado JA and Sage SO. Regulation of plasma membrane Ca^{2+}-ATPase by small GTPases and phosphoinositides in human platelets. J Biol Chem 2000; 275(26): 19529–19535.

Russo JM, Florian P, Shen L, Graham WV, Tretiakova MS, Gitter AH, Mrsny RJ, Turner JR. Distinct temporal-spatial roles for rho kinase and myosin light chain kinase in epithelial purse-string wound closure. Gastroenterology 2005; 128(4): 987–1001.

Sahai E and Marshall C. ROCK and Dia have opposing effects on adherens junctions downstream of Rho. Nat Cell Biol 2002; 4(6): 408–415.

Saitou M, Fujimoto K, Doi Y, Itoh M, Fujimoto T, Furuse M, Takano H, Noda T, Tsukita S. Occludin-deficient embryonic stem cells can differentiate into polarized epithelial cells bearing tight junctions. J Cell Biol 1998; 141(2): 397–408.

Salas PJ and López EM. Validity of the Goldman-Hodgkin-Katz equation in paracellular ionic pathways of gallbladder epithelium. Biochim Biophys Acta 1982; 691(1): 178–182.

Salas PJI and Moreno JH. Single-file diffusion multi-ion mechanism of permeation in paracellular epithelial channels. J Membr Biol 1982; 64: 103–112.

Sarli M, Hakim C, Rey P, Zanchetta J. Osteoperosis during pregnancy and lactation. Medicina (B Aires) 2005; 65(6): 533–540.

Schneeberger EE and Lynch RD. The tight junction: a multifunctional complex. Am J Physiol Cell Physiol 2004; 286(6): C1213–C1228.

Schreibelt G, Kooij G, Reijerkerk A, van Doorn R, Gringhuis SI, van der Pol S, Weksler BB, Romero IA, Piontek J, Blasig IE, Dijkstra CD, Ronken E, de

Vries HE. Reactive oxygen species alter brain endothelial tight junction dynamics via RhoA, PI3 kinase, and PKB signaling. FASEB 2007; 21(13): 3666–3676.

Schuler LA, Lu J-C, Brockman L. Prolactin receptor heterogeneity: processing and signaling of the long and short isoform during developement. Biochem Soc Trans 2001; 29(2): 52–56.

Seki T, Harada S, Hosoya O, Morimoto K, Juni K. Evaluation of the establishment of a tight junction in Caco-2 cell monolayers using a pore permeation model involving two different sizes. Biol Pharm Bull 2008; 31(1): 163–166.

Serri O, Chik CL, Ur E, Ezzat S. Diagnosis and management of hyperprolactinemia. Cmaj 2003; 169(6): 575–581.

Sheth P, Basuroy S, Li C, Naren AP, Rao RK. Role of phosphatidylinositol 3-kinase in oxidative stress-induced disruption of tight junctions. J Biol Chem 2003; 278(49): 49239–49245.

Sinha YN. Structural variants of prolactin: occurrence and physiological significance. Endocr Rev 1995; 16(3): 354–369.

Slepchenko BM and Bronner F. Modeling of transcellular Ca^{2+} transport in rat duodenum points to coexistence of two mechanisms of apical entry. Am J Physiol Cell Physiol 2001; 281: C270–C281.

Soldin SJ, Morales A, Albalos F, Lenherr S, Rifai N. Pediatric reference ranges on the Abbott IMx for FSH, LH, prolactin, TSH, T4, T3, free T4, free T3, T-uptake, IgE, and ferritin. Clin Biochem 1995; 28(6): 603–606.

Suzuki T and Hara H. Various non-digestible saccharides increase intracellular calcium ion concentration in rat small-intestinal enterocytes. Br J Nutr 2004; 92(5): 751–155.

Suzuki T and Hara H. Difructose anhydride III and sodium caprate activate paracellular transport via different intracellular events in Caco-2 cells. Life Sci 2006; 79(4): 401–410.

Taffetani S, Glaser S, Francis H, DeMorrow S, Ueno Y, Alvaro D, Marucci L, Marzioni M, Fava G, Venter J, Vaculin S, Vaculin B, Lam IP, Lee VH, Gaudio E, Carpino G, Benedetti A, Alpini G. Prolactin stimulates the

proliferation of normal female cholangiocytes by differential regulation of Ca2+-dependent PKC isoform. BMC Physiol 2007; 7: doi:10.1186/1472-6793-7-6

Tang VW and Goodenough DA. Paracellular ion channel at the tight junction. Biophys J 2003; 84(3): 1660–1673.

Tanrattana C, Charoenphandhu N, Limlomwongse L, Krishnamra N. Prolactin directly stimulated the solvent drage-induced calcium transport in the duodenum of femal rats. Biochim Biophys Acta 2004; 1665: 82–91.

Taparia S, Fleet JC, Peng JB, Wang XD, Wood RJ. 1,25-Dihydroxyvitamin D and 25-hydroxyvitamin D-mediated regulation of TRPV6 (a putative epithelial calcium channel) mRNA expression in Caco-2 cells. Eur J Nutr 2006; 45(4): 196–204.

Tian Y and Laychock SG. Prolactin regulates adenylyl cyclase and insulin secretion in rat pancreatic islets. Mol Cell Endocrinol 2003; 204(1-2): 75–84.

Triphan J, Aumuller G, Brandenburger T, Wilhelm B. Localization and regulation of plasma membrane Ca^{2+} ATPase in bovine spermatozoa. Eur J Cell Biol 2007; 86(5): 265–273.

Truong AT, Duez C, Belayew A, Renard A, Pictet R, Bell GI, Martial JA. Isolation and characterization of the human prolactin gene. Embo J 1984; 3(2): 429–437.

Tudpor K, Charoenphandhu N, Saengamnart W, Krishnamra N. Long-term prolactin exposure differentially stimulate the transcellular and solvent drage-induced calcium trnasport in the duodenum of ovarectomized rats. Exp Bio Med 2005; 11: 836–844.

Usachev YM, DeMarco SJ, Campbell C, Strehler EE, Thayer SA. Bradykinin and ATP accelerate Ca^{2+} efflux from rat sensory neurons via protein kinase C and the plasma membrane Ca^{2+} pump isoform 4. Neuron 2002; 33(1): 113–122.

Van Itallie C, Rahner C, Anderson JM. Regulated expression of claudin-4 decreases paracellular conductance through a selective decrease in sodium permeability. J Clin Invest 2001; 107(10): 1319–1327.

Van Itallie CM and Anderson JM. The role of claudins in determining paracellular charge selectivity. Proc Am Torac Soc 2004; 1: 38–41.

Van Itallie CM and Anderson JM. Claudins and epithelial paracellular transport. Annu Rev Physiol 2006; 68: 403–429.

Van Itallie CM, Fanning AS, Anderson JM. Reversal of charge selectivity in cation or anion-selective epithelial lines by expression of different claudins. Am J Physiol Renal Physiol 2003; 285(6): F1078–F1084.

Volpe D. Varieability in Caco-2 and MDCK cell-based intestinal permeability assays. J Pharm Sci 2007: doi 10.1002/jps.21010

Walker AM. Phosphorylated and non-phosphorylated prolactin isoforms. Trends Endocrinol Metab 1994; 5: 195–200.

Wangdee W, Limlomwongse L, Krishnamra N. Further studies on acute effect of prolactin on intestinal calcium absorption in rat. Bone Miner 1991; 15: 97–107.

Wasserman RH, Chandler JS, Meyer SA, Smith CA, Brindark ME, Fullmer CS, Penniston JT, Kumar R. Intestinal calcium transport and calcium extrusion process at the basolateral membrane. J Nutr 1992; 122: 662–671.

Weinstein AM and Stephenson JL. Coupled water transport in standing gradient model of the lateral intercellular space. Biophys J 1981; 35: 167–191.

Weitzman RE, Leake RD, Rubin RT, Fisher DA. The effect of nursing on neurohypophyseal hormone and prolactin secretion in human subjects. J Clin Endocrinol Metab 1980; 51: 836–839.

Wen H, Watry DD, Marcondes MC, Fox HS. Selective decrease in paracellular conductance of tight junctions: role of the first extracellular domain of claudin-5. Mol Cell Biol 2004; 24(19): 8408–8017.

Wennerberg K, Rossman KL, Der CL. The Ras superfamily at a glance. J Cell Sci 2005; 118: 843–846.

Wood RJ, Tchack L, Taparia S. 1,25-Dihydroxyvitamin D_3 increases the expression of the CaT1 epithelial calcium channel in the Caco-2 human intestinal cell line. BMC Physiol 2001; 1: doi:10.1186/1472-6793-1-11

Wright EM and Loo DF. Coupling between Na^+, sugar, and water transport across the intestine. Ann NY Acad Sci 2000; 915: 54–66.

Yamaguchi Y, Wada T, Handa H. Interplay between positive and negative elongation factors: drawing a new view of DRB. Genes Cells 1998; 3: 9–15.

Yankulov K, Yamachita K, Roy R, Egly J, Bentley DL. The transcriptional elongation inhibitor 5,6-dichloro-1β-D-ribofuranosylbenzimidazole inhibits transcription factor IIH-associated protein kinase. J Biol Chem 1995; 270: 23922–23925.

Yasuda A, Miyazima K, Kawauchi H, Peter RE, Lin HR, Yamaguchi K, Sano H. Primary structure of common carp prolactins. Gen Comp Endocrinol 1987; 66(2): 280–290.

Ye D, Ma I, Ma TY. Molecular mechanism of tumor neccrosis factor-α modulation of intestinal epithelial tight junction barrier. Am J Physiol Gastrointest Liver Physiol 2006; 290: G496–G504.

Yee S. In vitro permeability across Caco-2 (colonic) can predict in vivo (small intestine) absorption in man−fact or myth. Pharm Res 1997; 14(6): 763–766.

Yoshioka M, Erickson RH, Matsumoto H, Gum E, Kim ES. Expression of dipeptidyl aminopeptidase IV during enterocytic differentiation of human colon cancer (Caco-2) cells. Int J Cancer 1991; 47(6): 16–21.

Yu AS, Enck AH, Lencer WI, Schneeberger EE. Claudin-8 expression in Madin-Darby canine kidney cells augments the paracellular barrier to cation permeation. J Biol Chem 2003; 278(19): 17350–17359.

Yu H, Cook TJ, Sinko PJ. Evidence for diminished functional expression of intesinal transportters in Caco-2 cell monolayers at high passages. Pharm Res 1997; 14: 757–762.

Zhu Y, Goff JP, Reinhardt TA, Horst RL. Pregnancy and lactation increase vitamin D-dependent intestinal membrane calcium adenosine triphosphatase and calcium binding protein messenger ribonucleic acid expression. Endocrinology 1998; 139: 3520-3524.

Zhu Y, Pe'ery T, Peng J, Ramanathan Y, Marshall N, Marshall T, Amendt B, Mathews MB, Price DH. Transcription elongation factor P-TEFb is required for HIV-1 tat transactivation in vivo. Genes Dev 1997; 11: 2622–2632.

APPENDIX

APPENDIX A
RECOMBINANT HUMAN PROLACTIN PREPARATION

A. Principle

Recombinant human prolactin (rhPRL) is derived from *Escherichia coli.* which expresses DNA sequence encoding the mature human prolactin sequence (amino acid 29-227). It is recommended that rhPRL is dissolved in 4 mM HCL containing 1 mg/mL BSA.

B. Reagents

1. rhPRL 50 µg
2. sterile 4 mM HCL containing 1 mg/mL BSA
3. sterile distilled H_2O grade 2A
4. sterile standard phosphate buffer (PBS)

C. Procedures

1. Preparation of 80 mM HCL

To prepare 80 mM HCL, 66 µL of HCL (37% HCL analytical grade) is added into 100 mL volumic flask and then adjusted with autoclaved distilled H_2O grade 2A to obtain the final volume of 100 mL. The 80 mM HCL is kept in light protection bottle at room temperature.

2. Preparation of 2 mg/mL BSA

20 mg BSA is dissolved in 10 mL autoclaved PBS in 15 mL centrifuge tube, then, sealed and kept at 4 °C. This solution is prepared on the same day aspreparation of 4 mM HCL containing 1 mg/mL BSA solution.

3. Preparation of 4 mM HCL containing 1 mg/mL BSA solution

10 mL of 80 mM HCL and 10 mL of 2 mg/mL BSA are mixed gently in a 25 mL centrifuge tube. After being well mixing, the solution is filtered through a 0.2 µ filter membrane and kept at 4 °C.

4. Preparation of 10 µg/mL rhPRL

500 µL of sterile 4 mM HCL containing 1 mg/mL BSA solution is gently added into the bottle containing 50 µg of rhPRL powder, then gently mixed before the dissolved of rhPRL solution is removed and placed in a 15 mL centrifuge tube. This process is repeated 10 times to completely removed rhPRL and to obtain a final volume of 5 mL in a 15 mL tube. The final 10 µg/mL rhPRL stock solution is stored at –20 °C. This preparation is performed in a biosafety condition.

APPENDIX B
PREPARATION OF CULTURE MEDIA

A. Reagents

1. DMEM (D7777 of Sigma)
2. $NaHCO_3$
3. HEPES
4. sterile distilled H_2O grade 2A
5. sterile fetal bovine serum (FBS)
6. sterile L-Glutamine
7. sterile non-essential amino acid (NEAA)
8. sterile penicillin-streptomycin
9. sterile amphoteracin B
10. sterile standard phosphate buffer solution (PBS)

B. Procedures

1. Preparation of PBS

0.2 g KCL, 8 g NaCl, 2.16 g Na_2PHO_4, and 0.2 g KH_2PO_4 are placed in a 1–liter beaker and the volume is made up with autoclaved distilled H_2O grade 2A. The solution is gently mixed using magnetic stirrer. pH of the solution is adjusted to 7.2–7.3 by adding 1 M $NaHCO_3$ or 1 M HCL. Thereafter the solution is transferred to a 1 liter volumetric flask and autoclaved distilled H_2O grade 2A is added to obtain a final volume of 1000 mL. The PBS is then sterilized by autoclave.

2. Preparation of basal DMEM (Stock DMEM)

Autoclaved distilled H_2O grade 2A D7777 is added to DMEM, 3.7 g $NaHCO_3$, and 3.57 g HEPES in 1 liter beaker. After the solution is gently mixed using magnetic stirrer, pH of the solution is adjusted to 7.42 with 1 M $NaHCO_3$ or 1 M HCL.

Thereafter, the solution is poured into a 1 liter volumetric flask and made up to a final volume of 1000 mL with autoclaved distilled H_2O grade 2A. The basal DMEM is then sterilized by filtering through 0.2−μm filter membrane

3. Preparation of complete DMEM (Working DMEM)

All of the following processes are performed in a biosafety cabinet class II. 1 mL L-Glutamine, 1 mL NEAA, 1 mL penicillin-streptomycin, 0.2 mL amphoteracin B, 15 mL PBS, and 15 mL FBS were poured in a sterile 100 mL flask, then basal DMEM is gently added to obtain a final volume of 100 mL. The solution is mixed by manual shaking, and then poured into a sterile 100 mL bottle. Complete DMEM bottle is sealed and stored at 4 °C. The solution must be used within 5 days.

APPENDIX C
CACO-2 STORAGE PROTOCOL

A. Principle

According to ATCC protocol, the concept of slow-stepwise freezing is used to store Caco-2 cells. The slow-stepwise freezing protocol is, firstly, to cool down the cells to –4 °C in a specific freezing module (StrataColler®) for 30 min before incubating overnight at –80 °C. Finally, the frozen cells are kept in liquid nitrogen tank for long-term storage.

B. Reagents and Instruments

1. Freezing medium
2. Cryo-vials (Corning, Corning, NY, USA)
3. StrataColler® freezing module

C. Procedures

1. Preparation of freezing medium

5% v/v DMSO-containing complete DMEM is prepared in biosafety cabinet class II. The medium is sterilized by filtering through 0.2–μm filter and stored at –20 °C.

2. Caco-2 cells storage

The cells are harvested after trypsinization. Suspension of cells is then transferred to a sterile 15–mL centrifuge tube and was centrifuged at 1500 g for 5 min. Thereafter, the medium is removed and cells are re-suspended in ice-cold freezing medium. One mL of cell suspension is aliquoted into cryo-vials and cooled down in 4

°C pre-cooled StrataColler® for 30 min on ice. After cooling down, the StrataColler® containing cryo-vials is placed in –80 °C freezer overnight. Finally, the cry-vials containing frozen cells are transferred to the liquid nitrogen tank for long-term storage.

On the other hand, the thawing protocol follows the concept of quick-thaw. The cryo-vial containing frozen cells is quickly warmed in 37 °C autoclaved distilled H_2O grade 2A. Then, cells are re-suspended in 5 mL of complete DMEM in a 25–cm^2 culture flask.

APPENDIX D
RADIOACTIVE CALCIUM MEASUREMENT

A. Principle

Radioactive calcium, ^{45}Ca, decays with the production of β-particles, as shown in the following equation, with maximum energy of 255 KeV and a half life of 164 days.

$$_{20}Ca^{45} \longrightarrow {}_{21}Sc^{45} + \beta^{-}$$

For observation of Ca^{45} radioactivity, the liquid scintillation cocktail is used for dissolving the samples. The scintillation cocktail contains solvents and solutes, sometimes called fluors. The solutes, usually aromatics such as toluene or xylene, quench energy from ^{45}Ca decay and transmit energy to the solutes as molecular excitation. They must also be transparent to photons emitted by solutes and provide an adequate solubility for solvents and samples. The solutes contain primary and secondary solute. After being excited, the primary solute converts the excitation energy into visible light-photon. However, the emission spectrum of the high energy-short wavelength does not match and cannot be detected by the photodetector. Secondary solute, sometimes called wavelength shifters, takes up the photons emitted by primary solute and re-emit at a lower energy-long wavelength which is better detected by the photodetector.

B. Reagents of the liquid scintillation cocktail

1. 2,5-biphenyloxazole (PPO, primary solute which emits photon at 360 nm)
2. 1,4-bis(5-phenyloxazole-2-yl)benzene (POPOP, secondary solute which emit photon at 420 nm)
3. Triton X-100 (detergent)
4. Toluene (solvent)

C. Instrument

Liquid scintillation spectrophotometer (LKB-Wallac model 1219, LKB Wallac, Finland)

D. Liquid scintillation cocktail preparation

300 mL of toluene is added to 500 mL beaker containing 5 g PPO and 0.3 g POPOP. The solution is mixed using magnetic stirrer for 30 min, after which the solution is placed in a 1000 mL volumic flask. Additional 200 mL of toluene and 500 mL of Triton X-100 are addedeto the solution and mixed using magnetic stirrer. Finally, the solution is transferred into a light protection bottle.

E. Procedure

1. Aliquot 500 μL of scintillation cocktail into 2 mL transparent microcentrifuge tubes.
2. Pipette 100 mL of sample into the microcentrifuge tubes.
3. Mix well by a vortex.
4. Load each microcentrifuge tube into 25–mL transparent vial which is already checked for radioactivity background.

F. References

Mesquita CH, Duarte CL, Hamada MM. Radiation physical chemistry effects on organic detectors. Nucle Instru Method Physic Research 2003; 505:385–388.

Osterman LA, Isotopes, scintillator and scintillation counters. In: Methods of protein and nucleic research 1984. Germany: Springer-Verlag, 67–78.

APPENDIX E
PRLR-L KNOCKDOWN IN CACO-2 MONOLAYER

(*A*) Representative electrophoretic image and (*B–C*) quantitative real-time PCR demonstrate the expression of PRLR-S and PRLR-L in Caco-2 monolayer incubated for 48 h with siPORT (transfection agent) or siPORT plus 1 nmol/L PRLR-L siRNA. The absence of PRLR-L expression confirms the success of PRLR-L knockdown procedure. ** $P < 0.01$ compared with the control group (–siPORT/–siRNA). Numbers in parentheses represent the number of independent Snapwells.

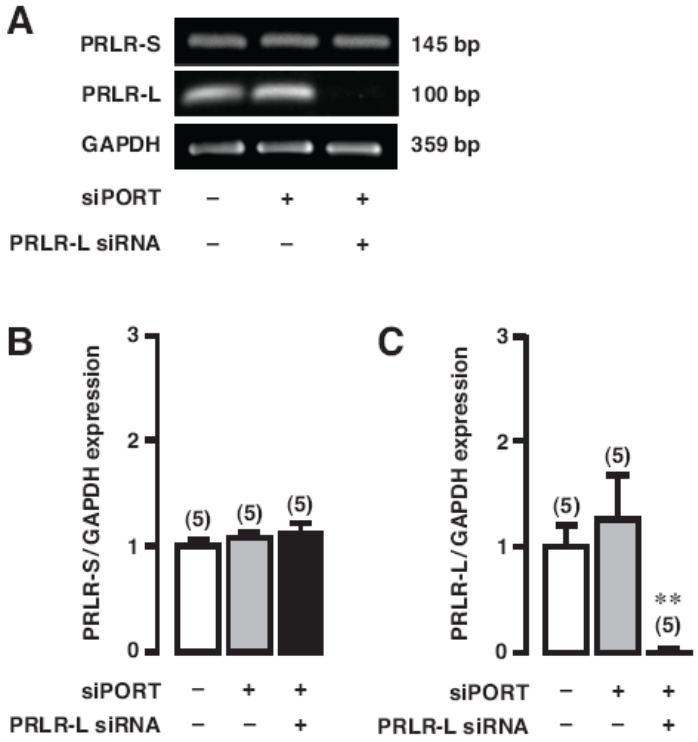

Reference

Thongon N, Nakkrasae L-i, Thongbunchoo J, Krishnamra N and Charoenphandhu N. *Prolactin stimulates transepithelial calcium transport and modulates paracellular permselectivity in Caco-2 monolayer: Mediation by PKC and ROCK pathways.* Am J Physiol Cell Physiol 2008: 294(5):C1158–C1168.

BIOGRAPHY

NAME	Mr. Narongrit Thongon
DATE OF BIRTH	5 February 1981
PLACE OF BIRTH	Ubonratchathanee, Thailand
INSTITUTIONAL ATTENDED	Khon Kaen University, 2000–2004 Bachelor of Science (Physical Therapy), Second Class Honors Mahidol University, 2004–2008 Doctor of Philosophy (Physiology)
HOME ADDRESS	28 Moo 4, Ban Kok, Aumpher Khueang Nai, Ubonratchathanee 34320 Thailand
RESEARCH GRANT	2005-2008 The Royal Golden Jubilee Ph.D. Program
AWARDS	Outstanding Oral Presentation Award at the 9th Annual RGJ–Ph.D. Congress on April 4 – 6, 2008, Jomtien Palm Beach Resort, Pattaya, Chonburi, Thailand Outstanding Oral Presentation Award at the 37th Physiological Society of Thailand's Annual Conference 2008 on May 7 – 9, 2008, Garden Sea View Resort, Pattaya, Chonburi, Thailand